

Winter 2014

Metal ion adsorption onto bacteria-mineral composites

Rachel E. Franzblau

University of Windsor, refranzblau@gmail.com

Follow this and additional works at: <http://scholar.uwindsor.ca/etd>

Recommended Citation

Franzblau, Rachel E., "Metal ion adsorption onto bacteria-mineral composites" (2014). *Electronic Theses and Dissertations*. Paper 5009.

This online database contains the full-text of PhD dissertations and Masters' theses of University of Windsor students from 1954 forward. These documents are made available for personal study and research purposes only, in accordance with the Canadian Copyright Act and the Creative Commons license—CC BY-NC-ND (Attribution, Non-Commercial, No Derivative Works). Under this license, works must always be attributed to the copyright holder (original author), cannot be used for any commercial purposes, and may not be altered. Any other use would require the permission of the copyright holder. Students may inquire about withdrawing their dissertation and/or thesis from this database. For additional inquiries, please contact the repository administrator via email (scholarship@uwindsor.ca) or by telephone at 519-253-3000ext. 3208.

**METAL ION ADSORPTION IN THE PRESENCE OF BACTERIA-MINERAL
COMPOSITES**

By

Rachel E. Franzblau

A Thesis
Submitted to the Faculty of Graduate Studies
through the Great Lakes Institute of Environmental Science
in Partial Fulfillment of the Requirements for
the Degree of Master of Science
at the University of Windsor

Windsor, Ontario, Canada

2013

© 2013 Rachel E. Franzblau

**METAL ION ADSORPTION IN THE PRESENCE OF BACTERIA-MINERAL
COMPOSITES**

By

Rachel E. Franzblau

APPROVED BY:

Dr. Iain Samson
Earth and Environmental Science

Dr. Brian Fryer
Great Lakes Institute for Environmental Research

Dr. Christopher Daughney
GNS Science, Lower Hutt, New Zealand

Dr. Christopher Weisener, Advisor
Great Lakes Institute for Environmental Research

December 17, 2013

DECLARATION OF CO-AUTHORSHIP AND PREVIOUS PUBLICATION

I. Co-Authorship Declaration

I hereby declare that this thesis incorporates material that is result of joint research, as follows:

This thesis also incorporates the outcome of a joint research undertaken in collaboration with C. Daughney under the supervision of C. Weisener. This collaboration is covered in Chapters 2 and 3 of this thesis. In all cases, the key ideas, primary contributions, experimental designs, data analysis and interpretation, were performed by the author, and the contribution of the co-authors was primarily through the provision of modeling assistance and comments on the manuscript.

I am aware of the University of Windsor Senate Policy on Authorship and I certify that I have properly acknowledged the contribution of other researchers to my thesis, and have obtained written permission from each of the co-author(s) to include the above material(s) in my thesis.

I certify that, with the above qualification, this thesis, and the research to which it refers, is the product of my own work.

II. Declaration of Previous Publication

This thesis includes 2 original papers that will be submitted for publication in peer reviewed journals, as follows:

Thesis Chapter	Publication title/full citation	Publication status*
<i>Chapter 2</i>	Selenate adsorption to composites of <i>Escherichia coli</i> and iron oxide during the addition, oxidation, and hydrolysis of Fe(II)	<i>Submitted to Chemical Geology</i>
<i>Chapter 3</i>	Copper (II) removal by <i>Escherichia coli</i> -iron oxide composites during the addition of Fe(II) _{aq}	<i>In preparation</i>

I certify that I have obtained a written permission from the copyright owner(s) to include the above published material(s) in my thesis. I certify that the above material describes work completed during my registration as graduate student at the University of Windsor.

I declare that, to the best of my knowledge, my thesis does not infringe upon anyone's copyright nor violate any proprietary rights and that any ideas, techniques, quotations, or any other material from the work of other people included in my thesis, published or otherwise, are fully acknowledged in accordance with the standard referencing practices. Furthermore, to the extent that I have included copyrighted material that surpasses the bounds of fair dealing within the meaning of the Canada Copyright Act, I certify that I have obtained a written permission from the copyright owner(s) to include such material(s) in my thesis.

I declare that this is a true copy of my thesis, including any final revisions, as approved by my thesis committee and the Graduate Studies office, and that this thesis has not been submitted for a higher degree to any other University or Institution.

ABSTRACT

Adsorption onto mineral and bacterial surfaces affects the fate of aqueous metal(loid)s but there is currently a poor understanding of adsorption onto mixtures of these two sorbents. This thesis used chemical analyses and imaging to track selenate and copper adsorption by iron oxide-*Escherichia coli* composites during $\text{Fe(II)}_{\text{aq}}$ addition. No selenate adsorbed onto *E. coli* under the conditions in this study. Selenate adsorption onto composites was reduced compared to iron oxide. Surface complexation models (SCMs) suggested that the reduction in selenate adsorption was due to masking of iron oxide sites and aggregation of the mineral over time. Copper adsorbed primarily to the cells under the conditions in this study; however, some removal was due to co-precipitation within the iron oxide. SCMs overestimated copper removal as they did not account for masking of bacterial sites. In conclusion, metal(loid) removal is significantly affected by the presence of sorbent mixtures and redox processes.

ACKNOWLEDGEMENTS

I would like to thank my advisor Dr. Chris Weisener and Dr. Chris Daughney for all of their help and guidance. I also am grateful to my other committee members Dr. Brian Fryer and Dr. Iain Samson for their support. Thank you to Sharon Lackie for her help with SEM and BET analyses, J.C. Barette for his help with my constant stream of samples for ICPOES analysis, and M. Reid and A. Korniak at McMaster University for their help with preparation and analysis of my TEM samples. Thank you to my lab mates and GLIER co-workers who have helped and supported me in my time here including (but not limited to): Nadine Loick, Nick Falk, Zach Diloreto, Danielle VanMensel, Ryan Boudens, Tom Reid, Sabari Prakasan, Christina Smeaton, Mark Ryder, and Linda Söderberg. Thank you to Mary Lou Scratch for all of her help getting me set up in a new country and making everything run smoothly for all of GLIER. Lastly thank you a big thank you to my friends and family who have supported me the whole way to where I am today!

TABLE OF CONTENTS

DECLARATION OF CO-AUTHORSHIP AND PREVIOUS PUBLICATION.....	iii
ABSTRACT.....	v
ACKNOWLEDGEMENTS.....	vi
LIST OF TABLES.....	x
LIST OF FIGURES.....	xi
CHAPTER 1 INTRODUCTION.....	1
1.1 Background.....	1
1.2 Adsorption.....	1
1.2.1 Chemistry of adsorption.....	1
1.2.2 Prior adsorption studies.....	2
1.2.3 Prior field studies.....	5
1.3 Thesis overview.....	6
1.3.1 Hypothesis and objectives.....	6
1.3.2 Overview of experimental components.....	7
1.3.3 Surface complexation modeling.....	9
1.4 References.....	11
CHAPTER 2 SELENATE ADSORPTION TO <i>ESCHERICHIA COLI</i> AND IRON OXIDE COMPOSITES DURING THE ADDITION, OXIDATION, AND HYDROLYSIS OF $\text{Fe(II)}_{\text{AQ}}$ TO Fe(III) OXIDE.....	17
2.1 Introduction.....	17
2.2 Methods.....	20
2.2.1 Bacterial growth conditions.....	20
2.2.2 Synthesis of abiotic iron oxides.....	21
2.2.3 Synthesis of bacteria-iron oxide composites.....	22
2.2.4 Adsorption to bacteria or iron oxide as a function of pH, selenate/sorbent ratio, and time.....	22
2.2.5 Selenate adsorption during the synthesis of abiotic iron oxides or bacteria-iron oxide composite.....	24
2.2.6 Electron microscopy.....	25

2.2.7 Modeling	26
2.3 Results and discussion	28
2.3.1 Selenate adsorption to bacterial cells	28
2.3.2 Selenate adsorption to abiotic iron oxides.....	29
2.3.3 Selenate adsorption to bacteria-iron oxide composites	32
2.3.4 Electron microscopy	34
2.4 Conclusions.....	35
2.5 References	47
CHAPTER 3 COPPER (II) REMOVAL BY <i>ESCHERICHIA COLI</i> -IRON OXIDE COMPOSITES DURING THE ADDITION OF $\text{Fe(II)}_{\text{AQ}}$	51
3.1 Introduction.....	51
3.2 Methods.....	54
3.2.1 Bacterial growth conditions.....	54
3.2.2 Synthesis of abiotic iron oxides.....	54
3.2.3 Synthesis of iron oxide-bacteria composites	55
3.2.4 Adsorption to bacteria or iron oxide as a function of pH, Cu(II) to sorbent ratio, and time.....	55
3.2.5 Copper adsorption experiments	57
3.2.6 Electron microscopy	58
3.2.7 Modeling	59
3.3 Results and discussion	60
3.3.1 Copper adsorption to bacterial cells	60
3.3.2 Copper adsorption to abiotic iron oxides	61
3.3.3 Copper adsorption to bacteria-iron oxide composites.....	64
3.4 Conclusions.....	66
3.5 References	77
CHAPTER 4 CONCLUSIONS	82
4.1 Summary	82
4.2 Discussion	84
4.3 Conclusions.....	86
4.4 Future work.....	87
4.5 References	88

VITA AUCTORIS	90
---------------------	----

LIST OF TABLES

Table 2.1: Overview of prior studies examining metal(loid) adsorption onto bacteria-iron oxide composites.....	44
Table 2.2: Features of the triple layer surface complexation models for iron oxide used in selenate adsorption modeling.....	45
Table 2.3: Features of the non-electrostatic surface complexation models for bacterial surfaces used in selenate adsorption modeling	46
Table 3.1: Overview of prior studies examining metal(loid) adsorption onto bacteria-iron oxide composites.....	74
Table 3.2: Features of the triple layer surface complexation models for iron oxide used in copper adsorption modeling.....	75
Table 3.3: Features of the non-electrostatic surface complexation models for bacterial surfaces used in copper adsorption modeling	76

LIST OF FIGURES

Figure 2.1: Selenate adsorption onto abiotic iron oxides and bacterial cells from 0 to 7 h	36
Figure 2.2: Selenate adsorption onto abiotic iron oxides as a function of pH (3-8) and mineral concentration (0.101 g/L, 0.054 g/L, 0.025 g/L) with models shown for each mineral concentration.....	37
Figure 2.3: $[\text{Fe(II)}]_{\text{aq}}$ during the synthesis of abiotic iron oxides and bacteria-iron oxides composites	38
Figure 2.4: Selenate adsorption during the synthesis of bacteria-iron oxide composites with models showing all data points modelled together and each data point modelled separately	39
Figure 2.5: Modelled iron oxide surface site concentrations over time for selenate adsorption.....	40
Figure 2.6: Backscatter electron-scanning electron microscopy images of bacteria-iron oxide composites equilibrated with selenate over time.....	41
Figure 2.7: Backscatter electron-scanning electron microscopy images of abiotic iron oxides equilibrated with selenate over time.....	42
Figure 2.8: Transmission electron microscopy images of bacteria-iron oxide composites equilibrated with selenate over time	43
Figure 3.1: Copper adsorption onto abiotic iron oxides and bacterial cells from over a range of pH, mineral or bacterial concentration, and time.....	68
Figure 3.2: $[\text{Fe(II)}]_{\text{aq}}$ during the synthesis of abiotic iron oxides and bacteria-iron oxides composites	69
Figure 3.3: Copper adsorption during the synthesis of bacteria-iron oxide composites with models showing all data points modelled together and each data point modelled separately	70
Figure 3.4: Backscatter electron-scanning electron microscopy images of bacteria-iron oxide composites equilibrated with copper over time.....	71
Figure 3.5: Transmission electron microscopy images of bacteria-iron oxide composites equilibrated with copper over time	72
Figure 3.6: Backscatter electron-scanning electron microscopy images of abiotic iron oxides equilibrated with copper over time.....	73

CHAPTER 1

INTRODUCTION

1.1 Background

In the environment, there are many controlling factors that can influence the chemistry of aqueous systems by adding or removing contaminants through abiotic or biotic means.¹⁻³ To better understand contaminant cycling in natural environments, these introduction and removal pathways must be understood so that polluted systems can be effectively remediated. Some of these removal pathways include oxidation, reduction, precipitation, and adsorption mechanisms.¹⁻⁹ Additionally, in natural systems abiotic (e.g. minerals) and biotic (e.g. bacterial cells) materials are often observed in close association with one another. The proximity of both organic and inorganic substrates can give rise to the formation of bacteria-mineral composites which can affect pollutant removal.² However these composites do not necessarily behave in the same manner as their end-member components (e.g. bacteria or minerals) in the presence of pollutants. As natural systems are incredibly complex it is useful to conduct systematic laboratory scale experiments to elucidate the effect that each pathway has on the release and/or sequestration of contaminants. To that end, this thesis focuses on adsorption to iron oxide-bacteria composites as a potential removal pathway for contaminant metal(loid) ions in aqueous systems.

1.2 Adsorption

1.2.1 Chemistry of adsorption

Adsorption is a reversible chemical reaction between a surface site on a given substrate and a free ion in solution.¹⁰⁻¹³ Functional surface sites are characterized by different binding energies or unsatisfied surface charge and cover surfaces. The type and density of sites vary between surfaces (e.g. mineral or bacterial) and, in the case of bacteria, the degree of this surface reactivity may often be controlled by cell surface receptors.^{1,14,15} Adsorption reactions are dependent on environmental conditions including pH, ionic strength, and the concentration of

sorbents and sorbates.^{4,6,13,16,17} These reactions are ubiquitous in nature and could potentially be used to remediate contaminated sites. Prior work has dealt with adsorption to either bacterial or mineral surfaces, giving a basic understanding of this process; however, natural systems are far more complex than just a single sorbate and sorbent studied in the laboratory. In order to understand and separate these complexities laboratory studies must undertake a more rigorous systematic approach by incrementally increasing the complexity of variables to advance our understanding of how natural environments function.

1.2.2 Prior adsorption studies

Microorganisms and minerals affect the speciation of metal cations and oxyanions in natural systems through complexation reactions with surface sites.^{3,6,7,11,12,17-23} Composites of bacteria and minerals can form and affect the mobility and transport of ions in solution.²¹ Prior work has been undertaken to determine the extent of metal ion sorption to bacterial or mineral surfaces, but little research has been performed on systems containing composite mixtures of both bacteria and minerals.^{17,24-26}

The studies that have examined ion sorption to bacteria-mineral composites have used both natural and synthetic composite materials. Small et al. studied Sr^{2+} sorption to *Shewanella alga*, *Shewanella putrefaciens*, hydrous ferric oxide, and *S. alga*-hydrous ferric oxide composites over a range of pH and ionic strength and concluded that the maximum sorption that occurred in the presence of the composite was less than the sum of that in the separate bacteria and iron oxide systems (i.e. non-additive sorption).^{4,24} The authors proposed that this non-additivity was due to masking of surface functional sites in the composite. Templeton et al. observed that Pb^{2+} sorption to *Burkholderia cepacia* biofilms coated with goethite was pH dependent with Pb^{2+} mainly sorbed to the biofilm fraction at low pH and primarily to the mineral fraction at high pH due to competition between the two sorbents.²⁷ Kulczycki et al. observed enhanced Cd^{2+} sorption in systems with either *Escherichia coli* or *Bacillus subtilis* as compared to composites of each with

ferrihydrite over a range of pH and Cd^{2+} concentrations, and attributed these observations to the masking of functional sites by ferrihydrite in the composite systems which caused there to be less sorption than predicted by one-site Langmuir models.²⁸ A study by Daughney et al. examined the sorption of Cd^{2+} to *Anoxybacillus flavithermus*-iron oxide composites during $\text{Fe(II)}_{\text{aq}}$ addition, oxidation, hydrolysis, and precipitation and found delayed iron oxide precipitation at low Fe/bacteria ratios, decreased Cd^{2+} sorption at intermediate Fe/bacteria ratios, and some recovered sorption capacity at high Fe/bacteria ratios.¹⁷ The authors concluded that Fe^{2+} and Cd^{2+} compete for bacterial functional sites and that masking of surface sites due to Fe^{2+} and Fe(III)-oxide sorption led to reduced Cd^{2+} adsorption under some of the experimental conditions. This study is the only prior work that assessed sorption to bacteria-iron oxide composites during Fe^{2+} precipitation as Fe(III)-oxide and, as the authors found that the progressive addition of Fe^{2+} and its subsequent precipitation as Fe(III)-oxide affected composite sorption capacity, this interaction is an important one to further investigate. Recent work by Moon et al. has examined Cu^{2+} sorption to *Bacillus subtilis*-ferrihydrite composites over a range of pH, Cu^{2+} concentrations, and ferrihydrite/bacteria ratios.^{16,29} In this study the authors found that sorption to the composites was non-additive: the sum of sorption in bacteria and ferrihydrite systems was greater than sorption in the composite system and this deviation increased with the ferrihydrite/bacteria ratio. However, these studies used pre-precipitated composite material which was then exposed to Cu^{2+} ions and so did not account for the effects of sorption during the formation of iron oxide-bacteria composites.

There have also been a number of studies examining sorption to bacteriogenic iron oxides (BIOS) and natural organic matter (NOM) from natural systems. Ferris et al. used BIOS collected from the Aspo Hard Rock Laboratory, Sweden which were dominated by *Gallionella ferruginea*, a lithotrophic iron oxidizing bacterium that forms stalks coated in iron oxides.²⁶ This study concluded that metal sorption was strongly affected by the species of bacteria in the

composite structure. Another study performed by Ferris et al. used BIOS from the Strassa Mine, Sweden made up of *Gallionella* and *Leptothrix* sp. and observed that the log K_D was inversely related to the mass of reducible iron in the BIOS samples, indicating that with more iron oxide present in the composite, metal ions became less strongly bound to the solid phase.³⁰ A study by Martinez et al. (2004) examined Cd^{2+} sorption to BIOS from a subterranean environment and found that sorption decreased in the presence of BIOS as compared to only bacterial surfaces and that this behavior was non-additive. Langley et al. studied the sorption of Sr^{2+} to BIOS over a pH range and found that Sr^{2+} sorption increased with pH and that sorption was enhanced at low ionic strength, indicating that Sr^{2+} can be easily removed by BIOS at low ionic strength and circumneutral pH.³² Vermeer et al. looked at Cd^{2+} sorption to Aldrich humic acid and hematite composites as compared to the end-member systems and discovered that sorption to the composite was non-additive and overall sorption to each sorbent was dependent on the affinity of the metal in question.¹⁴ A study conducted by Borrok et al. modeled the sorption capacity of bacteria versus that of humic substances using previously published data and found that humic substances have approximately 2 times as many sorption sites per gram compared to bacteria and a higher affinity for Cd^{2+} at circumneutral pH but that both bacteria and humic acids can control Cd^{2+} sorption depending on environmental conditions.³³ Borrok et al. tested for the existence of ternary bacteria-metal-humic complexes with *Bacillus subtilis* and Ni, Pb, Cd, or Cu in the laboratory and discovered that these ternary complexes form quickly and completely reversibly in solution with complex stability dependent on pH, concentration of humic substances, and type of metal cation.¹⁹ Another study by Craven et al. examined sorption of Cu^{2+} to dissolved organic matter (DOM) and observed that as the Cu/DOM ratio increased the binding constant decreased so the ratio of metal to sorbent is an important consideration for sorption capacity.³⁴ These studies performed with BIOS, humic substances, and DOM demonstrate the significance of bacteria-mineral composites for metal cycling in the environment. These studies also show that natural environments are more complex than the prior laboratory work with one sorbate and one

sorbent because non-additive sorption behavior was observed in many studies using natural and synthetic sorbent surfaces. These studies indicate that more laboratory work needs to be undertaken using bacteria-mineral composites to be able to accurately predict metal cycling in nature.

1.2.3 Prior field studies

In addition to the prior laboratory scale work, there have been a number of studies in the field to determine the effectiveness of sorption and other chemical and biological reactions on contaminant removal, primarily at acid mine drainage (AMD) sites. A number of these studies include a modeling component to enable the prediction of contaminant behavior in natural environments. A study by Chen et al. examined the sorption/desorption of Pb, Cd, and Zn by a contaminated soil from North Carolina that was made up of primarily apatite.³⁵ Apatite was found to remove Pb effectively due to dissolution/precipitation of secondary mineral phases. Cd and Zn removal was less extensive and occurred primarily via sorption instead of by precipitation of secondary minerals. Woulds et al. studied remediation via constructed wetlands and found that bacterial sulfate reduction occurred as well as sulfate removal through sorption; however, wetland performance decreased over time which led to low overall removal.³⁶ A study examining the effectiveness of Zn and Cu sorption to vegetal matter as a proxy for organic based passive remediation was conducted by Gibert et al.³⁷ This study developed a model for metal removal that assumed that there were two primary surface sites and that metal sorption increased with pH due to reduced competition with protons. Kairies et al. conducted a study of the properties of iron oxyhydroxides associated with passively treated coal mine drainage sites.³⁸ This study concluded that that lower crystallinity of the precipitates, which were primarily goethite, enhanced sorption capacity and that crystallinity is a function of how quickly Fe(II) oxidizes, precipitates, and aggregates so that precipitates formed later have lower crystallinity. Butler et al. assessed removal of Cu, Fe, Cd, Mn, or Zn by stream sediments from North Fork Clear Creek, Colorado (an AMD impacted system) as a function of pH, ionic strength, DOC, time and particle size.³⁹

The results indicated these variables affected each metal differently, with the most Cu and Fe released into solution overall from the sediments. Runkel et al. examined the hydrogeochemistry of untreated (low pH) versus treated (high pH) material and created a model to predict the outcomes.⁴⁰ The authors concluded that for Al, As, Fe, and Pb the model correctly predicted a reduction in dissolved concentrations but for Cd, Cu, and Zn were attributed to incorrect solid phase density inputs and can be corrected for through calibration. Overall, these field studies demonstrate the complexity of real-world systems and reinforce the conclusion that more advanced laboratory studies are necessary to further our understanding of metal removal in these environments.

1.3 Thesis overview

1.3.1 Hypothesis and objectives

In natural systems both bacteria and minerals can coexist and hence studies should focus on the effects that both sorbents may have on each other. In some cases both the bacteria and minerals will compete for sorbates in aqueous systems. Interactions between the two types of sorbent may lead to masking of reactive surface sites and thereby influence the overall reactivity of the composite. Metal cations and oxyanions are fundamentally different species and so studies should focus on comparing their respective adsorption mechanisms.

In this MSc thesis I hypothesize that a decrease in adsorption (e.g. non-additive behavior) will be observed in the presence of bacteria-iron oxide composites as compared to adsorption in the end-member systems (e.g. bacteria or iron oxide). This will be due to the masking of reactive surface sites through a process of competitive interactions between the two sorbents in the presence of selenate or copper. This hypothesis will be tested using laboratory experiments to test the abiotic (mineral only), biotic (bacteria only) and composite (mineral and bacteria) systems under constant pH and nongrowth conditions and during the addition, oxidation, hydrolysis, and precipitation of Fe(II) to Fe(III) oxide. In addition the hypothesis will be tested through the

creation of surface complexation models to describe the experimental data and to evaluate if current single sorbent models are capable of predicting the extent of adsorption in a two sorbent system. These assumptions will be tested and characterized using quantitative laboratory techniques of both the aqueous and solid phases (Ferrozine, 1,10-phenanthroline, ICP-OES) in combination with qualitative imaging techniques (SEM, TEM).

1.3.2 Overview of experimental components

This thesis will investigate the adsorption behaviors of selenate oxyanions (SeO_4^{2-}) and copper cations (Cu^{2+}) with composites of iron oxide minerals and *Escherichia coli* AB264.

Selenium is a pollutant metal, and it is most commonly found at naturally contaminated sites or sites where naturally high background levels have been amplified through bioaccumulation or human activities such as irrigation or water storage (e.g. Kesterson Reservoir).⁴¹⁻⁴⁴ Selenium oxyanions (SeO_4^{2-} , SeO_3^{2-}) are the most common species of selenium in aqueous systems, although selenide (Se^{2-}) and elemental Se (Se^0) may be present under some environmental conditions.^{41,42} This study will focus on selenate (SeO_4^{2-}) sorption as it is the more mobile of the two Se oxyanions, although selenite (SeO_3^{2-}) is more toxic.⁴¹ Selenate was selected for this project as there has been little research into the sorption behavior of oxyanions in the presence of bacteria and minerals and none to the knowledge of the author in the presence of mineral-bacteria composites.^{13,45-49}

Copper is a common metal pollutant, namely at mining sites and locations with naturally elevated background levels.⁵⁰⁻⁵³ However, the average background copper level is very low globally.⁵² Copper was selected not only because of its history as a pollutant but also for its comparability with previous work as a number of studies have been conducted on its sorption as Cu^{2+} to bacteria and iron oxides, both individually and in composites.^{3,7,11,12,19,20}

Iron oxide minerals form under a range of environmental conditions and the type of iron oxide formed depends greatly on pH during precipitation.⁵⁴ Iron oxides have one type of

amphoteric surface functional group, denoted in this thesis as $=\text{FeOH}$.⁵⁴ Depending on which iron oxide minerals are present, the concentration of surface functional groups varies due to differences in mineral structure.⁵⁴ Iron oxides are able to sorb fewer ions than bacteria as they have fewer functional sites overall and less diversity of sites, although they may have a larger surface area depending on particle type and size.¹⁷ However, it has been shown that bacteria adsorb fewer metal ions when there is iron oxide present than with no mineral as some surface binding sites may be masked by complexation with the iron oxides under specific experimental conditions.⁷

E. coli is a model Gram negative bacterium that has been well characterized and used in a number of prior geomicrobiological studies.^{3,6,7,11} Bacteria are classified by the Gram stain, which turns the cells purple (positive) or not (negative). This difference is due to Gram positive cells having solely a peptidoglycan cell wall and Gram negative cells having an additional outer membrane made of proteins, phospholipids, and lipopolysaccharides.^{55,56} Due to the differences between Gram positive and Gram negative bacterial surfaces there are different ratios of the same major classes of surface sites which are the carboxyl ($=\text{RCOOH}$), phosphoryl ($=\text{RPO}_4\text{H}$), hydroxyl ($=\text{ROH}$), and amino ($=\text{RNH}_3^+$) sites.^{17,57} Varying densities of each class of surface site could cause there to be differing amounts of sorption that occur in Gram positive versus Gram negative bacteria but few studies have compared sorption between these two classes of bacteria. One such study was by Yee et al. found that the sorption capacity could be similar between Gram negative and Gram positive bacteria while another by Borrok et al. found that Gram positive cells have approximately 40% more surface sites, but this is hard to assess as most studies are conducted using different experimental protocols and few use multiple strains of bacteria concurrently.^{58,59} The two studies that make up this thesis were conducted using identical experimental protocols that can be implemented in future studies to enable the direct comparison of results. Additionally, few prior studies have focused on the sorption of ions in the presence of

both minerals and bacteria, as stated previously, and as minerals and bacteria are ubiquitous in natural systems it is therefore important to include both in laboratory experiments.^{4,6,7,12,17,19,20,22,24,27–29}

1.3.3 Surface complexation modeling

Surface complexation models (SCMs) were developed to describe adsorption interactions between free ions in solution and mineral surfaces.⁶⁰ These models describe adsorption through a series of solution and surface chemical reactions in the form of the following general reactions for metal cation and anion sorption:



where XOH^0 represents a generic metal oxide surface site, M^{2+} is a metal cation, A^{2-} is a metal anion, a^{H^+} is the activity of the hydrogen ion, XOM^+ and XA^- are the adsorbed metal species, and K_M and K_A are the stability constants for these reactions. Similar equations have been used to model adsorption to bacterial surfaces in past studies as well.^{57,61} A set of mass law equations like equations 1.1 and 1.2 is created to describe all surface and solution reactions that could occur in a system and this set is input into the model. The model itself is adjusted to the actual experimental conditions including sorbent surface area, sorbate and sorbent concentration, ionic strength, and pH. Then the model is run through a number of iterations until it converges on the optimal fit for the adjustable parameters and data and ideally the model results match the experimental ones. Typically, the adjustable parameters include the stability constants for the adsorption reactions and/or the total concentration of surface functional groups present in the system. The fit of the model is judged by the variance $V(Y)$ which is represented by the following equation:⁶²

$$V(Y) = \frac{\sum_{P,Q} (\frac{Y}{s_Y})^2}{n_P \times n_Q - n_R} \quad (\text{Equation 1.3})$$

in which Y is the difference between the model and experimental mass balance over all data P and all components Q for which the total and free concentrations are known. s_Y is the standard deviation which is determined by propagation of uncertainty in the free and total concentrations of the system components. The sum of squares of Y/s_Y is normalized to the degrees of freedom in the system with n_P as the total number of points, n_Q as the number of components for which the total and free concentrations are known, and n_R as the number of parameters optimized in the model. A variance of 1 is ideal, indicating that the model and experimental errors are be equal.

In this thesis, a surface complexation modeling program called FITMOD was used to model the experimental data. FITMOD is a modified version of FITEQL 2.0 and was designed to enable a SCM to be fit to experimental data.^{62,63} FITMOD is unique in that it can automatically adjust stability constants to obtain the optimal fit and simultaneously model systems with different solid/solution ratios.⁶³ FITMOD incorporates the four FITEQL double and triple layer models as well as the Donnan model, which assumes that surface sites are distributed evenly over a volume instead of a plane at the solid-solution interface as the four other models do.⁶⁴

SCMs could potentially be used to predict pollutant cycling in nature once the models are advanced enough to account for all the potential interactions that occur. As the models are primarily used with a single sorbent and sorbate there is a lot of advancement that must occur. The previously mentioned studies which examined adsorption behavior onto composites are the first to add a new level of complexity to SCMs. More studies must be performed in these dual sorbent systems as well as those that are even more complex to enable us to model a natural environment.

1.4 References

- (1) Gadd, G. M. Metals, minerals and microbes: geomicrobiology and bioremediation. *Microbiology* **2010**, *156*, 609–43.
- (2) Fortin, D.; Langley, S. Formation and occurrence of biogenic iron-rich minerals. *Earth-Science Rev.* **2005**, *72*, 1–19.
- (3) Mullen, M. D.; Wolf, D. C.; Ferris, F. G.; Beveridge, T. J.; Flemming, C. A.; Bailey, G. W. Bacterial sorption of heavy metals. *Appl. Environ. Microbiol.* **1989**, *55*, 3143–9.
- (4) Small, T. D.; Warren, L. A.; Ferris, F. G. Influence of ionic strength on strontium sorption to bacteria, Fe(III) oxide, and composite bacteria-Fe(III) oxide surfaces. *Appl. Geochemistry* **2001**, *16*, 939 – 946.
- (5) Ferris, F. G.; Beveridge, T. J. Binding of a paramagnetic metal cation to *Escherichia coli* K-12 outer-membrane vesicles. *FEMS Microbiol. Lett.* **1984**, *24*, 43–46.
- (6) Kulczycki, E.; Ferris, F. G. Impact of cell wall structure on the behavior of bacterial cells as sorbents of cadmium and lead. *Geomicrobiol. J.* **2002**, *19*, 553–565.
- (7) Ferris, F. G.; Beveridge, T. J. Site specificity of metallic ion binding in *Escherichia coli* K-12 lipopolysaccharide. *Can. J. Microbiol.* **1986**, *32*, 52–55.
- (8) Yee, N.; Fein, J. Cd adsorption onto bacterial surfaces: A universal adsorption edge? *Geochim. Cosmochim. Acta* **2001**, *65*, 2037–2042.
- (9) Gadd, G. M.; White, C. Microbial treatment of metal pollution--a working biotechnology? *Trends Biotechnol.* **1993**, *11*, 353–9.
- (10) Beveridge, T. J.; Murray, R. G. Sites of metal deposition in the cell wall of *Bacillus subtilis*. *J. Bacteriol.* **1980**, *141*, 876–887.
- (11) Beveridge, T. J.; Koval, S. F. Binding of metals to cell envelopes of *Escherichia coli* K-12. *Appl. Environ. Microbiol.* **1981**, *42*, 325–335.
- (12) Fein, J. B.; Daughney, C. J.; Yee, N.; Davis, T. A. A chemical equilibrium model for metal adsorption onto bacterial surfaces. *Geochim. Cosmochim. Acta* **1997**, *61*, 3319–3328.
- (13) Kenward, P. A; Fowle, D. A; Yee, N. Microbial selenate sorption and reduction in nutrient limited systems. *Environ. Sci. Technol.* **2006**, *40*, 3782–6.

- (14) Vermeer, A. W. P.; McCulloch, J. K.; Van Riemsdijk, W. H.; Koopal, L. K. Metal ion adsorption to complexes of humic acid and metal oxides: Deviations from the additivity rule. *Environ. Sci. Technol.* **1999**, *33*, 3892–3897.
- (15) Gadd, G. M. Biosorption: critical review of scientific rationale, environmental importance and significance for pollution treatment. *J. Chem. Technol. Biotechnol.* **2009**, *84*, 13–28.
- (16) Moon, E. M.; Peacock, C. L. Adsorption of Cu(II) to ferrihydrite and ferrihydrite–bacteria composites: Importance of the carboxyl group for Cu mobility in natural environments. *Geochim. Cosmochim. Acta* **2012**, *92*, 203–219.
- (17) Daughney, C. J.; Fakhri, M.; Châtellier, X. Progressive sorption and oxidation/hydrolysis of Fe(II) affects cadmium immobilization by bacteria-iron oxide composites. *Geomicrobiol. J.* **2011**, *28*, 11–22.
- (18) Beveridge, T. J.; Murray, R. G. Uptake and retention of metals by cell walls of *Bacillus subtilis*. *J. Bacteriol.* **1976**, *127*, 1502–1518.
- (19) Borrok, D.; Aumend, K.; Fein, J. Significance of ternary bacteria–metal–natural organic matter complexes determined through experimentation and chemical equilibrium modeling. *Chem. Geol.* **2007**, *238*, 44–62.
- (20) Fang, L.; Cai, P.; Chen, W.; Liang, W.; Hong, Z.; Huang, Q. Impact of cell wall structure on the behavior of bacterial cells in the binding of copper and cadmium. *Colloids Surfaces A Physicochem. Eng. Asp.* **2009**, *19*, 553–565.
- (21) Chapelle, F. H. The significance of microbial processes in hydrogeology and geochemistry. *Hydrogeol. J.* **2000**, *8*, 41–46.
- (22) Fortin, D.; Ferris, F. G. Precipitation of iron, silica, and sulfate on bacterial cell surfaces. *Geomicrobiol. J.* **1998**, *15*, 309–324.
- (23) Randall, S. R.; Sherman, D. M.; Ragnarsdottir, K. V; Collins, C. R. The mechanism of cadmium surface complexation on iron oxyhydroxide minerals. *Geochim. Cosmochim. Acta* **1999**, *63*, 2971–2987.
- (24) Small, T. D.; Warren, L. A.; Roden, E. E. Sorption of strontium by bacteria, Fe(III) oxide, and bacteria-Fe(III) oxide composites. *Environ. Sci. Technol.* **1999**, *33*, 4465–4470.
- (25) Anderson, C. R.; Pedersen, K. In situ growth of *Gallionella* biofilms and partitioning of lanthanides and actinides between biological material and ferric oxyhydroxides. *Geobiology* **2003**, *1*, 169–178.

- (26) Ferris, F. Retention of strontium, cesium, lead and uranium by bacterial iron oxides from a subterranean environment. *Appl. Geochemistry* **2000**, *15*, 1035–1042.
- (27) Templeton, A. S.; Spormann, A. M.; Brown Jr., G. E. Speciation of Pb(II) sorbed by *Burkholderia cepacia*/goethite composites. *Environ. Sci. Technol.* **2003**, *37*, 2166–2172.
- (28) Kulczycki, E.; Fowle, D.; Fortin, D.; Ferris, F. G. Sorption of cadmium and lead by bacteria–ferrihydrite composites. *Geomicrobiol. J.* **2005**, *22*, 299–310.
- (29) Moon, E. M.; Peacock, C. L. Modelling Cu(II) adsorption to ferrihydrite and ferrihydrite–bacteria composites: Deviation from additive adsorption in the composite sorption system. *Geochim. Cosmochim. Acta* **2013**, *104*, 148–164.
- (30) Ferris, F. G.; Konhauser, K. O.; Lyven, B.; Pedersen, K. Accumulation of metals by bacteriogenic iron oxides in a subterranean environment. *Geomicrobiol. J.* **1999**, *16*, 181–192.
- (31) Martinez, R. E.; Pedersen, K.; Ferris, F. G. Cadmium complexation by bacteriogenic iron oxides from a subterranean environment. *J. Colloid Interface Sci.* **2004**, *275*, 82–9.
- (32) Langley, S.; Gault, A. G.; Ibrahim, A.; Takahashi, Y.; Renaud, R. O. B. Sorption of strontium onto bacteriogenic iron oxides. *Environ. Sci. Technol.* **2009**, *43*, 1008–1014.
- (33) Borrok, D.; Fein, J. B. Distribution of protons and Cd between bacterial surfaces and dissolved humic substances determined through chemical equilibrium modeling. *Geochim. Cosmochim. Acta* **2004**, *68*, 3043–3052.
- (34) Craven, A. M.; Aiken, G. R.; Ryan, J. N. Copper(II) binding by dissolved organic matter: Importance of the copper-to-dissolved organic matter ratio and implications for the biotic ligand model. *Environ. Sci. Technol.* **2012**, *46*, 9948–9955.
- (35) Chen, X.; Wright, J. V.; Conca, J. L.; Peurrung, L. M. Evaluation of heavy metal remediation using mineral apatite. *Water. Air. Soil Pollut.* **1997**, *98*, 57–78.
- (36) Woulds, C.; Ngwenya, B. T. Geochemical processes governing the performance of a constructed wetland treating acid mine drainage, Central Scotland. *Appl. Geochemistry* **2004**, *19*, 1773–1783.
- (37) Gibert, O.; de Pablo, J.; Cortina, J. L.; Ayora, C. Sorption studies of Zn(II) and Cu(II) onto vegetal compost used on reactive mixtures for in situ treatment of acid mine drainage. *Water Res.* **2005**, *39*, 2827–38.

- (38) Kairies, C. L.; Capo, R. C.; Watzlaf, G. R. Chemical and physical properties of iron hydroxide precipitates associated with passively treated coal mine drainage in the Bituminous Region of Pennsylvania and Maryland. *Appl. Geochemistry* **2005**, *20*, 1445–1460.
- (39) Butler, B. a Effect of pH, ionic strength, dissolved organic carbon, time, and particle size on metals release from mine drainage impacted streambed sediments. *Water Res.* **2009**, *43*, 1392–402.
- (40) Runkel, R. L.; Kimball, B. A.; Walton-day, K.; Verplanck, P. L.; Broshears, R. E.; Survey, U. S. G.; Stop, M.; States, U. Evaluating remedial alternatives for an acid mine drainage stream : A model post audit. *Environ. Sci. Technol.* **2012**, *46*, 340–347.
- (41) Barceloux, D. G. Selenium. *J. Toxicol. Clin. Toxicol.* **1999**, *37*, 145–72.
- (42) Conde, J. E.; Sanz Alaejos, M. Selenium concentrations in natural and environmental waters. *Chem. Rev.* **1997**, *97*, 1979–2004.
- (43) Frankenberger, W. T.; Arshad, M. Bioremediation of selenium-contaminated sediments and water. *Biofactors* **2001**, *14*, 241–54.
- (44) Macy, J. M.; Lawson, S.; Demoll-decker, H. Bioremediation of selenium oxyanions in San Joaquin drainage water using *Thauera selenatis* in a biological reactor system. *Appl. Microbiol. Biotechnol.* **1993**, *40*, 588–594.
- (45) Chen, Y.-W.; Truong, H.-Y. T.; Belzile, N. Abiotic formation of elemental selenium and role of iron oxide surfaces. *Chemosphere* **2009**, *74*, 1079–84.
- (46) Dowdle, P. R.; Oremland, R. S. Microbial oxidation of elemental selenium in soil slurries and bacterial cultures. *Environ. Sci. Technol.* **1998**, *32*, 3749–3755.
- (47) Myneni, S. C. B.; Tokunaga, T. K.; Brown Jr., G. E. Abiotic selenium redox transformations in presence of Fe(II,III) oxides. *Science* **2011**, *278*, 1106–1109.
- (48) Fukushi, K.; Sverjensky, D. a. A surface complexation model for sulfate and selenate on iron oxides consistent with spectroscopic and theoretical molecular evidence. *Geochim. Cosmochim. Acta* **2007**, *71*, 1–24.
- (49) Jordan, N.; Ritter, a.; Foerstendorf, H.; Scheinost, a. C.; Weiß, S.; Heim, K.; Grenzer, J.; Mücklich, A.; Reuther, H. Adsorption mechanism of selenium(VI) onto maghemite. *Geochim. Cosmochim. Acta* **2013**, *103*, 63–75.
- (50) Ginocchio, R.; Sánchez, P.; de la Fuente, L. M.; Camus, I.; Bustamante, E.; Silva, Y.; Urrestarazu, P.; Torres, J. C.; Rodríguez, P. H. Agricultural soils spiked with

copper mine wastes and copper concentrate: implications for copper bioavailability and bioaccumulation. *Environ. Toxicol. Chem.* **2006**, *25*, 712–8.

- (51) Mighall, T. M.; Abrahams, P. W.; Grattan, J. P.; Hayes, D.; Timberlake, S.; Forsyth, S. Geochemical evidence for atmospheric pollution derived from prehistoric copper mining at Copa Hill, Cwmystwyth, mid-Wales, UK. *Sci. Total Environ.* **2002**, *292*, 69–80.
- (52) Stern, B. R.; Solioz, M.; Krewski, D.; Aggett, P.; Aw, T.-C.; Baker, S.; Crump, K.; Dourson, M.; Haber, L.; Hertzberg, R.; Keen, C.; Meek, B.; Rudenko, L.; Schoeny, R.; Slob, W.; Starr, T. Copper and human health: biochemistry, genetics, and strategies for modeling dose-response relationships. *J. Toxicol. Environ. Health. B. Crit. Rev.* **2007**, *10*, 157–222.
- (53) Grattan, J. P.; Gilbertson, D. D.; Hunt, C. O. The local and global dimensions of metalliferous pollution derived from a reconstruction of an eight thousand year record of copper smelting and mining at a desert-mountain frontier in southern Jordan. *J. Archaeol. Sci.* **2007**, *34*, 83–110.
- (54) Cornell, R. M.; Schwertmann, U. *The Iron Oxides: Structure, Properties, Reactions, Occurrences and Uses*; 2nd ed.; Wiley & Sons, 2003.
- (55) Beveridge, T. J.; Davies, J. A. Cellular responses of *Bacillus subtilis* and *Escherichia coli* to the Gram stain. *J. Bacteriol.* **1983**, *156*, 846–58.
- (56) Bartholomew, J. W.; Mittwer, T. The Gram stain. *Bacteriol. Rev.* **1952**, *16*, 1–29.
- (57) Cox, J. S.; Smith, D. S.; Warren, L. a; Ferris, F. G. Characterizing heterogeneous bacterial surface functional groups using discrete affinity spectra for proton binding. *Environ. Sci. Technol.* **1999**, *33*, 4514–4521.
- (58) Yee, N.; Fein, J. B. Quantifying metal adsorption onto bacteria mixtures : A test and application of the surface complexation model. *Geomicrobiol. J.* **2003**, *20*, 43–60.
- (59) Borrok, D. A universal surface complexation framework for modeling proton binding onto bacterial surfaces in geologic settings. *Am. J. Sci.* **2005**, *305*, 826–853.
- (60) Dzombak, D. A.; Morel, F. M. M. *Surface Complexation Modeling, Hydrous Ferric Oxide*; Wiley Interscience: New York, 1990.
- (61) Daughney, C. J.; Fein, J. B.; Yee, N. A comparison of the thermodynamics of metal adsorption onto two common bacteria. *Chem. Geol.* **1998**, *144*, 161–176.

- (62) Westall, J. C. FITEQL: A computer program for the determination of chemical equilibrium constants from experimental data **1982**, Report 82-01.
- (63) Daughney, C. J.; Châtellier, X.; Chan, A.; Kenward, P.; Fortin, D.; Suttle, C. A.; Fowle, D. A. Adsorption and precipitation of iron from seawater on a marine bacteriophage (PWH3A-P1). *Mar. Chem.* **2004**, *91*, 101–115.
- (64) Ohshima, H.; Kondo, T. On the electrophoretic mobility of biological cells. *Biophys. Chem.* **1991**, *39*, 191–8.

CHAPTER 2

SELENATE ADSORPTION TO *ESCHERICHIA COLI* AND IRON OXIDE COMPOSITES DURING THE ADDITION, OXIDATION, AND HYDROLYSIS OF FE(II)_{AQ} TO FE(III) OXIDE

2.1 Introduction

The cycling of metal and metalloid ions in aqueous systems can be strongly affected by adsorption onto bacterial cells and/or secondary mineral surfaces. Bacterial surfaces are known to have high affinities for adsorption of many different metal(loid)s.¹⁻⁹ Likewise, secondary iron oxide minerals, which are of interest in this study, are also known to have high affinities for adsorption of many different metal(loid) ions.¹⁰⁻¹⁵ Bacterial cells and secondary minerals such as iron oxides are among the most important metal(loid) sorbents in near-surface fluid/rock systems, not just because of their adsorptive capacities, but also because they typically account for a large proportion of the reactive surface area exposed to solution, being both commonly occurring and typically present as coatings on primary mineral grains.

To date there have been surprisingly few studies that have investigated metal(loid) partitioning in the presence of mixtures of bacteria and minerals, even though this is the expected norm in nature (Table 2.1). The earliest studies evaluated metal adsorption onto composites having a single bacteria-to-mineral mass ratio. One series of experiments investigated adsorption of Cd²⁺, Pb²⁺ or Sr²⁺ by natural bacteria-iron oxide composites or synthetic equivalents incorporating a single species of *Bacillus*, *Escherichia* or *Shewanella*.¹⁶⁻²⁰ These studies reported that the metals investigated adsorbed preferentially to the bacterial component under the experimental conditions employed. Metal ion adsorption in these systems was observed to be non-additive, i.e. a significant decrease in adsorption onto the composites was observed relative to the end-member sorbents, which was interpreted to arise from masking of the bacterial

adsorption sites by the iron oxide particles. A second series of experiments investigated the adsorption of Pb^{2+} by composites of iron oxide and *Burkholderia cepacia*.^{21,22} These studies reported that Pb^{2+} adsorption was dominated by the mineral component above pH 6 with adsorption to the bacteria only appreciable at lower pH. These studies did not identify any significant non-additivity, suggesting that there was no masking of bacterial or mineral adsorption sites within the composite under the experimental conditions employed.

Recent studies have evaluated metal adsorption onto composites with various bacteria-to-mineral mass ratios. One such study evaluated Cu^{2+} and Zn^{2+} adsorption onto composites with various ratios of *P. putida* to goethite.²³ This study also evaluated the effect of viable versus non-viable cells. This study reported no significant departure from additivity for metal adsorption by the composites and also noted greater metal adsorption to composites containing living compared to non-living cells. A study by Song et al. evaluated Cd^{2+} adsorption onto composites with ferrihydrite-to-bacteria dry weight ratios of 10, 2, 1 and 0.2.²⁴ Non-additivity was detectable but only decreased Cd^{2+} adsorption by up to 10% compared to the additivity prediction. Moon and Peacock studied Cu^{2+} adsorption onto composites of ferrihydrite and *B. subtilis* having mass ratios of ca. 80:20, 60:40 and 30:70.^{25,26} These studies found that the bacterial fraction dominated Cu^{2+} adsorption onto the composites at low pH whereas the ferrihydrite fraction dominated at high pH, although the bacterial fraction became important at high pH as the biomass content of the composite was increased. Moon and Peacock reported that Cu^{2+} adsorption onto composites composed mainly of ferrihydrite deviated slightly from the prediction of additivity but the deviation was not larger than the predictive uncertainty of the additive model. In contrast, Moon and Peacock reported that Cu^{2+} adsorption by composites composed mainly of bacteria was significantly less than predicted by the additive model, which the authors proposed arose from physicochemical interactions between the bacteria and the mineral that altered their surface charges.

All of the above-listed studies were conducted with iron oxide minerals that were prepared abiotically (in the absence of bacteria) then mixed together with the cells to form the composites that were used in the experiments with the exception of Martinez et al. (2004) who used naturally formed bacteriogenic iron oxides. Typically the iron oxides were prepared by the abiotic hydrolysis of Fe(III), aged, mixed with the bacterial cells and only then was the composite exposed to the dissolved metal. In contrast, Daughney et al. (2011) evaluated adsorption of Cd^{2+} to *Anoxybacillus flavithermus*-iron oxide composites during the addition, oxidation, hydrolysis and precipitation of $\text{Fe(II)}_{\text{aq}}$. The authors observed that iron oxide precipitation was delayed at low Fe/bacteria ratios, and that Cd^{2+} sorption decreased at mid-range Fe/bacteria ratios, which was followed by increased sorption at high Fe/bacteria ratios. These results were interpreted to reveal competition between Fe^{2+} and Cd^{2+} for the bacterial surface sites. Increasing non-additivity was observed with increasing precipitation of iron oxide minerals, which the authors inferred to indicate progressive masking of the bacterial surface sites by the mineral particles.

Clearly there is currently a gap in knowledge of whether and to what extent the ion adsorption is additive and whether models that have been developed for single-sorbent systems can be used to predict ion adsorption onto mixtures of sorbents. The current lack of understanding arises in part because the previous studies have used different experimental procedures and making direct comparisons difficult. Previous studies have used different bacterial species and so results may not be directly comparable for this reason as well. Also previous studies have used only a few different metal cations and no studies have been performed with anions or oxyanions.

This study tracks the adsorption of dissolved selenate (SeO_4^{2-}) onto composites of iron oxide and *Escherichia coli* during the addition, oxidation, hydrolysis and precipitation of $\text{Fe(II)}_{\text{aq}}$. *E. coli* was chosen as because it is a Gram negative bacterium with well characterized surface properties.^{2,3,27} In this study the iron oxides are formed by the introduction, oxidation, hydrolysis

and precipitation of Fe(II) in order to allow comparison with Daughney et al. (2011) and Fakih et al. (2008). This approach allows SeO_4^{2-} adsorption to be tracked as the bacteria/mineral concentration ratio is gradually altered as a result of progressive oxidation of $\text{Fe(II)}_{\text{aq}}$ and concomitant precipitation of the iron oxides. SeO_4^{2-} was selected as the sorbate in part because of its environmental importance, given that it is toxic in relatively low doses and is more mobile than selenite (SeO_3^{2-}).^{27,28} In addition, SeO_4^{2-} was selected for this study because, as an oxyanion, it provides an excellent complement to the previous studies, all of which have all been performed with cations (Table 2.1). Specifically, SeO_4^{2-} is anticipated to have higher adsorptive affinity for the iron oxide and almost no adsorptive affinity for the bacteria, whereas the previously studied metal cations have all displayed the opposite affinity behavior. Hence we hypothesize that our study with SeO_4^{2-} will evaluate whether the bacterial cells interfere with adsorption onto the mineral, as compared to previous studies which have only been able to evaluate whether the mineral interferes with adsorption onto the bacteria. In this regard, the overall aim of this study is to contribute to understanding of the origin of non-additivity in ion adsorption that has been observed in some studies conducted with bacteria-iron oxide composites.

2.2 Methods

2.2.1 Bacterial growth conditions

Suspensions of *E. coli* AB264 (CGSC) were pre-cultured in 20 mL volumes of autoclaved (121°C, 60 min) trypticase soy broth (TSB). After 24 h of growth at 27°C, a 700 mL volume of autoclaved TSB was inoculated with 20 mL of the pre-cultured bacteria and placed in a shaking incubator for 24 h (27°C, 120 rpm) until late stationary phase. The cultures were then rinsed five times with 0.01 M NaNO_3 , which was the background electrolyte used in this study. The bacteria were recovered through centrifugation (1600 g, 10 min) and the supernatant was discarded after each rinse. The bacteria were re-suspended in 0.01 M NaNO_3 to give a biomass concentration of 0.44 dry g/l, based on measurements of optical density at 600 nm (OD_{600}) (see below). Electron microscopy was used to determine that the cells prepared in this manner were

intact. Cell metabolic state and viability were not evaluated. These growth and rinsing procedures were similar to those used in prior studies by Burnett et al. (2006), Burnett et al. (2007) and references therein.

The relationship between OD₆₀₀ and *E. coli* dry weight was determined through the growth of multiple separate cultures which were diluted with 0.01 M NaNO₃ to give a range of OD₆₀₀ values between 0.1-0.8. These cultures were then vacuum filtered onto pre-weighed 0.45 µm cellulose-acetate filters, rinsed with MilliQ water to remove the residual electrolyte, and dried at 60°C. Once the filtered cultures reached a constant weight (~24 h), the dry weights of the cultures were recorded. A linear regression was used to calculate the dry weight concentration of all cultures used in this study (Dry weight (g/L) = 0.6528 × OD₆₀₀, R² = 0.9657, OD₆₀₀ < 0.8, n = 37).

2.2.2 Synthesis of abiotic iron oxides

For the remainder of this paper, the minerals synthesized in the absence of bacterial cells will be referred to as abiotic iron oxides. Abiotic iron oxides were synthesized from a starting solution of 400 mL 0.01 M NaNO₃ that had been adjusted to pH 6. 48.00 ml of FeCl₂ solution ([FeCl₂]=1.25×10⁻² M, [HCl]=2.50×10⁻³ M, [NaNO₃]=0.01 M) were added at a constant rate of 0.12 mL/min (New Era syringe pump model NE-1000, Farmingdale, USA) over 6.66 h. This solution was aged for up to 24 h (including the period of addition of the FeCl₂ solution). Throughout the synthesis and aging of the iron oxides, the suspension was stirred and left open to the atmosphere, and a constant pH 6 was maintained by addition of NaOH solution ([NaOH]=0.03 M, [NaNO₃]=0.01 M) using a pH-stat automatic titrator (Radiometer Analytical model TIM 854, Lyon, France). This method has been used in prior studies to synthesize abiotic iron oxides.³⁰⁻³² This protocol leads to the formation of lepidocrocite, although mineral properties may differ in bacteria-bearing systems relative to the abiotic case, and so throughout this paper the term “iron oxide” is used generically without reference to crystallinity, particle size,

morphology or other properties. The surface area of the abiotic iron oxides, after 24 h aging in suspension, was determined through BET analysis to be 301 m²/g (n=3).

2.2.3 Synthesis of bacteria-iron oxide composites

For the remainder of this paper, the minerals synthesized in the presence of bacterial cells will be referred to as biotic iron oxides. Composites of *E. coli* and biotic iron oxide were prepared using the same method as for the synthesis of the abiotic iron oxides, except that the initial 400 mL of 0.01 M NaNO₃ contained bacterial cells at a concentration of 0.44 dry g/L. A similar procedure for preparation of bacteria-iron oxide composites was used by Daughney et al. (2011). The BET technique was not suitable for measurement of the surface area of the bacteria-iron oxide composites; this limitation is discussed below.

2.2.4 Adsorption to bacteria or iron oxide as a function of pH, selenate/sorbent ratio, and time

SeO₄²⁻ adsorption onto abiotic iron oxide (no bacteria present) was evaluated from pH 3 to 8 using three different SeO₄²⁻ to sorbent concentration ratios and a background electrolyte of 0.01 M NaNO₃. The abiotic iron oxide suspensions were synthesized as stated above, at pH 6, with constant stirring and in contact with the atmosphere. After aging for 24 h (including the period of addition of the FeCl₂ solution), the suspension was divided into three open glass beakers, resulting in three 200 mL suspensions after selenate addition having concentrations of 0.101 g/L, 0.054 g/L and 0.025 g/L iron oxide. To give a total concentration of 3 ppm and volume of 200 mL, 13.83 mL of a stock solution (43.4 ppm Na₂SeO₄, 0.01 M NaNO₃) was added to each suspension. These three suspensions were then adjusted to pH 3 by dropwise addition of HNO₃. The suspensions were allowed to equilibrate for 30 min with continuous stirring under an open atmosphere, after which 2 mL samples were taken from each suspension. The samples were centrifuged at 13200 g for 15 min, then the supernatant was acidified with 1% HNO₃ and analyzed by inductively couple plasma-optical emission spectroscopy (ICPOES) for [Se_{TOT}]_{aq} and [Fe_{TOT}]_{aq}. After sampling the pH in each of the three beakers was adjusted upwards by 0.5 units

by dropwise addition of NaOH and allowed to equilibrate for another 30 min, whereupon a second sample was collected, centrifuged and analyzed by ICPOES. This procedure of pH adjustment, sampling and analysis was repeated until an endpoint of pH 8 was reached. These experiments were repeated in triplicate and were also run from an initial pH of 8 to a final pH of 3 in order to identify any adsorption hysteresis or any aging effects.

An analogous procedure was used to evaluate SeO_4^{2-} adsorption onto the bacteria (no iron oxide present). Bacteria were cultured and rinsed as described above and used to prepare three 200 ml cell suspensions with concentrations of 0.44, 0.22 and 0.11 dry g/L in a background electrolyte of 0.01 M NaNO_3 . 0.85 mL of a stock solution (42.6 ppm Na_2SeO_4 , 0.01M NaNO_3) was added to each suspension to give a total concentration of 3 ppm and a total concentration of 200 mL. The pH was adjusted from 3 to 8 or from 8 to 3 in increments of 0.5 pH units, with 30 min equilibration and constant stirring under an open atmosphere at each pH point, followed by sampling, centrifugation and analysis by ICPOES as described above.

Kinetic adsorption experiments were also conducted. These experiments were conducted at pH 4, for which the pH experiments indicated significant SeO_4^{2-} adsorption to the iron oxide but no adsorption to the bacterial cells. These pH conditions were selected to interrogate the effects of the bacteria on ion adsorption to the mineral, for comparison with previous studies that have all evaluated the effect of the mineral on ion adsorption by the bacteria. Suspensions containing either iron oxide (0.108 g/L) or bacteria (0.44 dry g/L) were prepared as described above, spiked with the stock solution to give $[\text{Se}_{\text{TOT}}] = 3$ ppm, adjusted to pH 4 and equilibrated with constant stirring under an open atmosphere. A 2 mL sample was extracted every 30 min over 7 h, followed by centrifugation and ICPOES analysis as described above.

2.2.5 Selenate adsorption during the synthesis of abiotic iron oxides or bacteria-iron oxide composite

The SeO_4^{2-} adsorption experiments described above were all conducted *after* the sorbent had aged for 24 h. In contrast, the experiments described below were used to track the fate of SeO_4^{2-} *during* the synthesis and aging of the sorbents. SeO_4^{2-} adsorption was evaluated in three systems: bacteria only with no added iron; abiotic iron oxide without bacteria; and bacteria-iron oxide composites. Each system was investigated in triplicate using independently prepared batches of the sorbent (including independent cultures of the bacteria in the biotic systems) and all tables and graphs depict the average and standard deviation of the three replicate values.

All syntheses were initiated with 400 mL of 0.01 M NaNO_3 , continuously stirred in a glass beaker that was left open to the atmosphere. For the experiments that involved the bacteria alone or the bacteria-iron oxide composites, this 400 mL volume contained rinsed *E. coli* cells at a biomass concentration of 0.44 dry g/l; for the experiments conducted with the abiotic iron oxide, this 400 mL solution was free of bacteria. For all experiments this starting solution or suspension was adjusted to pH 6. As per the protocol described above, 48.0 mL of a solution were added to the beaker at a constant rate of 0.12 mL/min while maintaining the suspension at pH 6. For the experiments involving the abiotic iron oxide or the bacteria-iron oxide composites, this solution contained $[\text{FeCl}_2]=1.25 \times 10^{-2}$ M, $[\text{HCl}]=2.50 \times 10^{-3}$ M and $[\text{NaNO}_3]=0.01$ M. For the experiments that involved the bacteria in the absence of iron, this solution contained $[\text{HCl}]=2.50 \times 10^{-3}$ M and $[\text{NaNO}_3]=0.01$ M.

For all experiments, two samples (2 mL and 15 mL) of the suspension were collected every 60 min for 10 h and a final sample was collected after 24 h. The 2 mL sample was immediately centrifuged (13200 g, 15 min) and the supernatant was analyzed using 1,10-phenanthroline, a colorimetric indicator for $\text{Fe(II)}_{\text{aq}}$. The 15 mL sample was spiked with a solution of sodium selenate (50 ppm Na_2SeO_4 , 0.01 M NaNO_3) to give a final $[\text{SeO}_4]_{\text{TOT}}$ of 3 ppm. The sample was then equilibrated for 2 h at pH 4 ± 0.03 by small additions (5-10 μL) of 0.1

M, 0.01 M, or 0.001 M HNO₃ or NaOH, and stirred continuously while open to the atmosphere. The 2 h equilibration time was selected on the basis of the kinetics experiments (see below). After the 2 h equilibration, the 15 mL sample was divided into three subsamples. One 2 mL subsample was centrifuged (13200 g, 15 min) and the supernatant was analyzed for [Fe(II)]_{aq} using 1,10-phenanthroline. A second 2 mL subsample was centrifuged (13200 g, 2 min), half the supernatant was discarded, then 2.5% glutaraldehyde was added to give a volume ratio of 1:1 for sample relative to glutaraldehyde solution. These samples were stored at 4°C for subsequent analysis by electron microscopy (see below). An ethanol dehydration series was not done to dry the samples as an environmental scanning electron microscope (ESEM) was used so drying was unnecessary. The third 2 mL subsample was centrifuged (13200 g, 15 min) and the supernatant was acidified with 1% HNO₃ and analyzed for [Fe_{TOT}]_{aq} and [Se_{TOT}]_{aq} using ICPOES. The solid (pellet) from the third subsample was digested in 0.5 mL 5 M HCl and the acid digest was analyzed using the ferrozine method and ICPOES for [Fe(II)]/[Fe(III)] in the solid phase.^{33,34}

The sampling and analytical regime described above was used to allow tracking of Se and Fe throughout the experiments. Notably, one subsample was analyzed for [Fe(II)]_{aq} immediately after collection of each 15 mL sample of the suspension, before the addition of SeO₄²⁻, and another subsample was analyzed for Fe(II)_{aq} after 2 h of equilibration with SeO₄²⁻. Comparison of the [Fe(II)]_{aq} in these two subsamples was used to quantify the amount of iron oxide that had precipitated while SeO₄²⁻ was present. This fraction of iron oxide could potentially remove SeO₄²⁻ from solution via co-precipitation, as has been observed for PO₄³⁻ (Châtellier et al., 2013), whereas the remaining fraction of iron oxide was presumed to be capable of SeO₄²⁻ removal only via adsorption.

2.2.6 Electron microscopy

Samples for scanning electron microscopy (SEM) were prepared as stated previously. Back scatter (BSE) and secondary electron (SE) images of uncoated samples were taken under low vacuum pressure (~80 Pa) at 10.0 kV using a field emission-environmental scanning electron

microscope (FE-ESEM) (FEI Quanta200F).^{35–37} Elemental composition was investigated using energy dispersive X-ray (EDX) spectroscopy of the solids.

Samples for transmission electron microscopy (TEM) were initially prepared in the same manner as for SEM analysis but were stored at 4°C until all replicates were completed. These samples were then shipped to McMaster University, Hamilton, ON, Canada and prepared for analysis.³⁵ The main fixative used was 0.2 M glutaraldehyde in a 0.1 M phosphate buffer (pH 6.8). The samples were rinsed twice in the buffer solution and fixed in 1% osmium tetroxide in 0.1 M phosphate buffer for 1 h. The samples were then dehydrated through a graded ethanol series with the final dehydration in 100% propylene oxide. Samples were infiltrated with Spurr's resin in a series, rotating samples between solution changes. The samples were then transferred to molds and filled with Spurr's resin and polymerized at 60°C overnight. Thin sections were cut on a Leica UCT Ultramicrotome and put on uncoated and Formvar-coated grids. Formvar-coated samples were then examined using field emission TEM (FEI Titan 80-300). Bright field (BF) images were collected at 300 kV and EDX spectra were collected in scanning TEM mode at a probe size of 1 nm.

2.2.7 Modeling

Surface complexation models (SCMs) were developed using FITMOD (Daughney et al., 2004), a modified version of FITEQL 2.0 (Westall, 1982). All SCMs incorporated equilibrium reactions to describe the dissociation of water, acid, base, and the electrolyte used in this study (0.01M NaNO₃). All SCMs also included equilibrium reactions for SeO₄²⁻ and Fe²⁺ hydrolysis, reactions with electrolyte ions, and reactions with dissolved carbonate. All stability constants were taken from the MINTEQ database (Visual MINTEQ Version 3.0). All stability constants were adjusted for ionic strength using the Davies equation and all values tabulated in this paper were referenced to zero ionic strength, zero surface charge and 25°C.⁴⁰

Models of SeO_4^{2-} adsorption onto iron oxides were based on the triple layer SCMs compiled by Fukushima and Sverjenski (2007) with incorporation of CO_2 adsorption based on the SCMs of Villalobos and Leckie (2001) (Table 2.2). The iron oxide was assumed to display one type of amphoteric surface site, denoted here as $\equiv\text{FeOH}$. Concentrations of iron oxide in the experimental systems were calculated based on the known volume of FeCl_2 solution that had been added at any given time point, in combination with the measured concentration of $\text{Fe(II)}_{\text{aq}}$ and assuming a gram formula weight of 88.85 g/mol for the precipitated iron oxide. It was also assumed that the iron oxide has capacitance values of 1.0 and 0.2 F/m^2 for the 0 and B planes, respectively, after Fukushima and Sverjenski (2007) and a surface area of 301 m^2/g based on the BET measurements of the aged abiotic iron oxide made in this study. The surface area value agrees well with prior studies in similar systems.^{26,31,41} However, we acknowledge the limitation of assuming that the surface area is constant at all time points and is equal in the abiotic and biotic systems (see discussion below).

SCMs for the bacterial cells were based on the non-electrostatic models of Borrok et al. (2005) and Johnson et al. (2007). These models define four types of cell wall functional groups, denoted as R_1 , R_2 , R_3 and R_4 , where R represents the cell wall to which the functional group is attached (Table 2.3). As will be shown below, the results of this study did not reveal any SeO_4^{2-} adsorption onto the cells, and hence corresponding reactions are not incorporated into the SCMs. However, bacterial surfaces are known to interact with protons and potentially Fe^{2+} (Daughney et al., 2011) and are therefore included in the SCMs developed in this study in order to account for any possible indirect effects on SeO_4^{2-} adsorption onto the bacteria-iron oxide composites.

Optimization of the SCMs was achieved using FITMOD, which like FITEQL calculates the variance $V(Y)$ as a measure of goodness of model fit:

$$V(Y) = \frac{\sum_{P,Q} \left(\frac{Y}{s_Y}\right)^2}{n_P \times n_Q - n_R} \quad (\text{Equation 2.1})$$

in which Y was the difference between the model and experimental mass balance over all data points P and all components Q for which both total and free concentration were known. The standard deviation s_Y was calculated by propagation of the estimated experimental errors associated with the determination of total and free concentrations. The sum of squares of the weighted error Y/s_Y was normalized to the degrees of freedom in the system as determined from the total number of data points (n_P), the number of components for which the total and free concentrations were known (n_Q) and the number of parameters optimized in the model (n_R). Our general approach was to fix the stability constants at the values compiled in Tables 2.2 and 2.3 and optimize the total concentration of adsorption sites. A variance of less than 10 was interpreted as a good fit, with $V(Y)$ of 1 being the ideal where the experimental and model errors are equal.^{30,38,39}

2.3 Results and discussion

2.3.1 Selenate adsorption to bacterial cells

No SeO_4^{2-} adsorption to bacteria was observed at any pH, biomass concentration, or reaction time used in this study. For comparison, a prior study by Kenward et al. (2006) reported adsorption of approximately 12% of a total concentration of 0.1 M selenate (~ 1.2 M or $\sim 9.5 \times 10^4$ ppm) at pH 4 with 1 dry g/L *Shewanella putrefaciens* in 0.001 M NaCl. These authors further reported that the extent of adsorption decreased with increasing ionic strength. The present study had 0.44 g/L *E. coli* at pH 4 in 0.01 M NaNO_3 and so, based on the study of Kenward et al. (2006), approximately 6% adsorption or less would be expected.

As an example, the results of the kinetic experiments are displayed in Figure 2.1. These results suggest ‘negative’ sorption of ca. 5% throughout the duration of the experiment. This could be interpreted as release of SeO_4^{2-} from the cells, such that the supernatants contained concentrations in excess of the $[\text{SeO}_4]_{\text{TOT}}$ that was added during the experiments. However, we interpret this result to indicate an analytical bias that is introduced by exudates released by the

bacteria during the equilibration period. This matrix effect was validated by comparing ICPOES results for Se standards that had been prepared in supernatants from the bacterial suspensions in contrast to Se standards that had been prepared in 0.01 M NaNO₃.

2.3.2 Selenate adsorption to abiotic iron oxides

At pH 4, SeO₄²⁻ adsorption to the abiotic iron oxide increased from 37.7±8.2% at 0.5 h to 45.4±6.6% at 7.0 h (Fig. 2.1). Hence all experimental results were indistinguishable within the measurement standard deviation. An equilibration time of 2 h was selected for convenience and used for all subsequent SeO₄²⁻ adsorption experiments.

SeO₄²⁻ adsorption was observed to decrease with increasing pH and increasing ratio of [SeO₄]_{aq} to mineral concentration (Fig. 2.2). These results are consistent with previous work¹⁴. In addition, the direction of pH adjustment used in the experiments had no influence on the extent of SeO₄²⁻ adsorption. This pH reversibility indicated that there were no effects of aging apparent within the initial 24 h period under the conditions of this study, and that an equilibrium framework would be appropriate for modeling. A pH of 4 was chosen for subsequent experiments because it corresponded to SeO₄²⁻ adsorption of 47.4±5.2%, which would allow for the greatest sensitivity in detecting either increased or decreased adsorption onto the bacteria-iron oxide composites relative to the abiotic case.

A SCM was developed to fit all of the data from the experiments that investigated the effect of pH on SeO₄²⁻ adsorption. This SCM employed the stability constants and other system characteristics listed in Table 2.2. The only adjustable parameter was the total concentration of surface sites, [≡FeOH]_{TOT}. The best-fitting model had [≡FeOH]_{TOT} = 4.70×10⁻⁵ mol/l and V(Y) = 2.35 and was considered to provide an acceptable fit to the experimental data. Given a surface area of 301 m²/g as determined by BET analysis, this surface site concentration equates to a site density of 4.7×10⁻⁴ mol sites/g iron oxide (0.94 sites/nm²). Previously site densities have been calculated to be higher, Fukushima et al. (2007) reported densities of 3.8 sites/nm² for the four

studies which they reviewed on selenate adsorption onto hydrous ferric oxide. The site densities calculated in this study were likely lower as the iron oxides synthesized were used immediately without rinsing and precipitated at a lower pH than most prior work (pH 6 versus pH 6.5 or 7) which would affect the iron oxide phase formed and therefore the surface site concentration.

Iron exhibited complex behavior during the synthesis of the abiotic iron oxides. All Fe in the solid phase was found to be present as Fe(III), based on the Ferrozine method after acid digestion of the solid which was done immediately after the sample was centrifuged (13200 g, 15 min).^{33,34} In contrast, all Fe in the aqueous phase was found to be present as Fe(II). For aqueous samples analyzed prior to the addition of SeO_4^{2-} , the $[\text{Fe(II)}]_{\text{aq}}$ increased from 0.0 ppm at 0 h to a maximum of 17.5 ± 7.8 ppm at 2 h, then decreased again to 0.0 ppm at 24 h (Fig. 3). A very similar pattern was observed for samples analyzed after 2 h equilibration with SeO_4^{2-} , in which a peak $[\text{Fe(II)}]_{\text{aq}}$ of 15.7 ± 5.3 was reached after 2 h. Indeed, at every time point, the $[\text{Fe(II)}]_{\text{aq}}$ were indistinguishable for samples collected before and after equilibration with SeO_4^{2-} . This important result shows that there was essentially no precipitation of iron oxide during the period of equilibration with SeO_4^{2-} , meaning that it is unlikely that any SeO_4^{2-} removal from solution occurred as a result of co-precipitation. In comparison, Châtellier et al. (2013) observed that substantial levels of PO_4^{3-} were incorporated into iron oxide formed as a result of $\text{Fe(II)}_{\text{aq}}$ oxidation and precipitation, albeit under different experimental conditions than used in the present study. Further, Châtellier et al. (2013) determined that PO_4^{3-} co-precipitation could affect the reaction kinetics and the mineralogy, particle size and stability of the iron oxides formed. While such effects might occur due to SeO_4^{2-} co-precipitation with iron oxides under some conditions, they can be ruled out as possible influences in our experiments simply because no iron oxide was precipitating while SeO_4^{2-} was present. Hence we conclude that, for the abiotic system at least, SeO_4^{2-} removal from solution only occurs due to adsorption.

Figure 2.4 displays the behavior of Se during the synthesis of the abiotic iron oxides. SeO_4^{2-} adsorption onto the abiotic iron oxide was 0.0% at 0 h, followed by an increase to a maximum of $71.4 \pm 6.5\%$ at 8 h, followed by a decrease to $47.3 \pm 7.6\%$ at 24 h. The increasing SeO_4^{2-} removal observed over the first 8 h can be attributed to the fact that the FeCl_2 solution was added at a constant rate over the first 6.66 h of the synthesis, and progressive precipitation of the introduced iron led to an increasing concentration of $\equiv\text{FeOH}$ sites in the system. The decrease in sorption after 8 h was interpreted to arise from aggregation and/or densification of the iron oxide during aging, leading to a decrease in $\equiv\text{FeOH}$ sites available for adsorption of SeO_4^{2-} . A comparison of the SeO_4^{2-} adsorption observed in Figs. 1, 2 and 4 supports the interpretation that the concentration of available $\equiv\text{FeOH}$ surface sites declines with time. Under comparable conditions, the kinetic experiments (Fig. 2.1) and the pH experiments (Fig. 2.2) revealed a similar level of SeO_4^{2-} adsorption. These experiments were both conducted with abiotic iron oxide that had been precipitated and aged for 24 h. In contrast, during the synthesis of the iron oxides, i.e. with little or no aging, there was a comparatively greater level of SeO_4^{2-} removal, consistent with a greater concentration of $\equiv\text{FeOH}$ surface sites, which in turn is consistent with less aggregation of the solid at short synthesis times.

A SCM was developed for SeO_4^{2-} adsorption during the synthesis of the abiotic iron oxides. Initially, the surface site density was assumed to be 4.7×10^{-4} mol sites/g for all time points (assuming a surface area of $301 \text{ m}^2/\text{g}$), based on the SCM that had been optimized to fit the data from the pH experiments. This model produced a reasonable fit with $V(Y) = 2.83$. However, visual comparison to the data revealed that this model under-predicted the SeO_4^{2-} adsorption for the 0 to 10 h time points and over-predicted the SeO_4^{2-} adsorption for the 24 h time point (Fig. 2.4). The SCM was subsequently refined by individually optimizing the $[\equiv\text{FeOH}]_{\text{TOT}}$ concentration for each time point. The optimized surface site densities (again assuming a surface area of $301 \text{ m}^2/\text{g}$ for all time points) ranged from $5.5 \pm 0.6 \times 10^{-4}$ mol sites/g iron oxide at the 3 h

time point to $2.3 \pm 0.2 \times 10^{-4}$ mol sites/g iron oxide at the 24h time point (Fig. 2.5). For comparison, the pH experiments conducted abiotic iron oxide that had been aged for 24h were best modeled with a surface site density of 4.7×10^{-4} mol sites/g iron oxide. We conclude that the difference in the optimized site density for the 24h time point arises because the model developed for the pH experiments was applied to a pH range of 3-8 and solid concentrations from 0.03 to 0.10 g/l, whereas the model developed for the 24h time point during the synthesis of the abiotic iron oxides only needed to fit data at pH 4 and a single solid concentration. Regardless of any differences between the different types of experiments conducted in this study, the modeling suggested that the abiotic iron oxides lost approximately 67% of their available surface sites during the 24 h period of synthesis. This is interpreted to arise from aggregation of the mineral particles.

2.3.3 Selenate adsorption to bacteria-iron oxide composites

For samples analyzed prior to the addition of the SeO_4^{2-} , the $\text{Fe}(\text{II})_{\text{aq}}$ increased from 0.0 ppm at 0 h to 18.3 ± 2.3 ppm at 2h and then decreased to 0.0 ± 0.4 ppm at 24 h (Fig. 2.3). Samples analyzed after the 2 h equilibration with SeO_4^{2-} followed a very similar pattern, with $[\text{Fe}(\text{II})]_{\text{aq}}$ reaching a maximum of 16.7 ± 1.0 ppm at 2 h (Fig. 2.3). Just as for the samples collected during the synthesis of the abiotic iron oxides, the comparison of $[\text{Fe}(\text{II})]_{\text{aq}}$ concentrations before and after the equilibration period revealed that no iron oxide was forming while SeO_4^{2-} was present. Again this indicates that any SeO_4^{2-} removal would be due to adsorption and not co-precipitation.

Higher concentrations of $[\text{Fe}(\text{II})]_{\text{aq}}$ were observed in the bacteria-bearing systems for the first several hours of the synthesis compared to the abiotic case (Fig. 2.3). This result suggested that the presence of the bacteria inhibited the rate of Fe(II) oxidation, possibly through adsorption of Fe(II) onto the cells and/or complexation of Fe(II) by bacterial exudates in solution. This interpretation was supported by Ferrozine analyses of the acid digested solid phase, which revealed a maximum of 5.8 ± 0.2 ppm Fe(II) in the solid phase at the 3 h time point, decreasing to

0 ppm Fe(II) in the solid phase at the 5 h time point (results not shown). Fakih et al. (2008) also reported that the presence of bacterial cells decreased the rate of Fe(II) oxidation, which was interpreted by the authors to arise from adsorption of Fe(II) by the cells or interactions with exudates in solution.

SeO_4^{2-} adsorption onto the bacteria-iron oxide composites increased from 0.0% at 0 h to a maximum of $45.4 \pm 3.8\%$ at 7 h and decreased to $16.5 \pm 6.9\%$ at 24 h, a similar pattern as observed in the abiotic case (Fig. 2.4). However, SeO_4^{2-} adsorption at all time points was consistently ca. 20% less in for the bacteria-iron oxide composites compared to the abiotic iron oxides. We interpret this as an indication that the bacterial cells mask a proportion of the iron oxide surface sites. We emphasize that identification of this effect is only possible by evaluating the behavior of a sorbate that has high affinity for the iron oxide but low affinity for the bacteria. In contrast, all previous studies of this type have been conducted with metal ions, which have high affinity for the bacteria but low affinity for the iron oxide under most experimental conditions employed.^{16,21,25,26,30} Hence, the combination of cation and anion adsorption data show that masking affects both sorbates: the mineral particles cause a reduction in the availability of bacterial adsorption sites and the bacteria cause a reduction in the availability of iron oxide adsorption sites.

A SCM was developed for SeO_4^{2-} adsorption during the synthesis of the bacteria-iron oxide composites. Initially, an SCM was optimized to fit the data by assuming a constant concentration of $[\equiv\text{FeOH}]_{\text{TOT}}$ for all time points. This model yielded an optimized $[\equiv\text{FeOH}]_{\text{TOT}}$ of 4.1×10^{-5} mol/l and a $V(Y)$ of 4.2 (Fig. 2.4). Assuming a surface area of $301 \text{ m}^2/\text{g}$, this surface site concentration translates to a site density of 3.8×10^{-4} mol sites/g. However, the visual fit of this model is poor, with under-estimation of SeO_4^{2-} removal at the shorter time points and over-estimation of SeO_4^{2-} removal at the later time points. Thus, following the approach presented above, the $[\equiv\text{FeOH}]_{\text{TOT}}$ was optimized individually for each time point (Fig. 2.5). This model

indicated that there were $2.2 \pm 4.3 \times 10^{-4}$ mol sites/g at 2 h, which then decreased to $1.5 \pm 0.3 \times 10^{-4}$ mol sites/g at 24 h (again assuming a surface area of $301 \text{ m}^2/\text{g}$ for all time points). This was the same trend as for the abiotic iron oxides however the composite samples had significantly more available surface sites until 7 h. Rancourt et al. (2005) also reported that iron oxides formed in the presence of bacteria have greater surface site density compared to the abiotic case, as a result of smaller particle size and greater crystallographic disorder. Rancourt et al. (2005) concluded that the smaller particle size and greater crystallographic disorder for biogenic iron oxides both result from stoppage of particle growth due to adsorption of organic compounds of bacterial origin.

2.3.4 Electron microscopy

SEM and TEM images of the bacteria-iron oxide composite over time depict the progressive formation of iron oxide (Figs. 2.6, 2.7, and 2.8). At 0 h only the bacterial cells were present with no added Fe and the characteristic rod-shaped *E. coli* cells were clearly visible (Fig. 2.6). After 1 h, there were small nodes of iron oxide present on the cells (Fig. 2.8). After 3 h of FeCl_2 addition a thin coating of Fe had begun to form over the cell surfaces which was verified through SEM-EDX ($6.6 \pm 0.4 \text{ wt\% Fe}$, $n=3$) and observed as an opaque layer partially obscuring and surrounding the cells. After 7 h the layer of Fe oxide was more pronounced and it was difficult to discern individual cells and loose aggregates of iron oxide were observed surrounding the cells as well as a nearly complete layer of iron oxide surrounding the cell surface. After 10 h the iron oxide had begun to aggregate into larger particles which were still associated with the bacterial cells and the layer of iron oxide was complete around the cells. At the last time point of 24 h, the iron oxides had condensed into still larger particles some of which had broken off the cells and were present in suspension. These images confirmed the hypothesis that as $\text{Fe(II)}_{\text{aq}}$ was added to the suspension it oxidized and precipitated as Fe(III) oxides which were closely associated with the bacterial cells and led to masking of iron oxide surface sites. These images also showed that the aggregation of the iron oxide particles increased with time.

2.4 Conclusions

This study has demonstrated that adsorption of SeO_4^{2-} onto iron oxide minerals is affected significantly by the presence of bacteria which, although SeO_4^{2-} was found not to adsorb to the cells, did affect adsorption through masking of iron oxide surface sites. The progressive addition of $\text{Fe(II)}_{\text{aq}}$ and its eventual precipitation as Fe(III)-oxides was not affected by the presence of SeO_4^{2-} . With increasing aging time, there was a decrease in SeO_4^{2-} adsorption arising from aggregation of the mineral in both the abiotic and composite systems and masking of iron oxide surface sites by bacterial cells in the composite system. This leads to the conclusion that metal oxyanion removal in the water-rock systems is significantly affected by the presence of various sorbents including iron oxide minerals and bacterial cells and also redox processes that occur including $\text{Fe(II)}_{\text{aq}}$ oxidation, hydrolysis, and precipitation.

There are still many various areas of research into metal(loid) cycling in near-surface water-rock systems that should be investigated. This study was the first to examine anion removal in the presence of mixtures of bacteria and minerals and so there is much more work to be done on various metal anion and oxyanion adsorption in the presence of composites. Also this is only the second study to explore metal(loid) removal during the addition of $\text{Fe(II)}_{\text{aq}}$ and the accompanying redox reactions leading to iron oxide precipitation. Currently the understanding of water-rock systems in nature is very basic and more complex studies, like this one, should be conducted to comprehend metal(loid) cycling in these systems.

Figure 2.1: SeO_4^{2-} adsorption to abiotic iron oxides (0.11 g/l, closed diamonds) or bacteria (0.44 g/l, open diamonds) at pH 4 as a function of time. $[\text{SeO}_4]_{\text{TOT}} = 3$ ppm for all data points. Error bars represent one standard deviation (n=3). ‘Negative’ adsorption observed for the experiments with bacteria is interpreted to arise from a matrix effect due to the presence of bacterial cells. Potentially the extracellular matrix of secreted by the cells caused this effect but cell exudates were not characterized as part of this study.

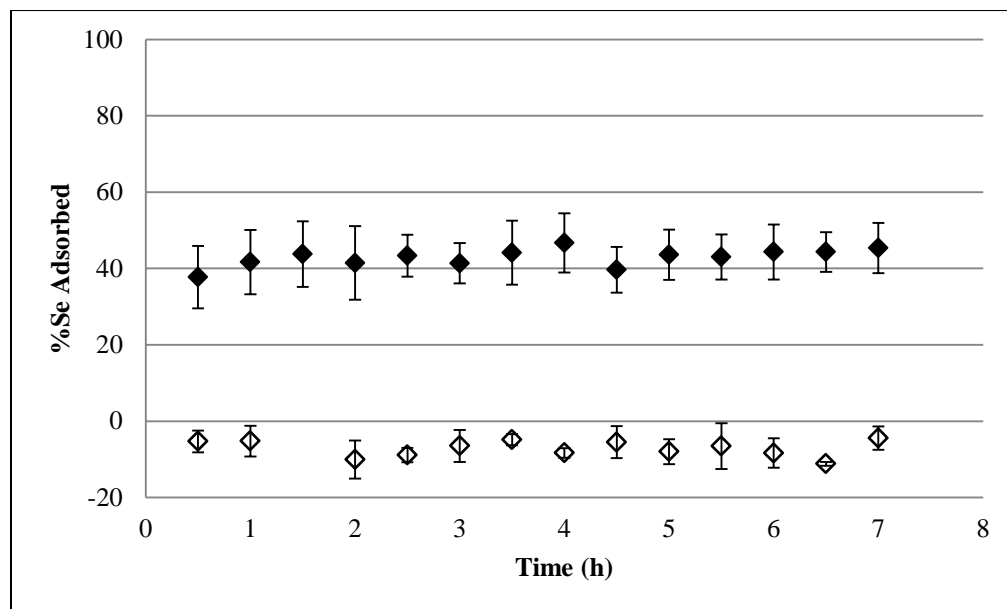


Figure 2.2: SeO_4^{2-} adsorption to abiotic iron oxides as a function of pH and sorbent concentration (diamonds 0.101 g/L iron oxide; squares 0.054 g/L; triangles 0.025 g/L). $[\text{SeO}_4]_{\text{TOT}} = 3 \text{ ppm}$ for all data points. Error bars represent one standard deviation ($n=3$). Lines represent models (0.101 g/L solid, 0.054 g/L dashed, 0.025 g/L dotted) described in the text.

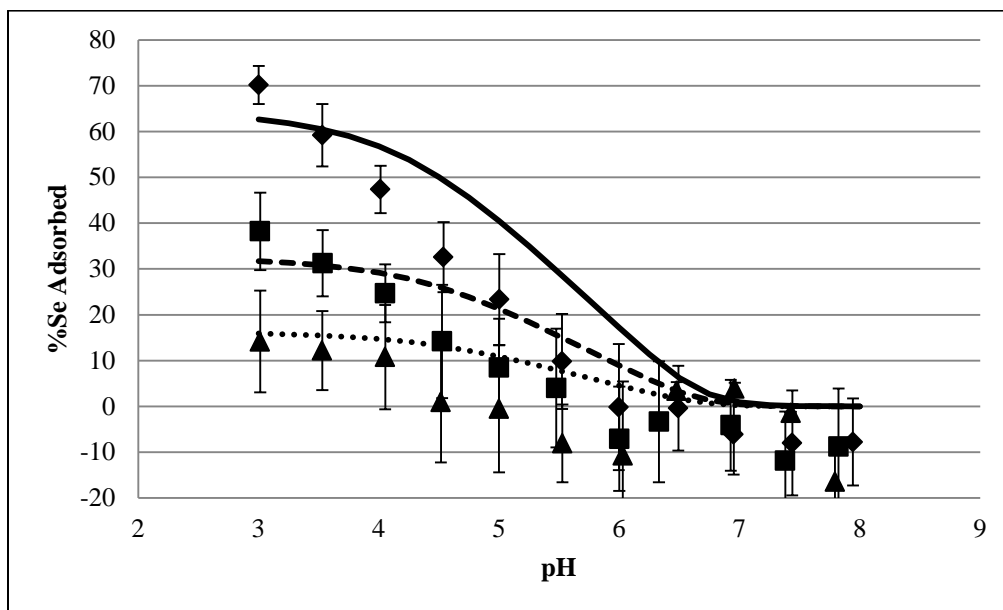


Figure 2.3: $[\text{Fe(II)}]_{\text{aq}}$ during the synthesis of (A) abiotic iron oxides and (B) bacteria-iron oxide composites. Black diamonds represent $[\text{Fe(II)}]_{\text{aq}}$ concentrations prior to the addition of SeO_4^{2-} and grey diamonds represent $[\text{Fe(II)}]_{\text{aq}}$ concentrations after 2 h equilibration with 3 ppm SeO_4^{2-} . The error bars denote one standard deviation ($n=3$) and the vertical lines denote 5 h and 10 h.

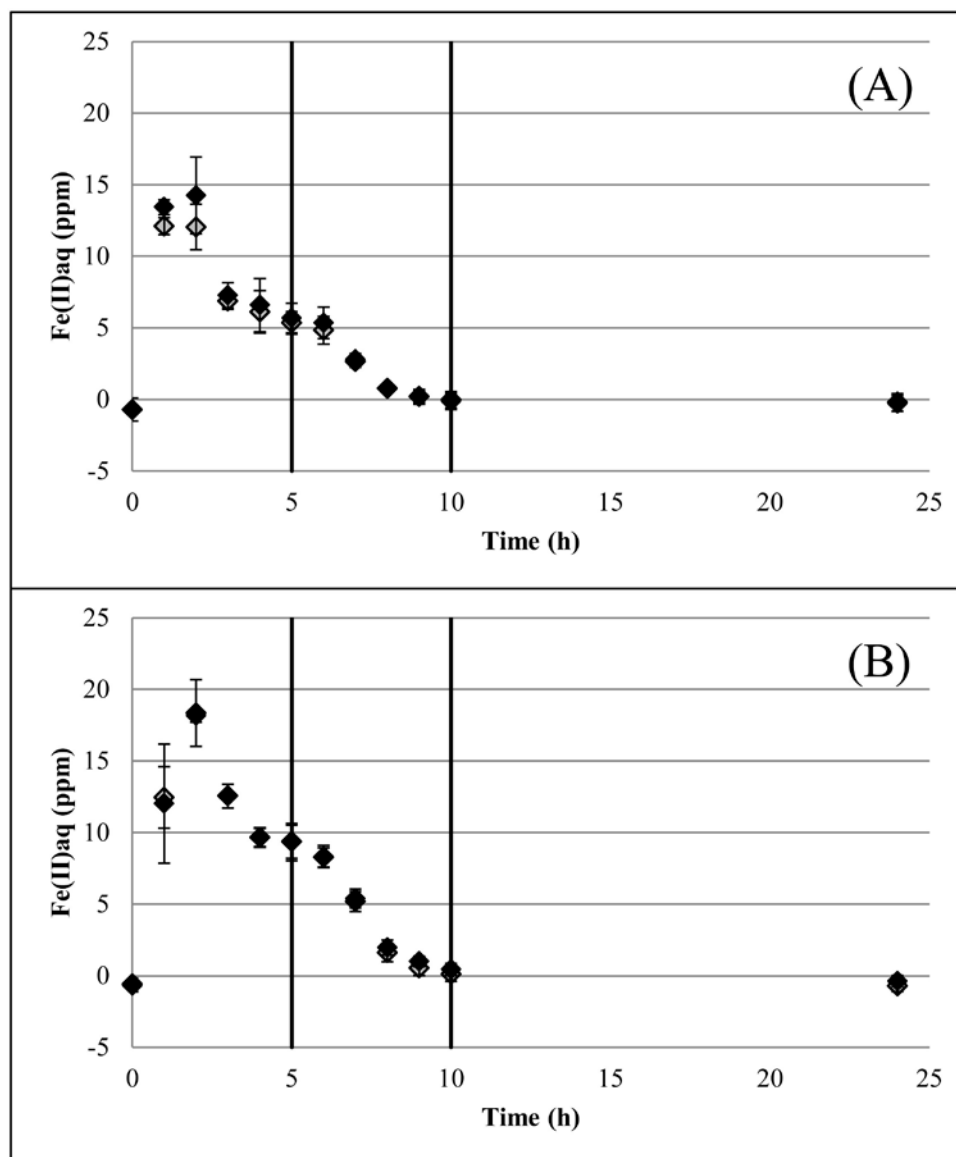


Figure 2.4: SeO_4^{2-} adsorption during the synthesis of abiotic iron oxides (closed diamonds) and bacteria-iron oxide composites (shaded diamonds). Modeling results are included for the abiotic (solid line) and composite (dotted line) systems. Additionally the abiotic (dash-dot line) and composite (dashed line) system were modelled by separately optimizing the concentration of iron oxide surface sites for each time point. All data points are averages with error bars showing one standard deviation (n=3).

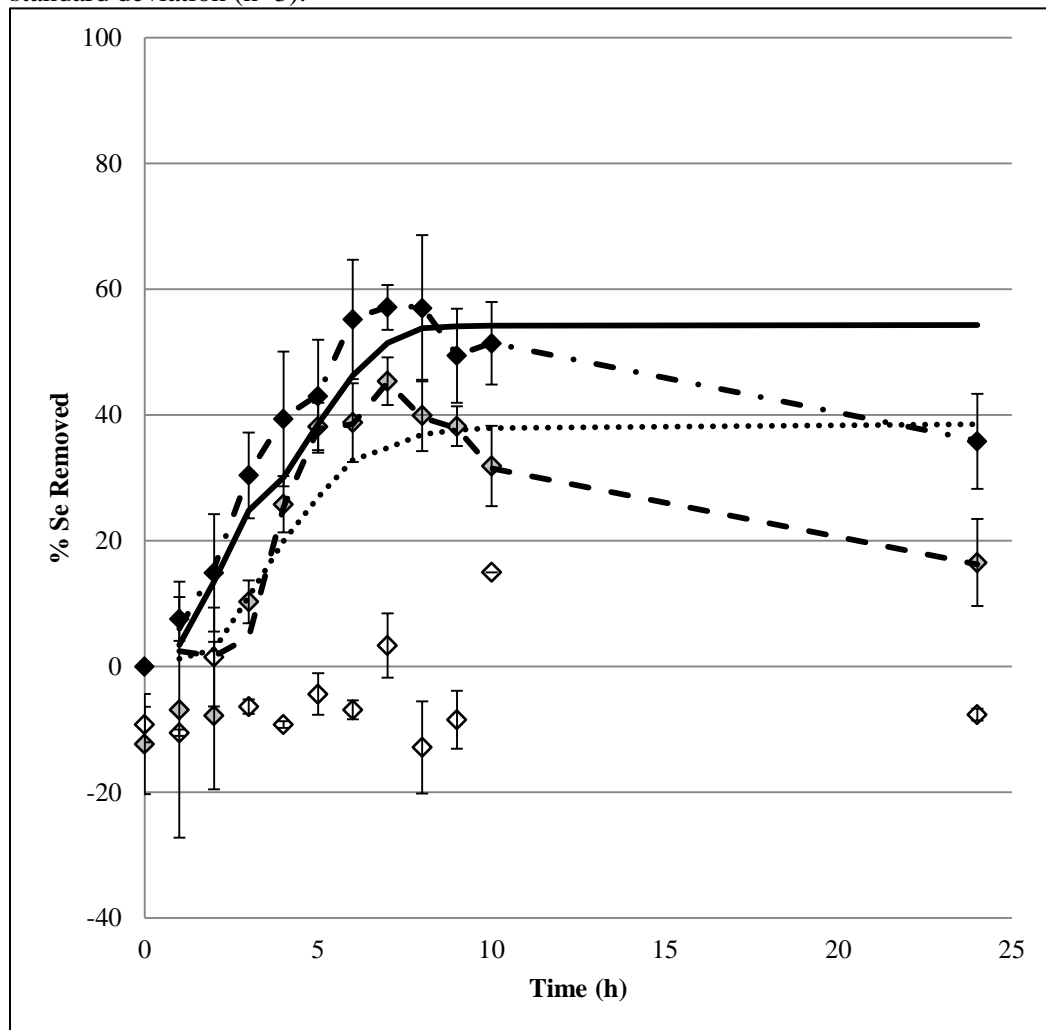


Figure 2.5: Modeled concentration of available iron oxide surface sites in mol sites/g iron oxide over the 24 h period, assuming a surface area of 301 m²/g for all time points. (Abiotic iron oxides in black diamonds, bacteria-iron oxide composite in grey diamonds.) Error bars represent one standard deviation (n=3).

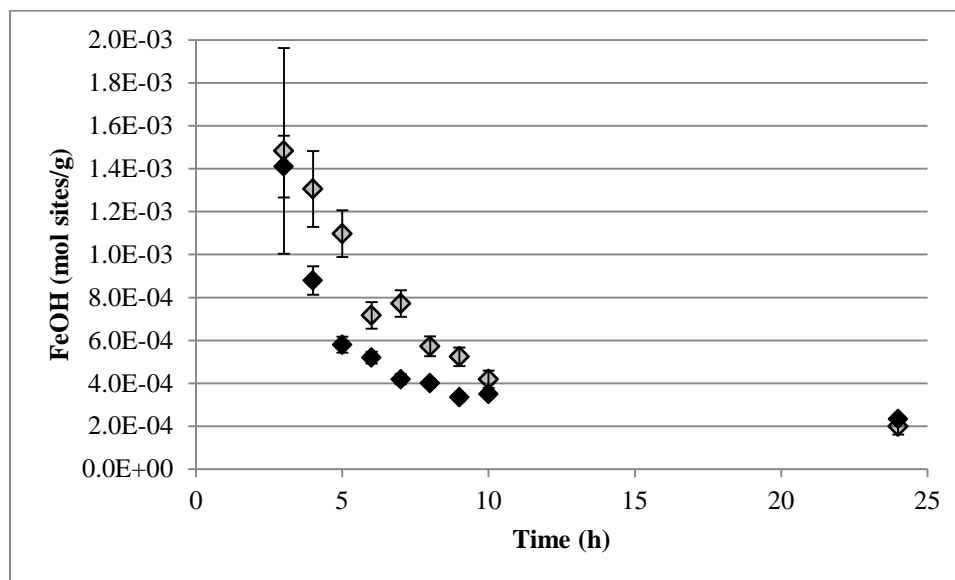


Figure 2.6: Backscatter electron-scanning electron microscopy (BSE-SEM) images of bacteria-iron oxide composites after a 2 h equilibration with 3 ppm selenate added to solution showing (A) 0 h, (B) 3 h, (C) 7 h, and (D) 24 h. The white scale bars all denote 10 μm . All images were taken at 10.0 kV and ~ 80 Pa (low vacuum).

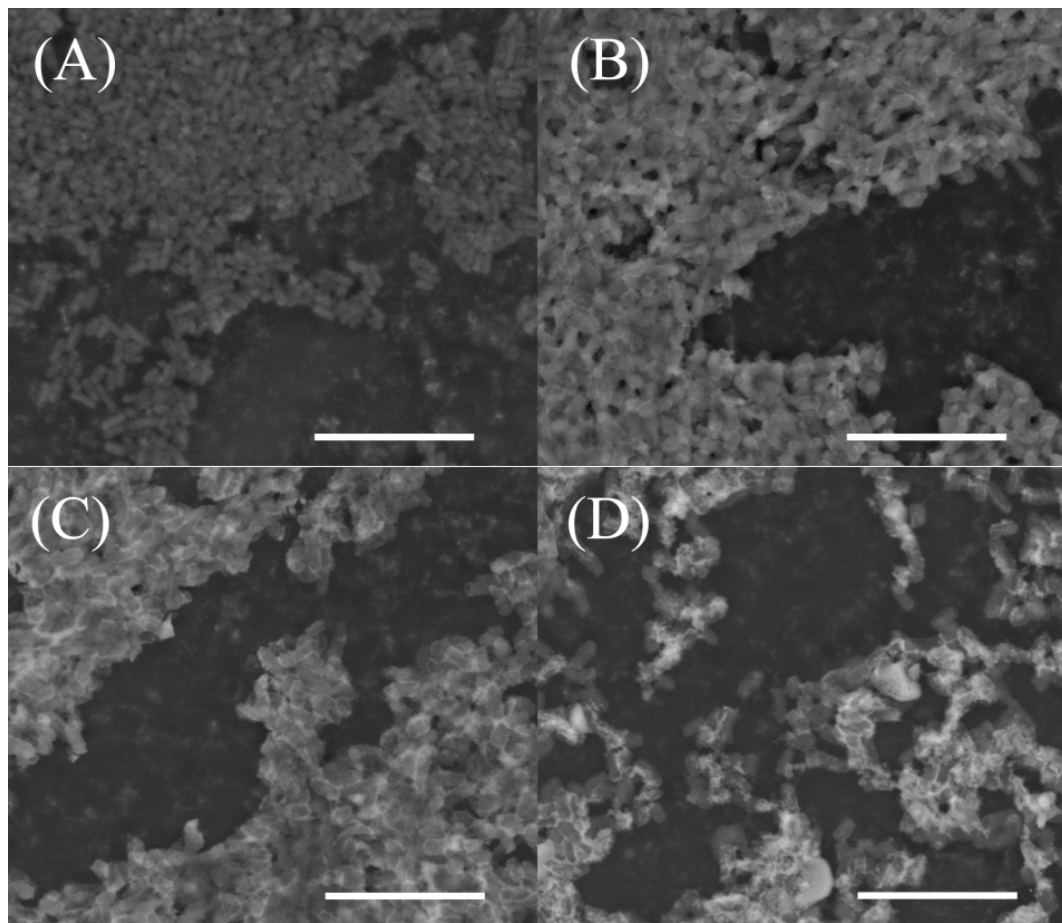


Figure 2.7: Backscatter electron-scanning electron microscopy (BSE-SEM) images of abiotic iron oxides at (A) 3 h, (B) 10 h, and (C) 24 h with white scale bars showing 10 μm . The cubic structures in (C) were identified as salt (NaCl) crystals through scanning electron microscopy-energy dispersive X-ray spectroscopy (SEM-EDS) and a result of salt saturation and considered to be an artifact resulting from water vapor evaporation under vacuum within the SEM .

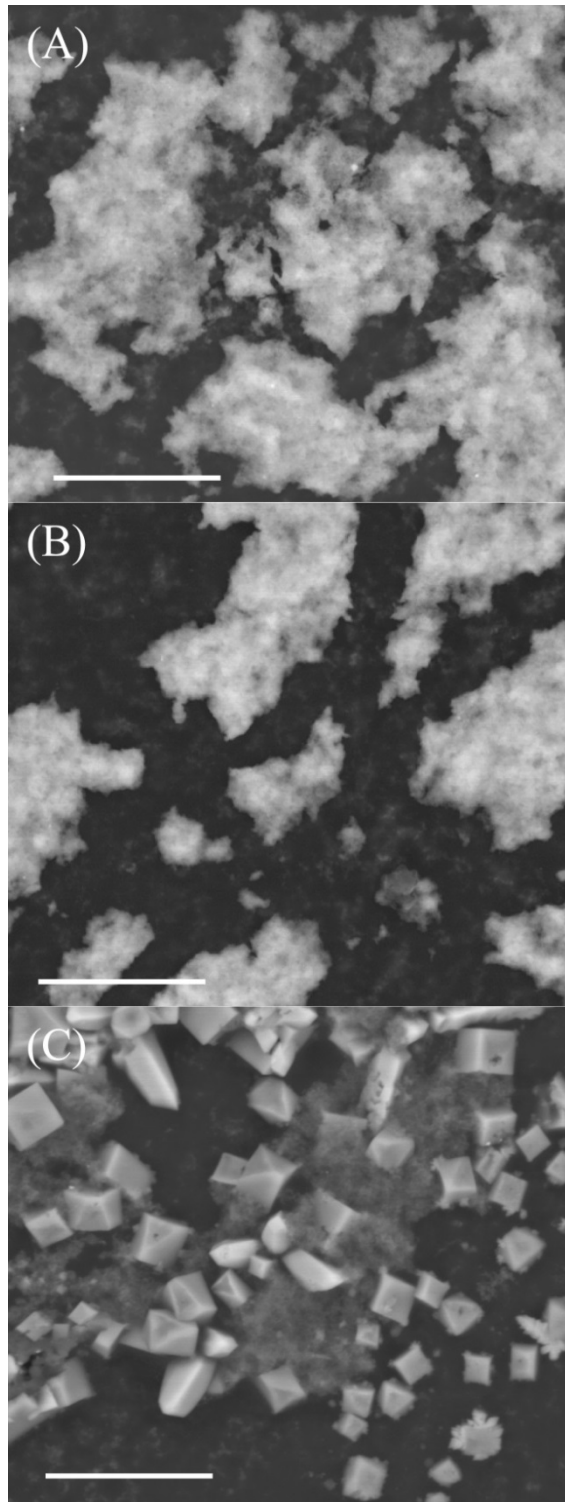


Figure 2.8: Transmission electron microscopy (TEM) images of bacteria-iron oxide composites at (A) 1 h, (B) 3 h, (C) 7 h, (D) 10 h, and (E) 24 h with white scale bars showing 0.2 μm and (F) 1 h, (G) 3 h, (H) 7 h, (I) 10 h, and (J) 24 h and white scale bars showing 0.1 μm .

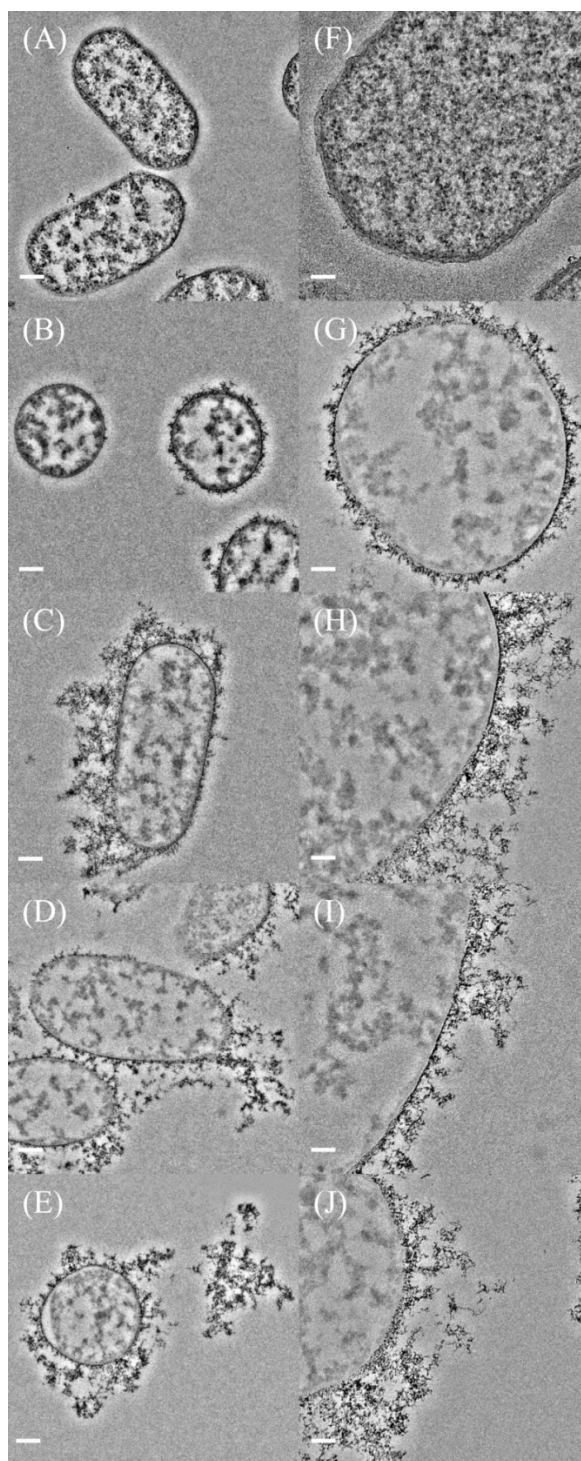


Table 2.1: Overview of prior studies examining metal(loid) adsorption onto composite mixtures of bacteria and iron oxide minerals showing the sorbate ion, the dominant sorbent (bacteria or mineral) under the experimental conditions employed, and the observed additive or non-additive behavior of the system.

Study	Sorbate	Dominant Sorbent	Additive? ^a
Small et al. (1999)	Sr ²⁺	Bacteria	No
Templeton (2003a,b)	Pb ²⁺	Mineral	Yes
Martinez et al. (2004)	Cd ²⁺	Bacteria	No
Kulczycki et al. (2005)	Cd ²⁺ , Pb ²⁺	Bacteria	No
Chen et al. (2008)	Cu ²⁺ , Zn ²⁺	Bacteria	Yes
Langley et al. (2009)	Sr ²⁺	Not determined	Not determined
Song et al. (2009)	Cd ²⁺	Both	No
Daughney et al. (2011)	Cd ²⁺	Bacteria	No
Moon et al. (2012, 2013)	Cu ²⁺	Both	Both

^a In an additive system, adsorption onto the bacteria-iron oxide composite can be accurately predicted from the mass concentration of the bacteria and the mineral within the mixture, in conjunction with models of adsorption onto these end-members. One study has reported both additive and non-additive behavior in the same system but under different experimental conditions.

Table 2.2: Features of triple layer surface complexation models for iron oxide.

Characteristic	Value	Source ^b
Iron oxide surface area (m ² /g)	301 ^a	This study
Capacitance, 0 Plane (F/m ²)	1.0	1
Capacitance, B Plane (F/m ²)	0.2	1
Log K, $\equiv\text{FeOH} + \text{H}^+ + \text{SeO}_4^{2-} \rightleftharpoons \equiv\text{FeOSeO}_3^- + \text{H}_2\text{O}$	9.6	1
Log K, $\equiv\text{FeOH} + 2\text{H}^+ + \text{SeO}_4^{2-} \rightleftharpoons \equiv\text{FeOH}_2^+ \cdots \text{HSeO}_4^-$	16.8	1
Log K, $2\equiv\text{FeOH} + 2\text{H}^+ + \text{SeO}_4^{2-} \rightleftharpoons (\equiv\text{FeOH}_2^+)_2 \cdots \text{SeO}_4^{2-}$	21.0	1
Log K, $\equiv\text{FeOH} + \text{H}^+ \rightleftharpoons \equiv\text{FeOH}_2^+$	6.9	2
Log K, $\equiv\text{FeOH} \rightleftharpoons \equiv\text{FeO}^- + \text{H}^+$	-10.9	2
Log K, $\equiv\text{FeOH} + \text{Na}^+ \rightleftharpoons \equiv\text{FeO}^- \cdots \text{Na}^+ + \text{H}^+$	-9.6	2
Log K, $\equiv\text{FeOH} + \text{NO}_3^- \rightleftharpoons \equiv\text{FeOH}_2^+ \cdots \text{NO}_3^-$	8.4	2
Log K, $\equiv\text{FeOH} + \text{H}_2\text{CO}_3 \rightleftharpoons \equiv\text{FeOCOO}^- + \text{H}^+ + \text{H}_2\text{O}$	-2.68	2
Log K, $\equiv\text{FeOH} + \text{H}_2\text{CO}_3 \rightleftharpoons \equiv\text{FeOCOOH} + \text{H}_2\text{O}$	2.15	2
Log K, $\equiv\text{FeOH} + \text{H}_2\text{CO}_3 + \text{Na}^+ \rightleftharpoons \equiv\text{FeOCOONa} + \text{H}^+$	-3.23	2

^a The surface area was assumed to be 301 m²/g at all time points.

^b Sources: 1) Fukushi and Sverjenski (2007); 2) Villalobos and Leckie (2001).

Table 2.3: Features of the non-electrostatic surface complexation models for bacterial surfaces.

Characteristic	Mean $\pm \sigma$	Source
Dry biomass concentration (g/l)/optical density (600 nm)	0.6528	This study
Site 1 concentration (10^{-4} mol/dry g/l)	6.50 \pm 1.7	Borrok et al., 2005
Site 2 concentration (10^{-4} mol/dry g/l)	7.34 \pm 0.52	Borrok et al., 2005
Site 3 concentration (10^{-4} mol/dry g/l)	5.02 \pm 0.52	Borrok et al., 2005
Site 4 concentration (10^{-4} mol/dry g/l)	3.82 \pm 0.39	Borrok et al., 2005
Log K, $R_1\text{-H} \rightleftharpoons R_1^- + H^+$	-3.1	Johnson et al., 2007
Log K, $R_2\text{-H} \rightleftharpoons R_2^- + H^+$	-4.7	Johnson et al., 2007
Log K, $R_3\text{-H} \rightleftharpoons R_3^- + H^+$	-6.6	Johnson et al., 2007
Log K, $R_4\text{-H} \rightleftharpoons R_4^- + H^+$	-9.0	Johnson et al., 2007

2.5 References

- (1) Beveridge, T. J.; Murray, R. G. Sites of metal deposition in the cell wall of *Bacillus subtilis*. *J. Bacteriol.* **1980**, *141*, 876–887.
- (2) Beveridge, T. J.; Koval, S. F. Binding of metals to cell envelopes of *Escherichia coli* K-12. *Appl. Environ. Microbiol.* **1981**, *42*, 325–335.
- (3) Ferris, F. G.; Beveridge, T. J. Site specificity of metallic ion binding in *Escherichia coli* K-12 lipopolysaccharide. *Can. J. Microbiol.* **1986**, *32*, 52–55.
- (4) Fein, J. B.; Daughney, C. J.; Yee, N.; Davis, T. A. A chemical equilibrium model for metal adsorption onto bacterial surfaces. *Geochim. Cosmochim. Acta* **1997**, *61*, 3319–3328.
- (5) Daughney, C. J.; Fowle, D. A.; Fortin, D. E. The effect of growth phase on proton and metal adsorption by *Bacillus subtilis*. *Geochim. Cosmochim. Acta* **2001**, *65*, 1025–1035.
- (6) Châtellier, X.; Fortin, D. Adsorption of ferrous ions onto *Bacillus subtilis* cells. *Chem. Geol.* **2004**, *212*, 209–228.
- (7) Boyanov, M. I.; Kelly, S. D.; Kemner, K. M.; Bunker, B. A.; Fein, J. B.; Fowle, D. A. Adsorption of cadmium to *Bacillus subtilis* bacterial cell walls : A pH-dependent X-ray absorption fine structure spectroscopy study. *Geochim. Cosmochim. Acta* **2003**, *67*, 3299–3311.
- (8) Burnett, P.-G.; Heinrich, H.; Peak, D.; Bremer, P. J.; McQuillan, a. J.; Daughney, C. J. The effect of pH and ionic strength on proton adsorption by the thermophilic bacterium *Anoxybacillus flavithermus*. *Geochim. Cosmochim. Acta* **2006**, *70*, 1914–1927.
- (9) Kenward, P.; Fowle, D.; Yee, N. Microbial selenate sorption and reduction in nutrient limited systems. *Environ. Sci. Technol.* **2006**, *40*, 3782–6.
- (10) Dzombak, D. A.; Morel, F. M. M. *Surface Complexation Modeling, Hydrous Ferric Oxide*; Wiley Interscience: New York, 1990.
- (11) Hayes, K. F.; Roe, A. L.; Brown, G. E.; Hodgson, K. O.; James, O.; Parks, G. A. In situ X-ray absorption study of surface complexes: Selenium oxyanions on α -FeOOH. *Science* (80-.). **1987**, *238*, 783–786.
- (12) Manceau, A.; Charlet, L. The mechanism of selenate adsorption on goethite and hydrous ferric oxide. *J. Colloid Interface Sci.* **1994**, *168*, 87–93.

- (13) Peak, D.; Sparks, D. L. Mechanisms of selenate adsorption on iron oxides and hydroxides. *Environ. Sci. Technol.* **2002**, *36*, 1460–6.
- (14) Duc, M.; Lefèvre, G.; Fédoroff, M. Sorption of selenite ions on hematite. *J. Colloid Interface Sci.* **2006**, *298*, 556–563.
- (15) Karthikeyan, K.; Elliott, H. Surface complexation modeling of copper sorption by hydrous oxides of iron and aluminum. *J. Colloid Interface Sci.* **1999**, *220*, 88–95.
- (16) Martinez, R. E.; Pedersen, K.; Ferris, F. G. Cadmium complexation by bacteriogenic iron oxides from a subterranean environment. *J. Colloid Interface Sci.* **2004**, *275*, 82–9.
- (17) Small, T. D.; Warren, L. A.; Ferris, F. G. Influence of ionic strength on strontium sorption to bacteria, Fe(III) oxide, and composite bacteria-Fe(III) oxide surfaces. *Appl. Geochemistry* **2001**, *16*, 939 – 946.
- (18) Small, T. D.; Warren, L. A.; Roden, E. E. Sorption of strontium by bacteria, Fe(III) oxide, and bacteria-Fe(III) oxide composites. *Environ. Sci. Technol.* **1999**, *33*, 4465–4470.
- (19) Kulczycki, E.; Fowle, D.; Fortin, D.; Ferris, F. G. Sorption of cadmium and lead by bacteria–ferrihydrite composites. *Geomicrobiol. J.* **2005**, *22*, 299–310.
- (20) Langley, S.; Gault, A. G.; Ibrahim, A.; Takahashi, Y.; Renaud, R. O. B. Sorption of strontium onto bacteriogenic iron oxides. *Environ. Sci. Technol.* **2009**, *43*, 1008–1014.
- (21) Templeton, A. S.; Spormann, A. M.; Brown Jr., G. E. Speciation of Pb(II) sorbed by *Burkholderia cepacia*/goethite composites. *Environ. Sci. Technol.* **2003**, *37*, 2166–2172.
- (22) Templeton, A. S.; Trainor, T. P.; Spormann, A. M.; Newville, M.; Sutton, S. R.; Dohnalkova, A.; Gorby, Y.; Brown, G. E. Sorption versus biomineralization of Pb(II) within *Burkholderia cepacia* biofilms. *Environ. Sci. Technol.* **2003**, *37*, 300–307.
- (23) Chen, X.; Chen, L.; Shi, J.; Wu, W.; Chen, Y. Immobilization of heavy metals by *Pseudomonas putida* CZ1/goethite composites from solution. *Colloids Surf. B. Biointerfaces* **2008**, *61*, 170–5.
- (24) Song, Y.; Swedlund, P. J.; Singhal, N.; Swift, S. Cadmium(II) speciation in complex aquatic systems: A study with ferrihydrite, bacteria, and an organic ligand. *Environ. Sci. Technol.* **2009**, *43*, 7430–7436.

- (25) Moon, E. M.; Peacock, C. L. Modelling Cu(II) adsorption to ferrihydrite and ferrihydrite–bacteria composites: Deviation from additive adsorption in the composite sorption system. *Geochim. Cosmochim. Acta* **2013**, *104*, 148–164.
- (26) Moon, E. M.; Peacock, C. L. Adsorption of Cu(II) to ferrihydrite and ferrihydrite–bacteria composites: Importance of the carboxyl group for Cu mobility in natural environments. *Geochim. Cosmochim. Acta* **2012**, *92*, 203–219.
- (27) Mullen, M. D.; Wolf, D. C.; Ferris, F. G.; Beveridge, T. J.; Flemming, C. A.; Bailey, G. W. Bacterial sorption of heavy metals. *Appl. Environ. Microbiol.* **1989**, *55*, 3143–9.
- (28) Winkel, L. H. E.; Johnson, C. A.; Lenz, M.; Grundl, T.; Leupin, O. X.; Amini, M.; Charlet, L. Environmental selenium research: from microscopic processes to global understanding. *Environ. Sci. Technol.* **2012**, *46*, 571–9.
- (29) Burnett, P.-G. G.; Handley, K.; Peak, D.; Daughney, C. J. Divalent metal adsorption by the thermophile *Anoxybacillus flavithermus* in single and multi-metal systems. *Chem. Geol.* **2007**, *244*, 493–506.
- (30) Daughney, C. J.; Fakih, M.; Châtellier, X. Progressive sorption and oxidation/hydrolysis of Fe(II) affects cadmium immobilization by bacteria-iron oxide composites. *Geomicrobiol. J.* **2011**, *28*, 11–22.
- (31) Châtellier, X.; West, M. M.; Rose, J.; Fortin, D.; Leppard, G.; Ferris, F. G. Characterization of iron-oxides formed by oxidation of ferrous ions in the presence of various bacterial species and inorganic ligands. *Geomicrobiol. J.* **2004**, *21*, 99–112.
- (32) Châtellier, X.; Grybos, M.; Abdelmoula, M.; Kemner, K. M.; Leppard, G. G.; Mustin, C.; West, M. M.; Paktunc, D. Immobilization of P by oxidation of Fe(II) ions leading to nanoparticle formation and aggregation. *Appl. Geochemistry* **2013**, *35*, 325–339.
- (33) Viollier, E.; Inglett, P. W.; Hunter, K.; Roychoudhury, A. N.; Van Cappellen, P. The ferrozine method revisited: Fe(II)/Fe(III) determination in natural waters. *Appl. Geochemistry* **2000**, *15*, 785–790.
- (34) Stookey, L. L. Ferrozine---a new spectrophotometric reagent for iron. *Anal. Chem.* **1970**, *42*, 779–781.
- (35) Smeaton, C. M.; Fryer, B. J.; Weisener, C. G. Intracellular precipitation of Pb by *Shewanella putrefaciens* CN32 during the reductive dissolution of Pb-jarosite. *Environ. Sci. Technol.* **2009**, *43*, 8086–91.

- (36) Smeaton, C. M.; Walshe, G. E.; Smith, A. M. L.; Hudson-Edwards, K. A.; Dubbin, W. E.; Wright, K.; Beale, A. M.; Fryer, B. J.; Weisener, C. G. Simultaneous release of Fe and As during the reductive dissolution of Pb-As jarosite by *Shewanella putrefaciens* CN32. *Environ. Sci. Technol.* **2012**, *46*, 12823–31.
- (37) Smeaton, C. M.; Walshe, G. E.; Fryer, B. J.; Weisener, C. G. Reductive dissolution of Tl(I)-jarosite by *Shewanella putrefaciens*: providing new insights into Tl biogeochemistry. *Environ. Sci. Technol.* **2012**, *46*, 11086–94.
- (38) Westall, J. C. FITEQL: A computer program for the determination of chemical equilibrium constants from experimental data. **1982**, Report 82–01.
- (39) Daughney, C. J.; Châtellier, X.; Chan, A.; Kenward, P.; Fortin, D.; Suttle, C. A.; Fowle, D. A. Adsorption and precipitation of iron from seawater on a marine bacteriophage (PWH3A-P1). *Mar. Chem.* **2004**, *91*, 101–115.
- (40) Langmuir, D. *Aqueous Environmental Geochemistry*; Prentice Hall: Upper Saddle River, 1997.
- (41) Spadini, L.; Schindler, P. W.; Charlet, L.; Manceau, A.; Vala Ragnarsdottir, K. Hydrous ferric oxide: evaluation of Cd-HFO surface complexation models combining Cd(K) EXAFS data, potentiometric titration results, and surface site structures identified from mineralogical knowledge. *J. Colloid Interface Sci.* **2003**, *266*, 1–18.
- (42) Rancourt, D. G.; Hibault, P. E.; Avrocordatos, D. M.; Amarche, G. L. Hydrous ferric oxide precipitation in the presence of nonmetabolizing bacteria : Constraints on the mechanism of a biotic effect. *Geochim. Cosmochim. Acta* **2005**, *69*, 553–577.

CHAPTER 3

COPPER (II) REMOVAL BY *ESCHERICHIA COLI*-IRON OXIDE COMPOSITES DURING THE ADDITION OF $\text{Fe(II)}_{\text{AQ}}$

3.1 Introduction

The fate and mobility of metal and metalloid ions in the environment is affected by a variety of processes including adsorption. Secondary iron oxide minerals and bacterial cells are among the most important metal(loid) sorbents in near-surface water-rock systems. Both types of sorbent often exist as coatings on the surfaces of primary mineral grains, hence represent a significant fraction of the reactive surface area exposed to the solution phase. Both types of sorbent have high affinities for dissolved metals, and iron oxide minerals are further known to adsorb metalloid ions too. Previously there have been many studies focused on the adsorption of metal(loid) ions onto bacterial or iron oxide surfaces.¹⁻¹⁰ The extent of adsorption is observed to be dependent on environmental conditions including pH, ionic strength, and sorbate and sorbent concentrations. Prior studies have developed a variety of surface complexation models to describe metal(loid) adsorption to bacteria or iron oxide minerals as there is considerable interest in the relationship between metal toxicity and transport, both of which are affected by adsorption.^{7,8,10-14}

Few previous studies have evaluated metal(loid) adsorption onto composites (mixtures) of bacteria and iron oxide minerals and laboratory experiments of metal(loid) ion adsorption by iron oxide-bacteria composites have been conducted with a variety of bacteria (Table 3.1).¹⁵⁻²⁶ However, only one prior study has examined metal adsorption during the addition, oxidation, hydrolysis, and precipitation of $\text{Fe(II)}_{\text{aq}}$ which was found to significantly affect the removal of Cd(II) from solution.²¹

The earliest set of experiments investigated adsorption of cadmium, lead or strontium by natural bacteria-iron oxide composites or synthetic equivalents using a single species of *Bacillus*,

Escherichia or *Shewanella*.^{16,17,23,25} It was observed that the metals adsorbed primarily to the bacterial cells and a significant decrease in adsorption occurred when iron oxide minerals were present, which was attributed to masking of bacterial surface sites by the iron oxide.

A second set of experiments investigated Pb adsorption by iron oxide-*Burkholderia cepacia* composites and found that Pb adsorbed primarily to the mineral component above pH 6 and adsorption to the cells was only observed at lower pH.^{18,22} The authors concluded there was no significant masking of bacterial or mineral adsorption sites. A third study examined Cu and Zn adsorption onto composites with fixed *P. putida*/goethite ratios and also evaluated the effect of living versus non-living cells.²⁴ This study found that the sorption behavior was additive and further noted that adsorption was greater when the composites were comprised of living rather than non-living cells. Song et al. (2009) evaluated Cd adsorption onto composites over a range of set ferrihydrite/bacteria dry weight ratios and found that adsorption was non-additive but only decreased Cd adsorption by up to 10%.

Moon and Peacock (2012, 2013) studied Cu adsorption onto composites of ferrihydrite and *B. subtilis* with mass ratios of 80:20, 60:40, and 30:70 as well as the end-members. These studies found that Cu adsorbed mainly to the bacterial fraction of the composites at low pH while the ferrihydrite fraction dominated at high pH, although the bacterial fraction became important in the high pH region at higher bacteria/iron oxide ratios. Cu adsorption onto composites of mainly ferrihydrite deviated slightly from the prediction of additivity, but the deviation was not significantly greater than the experimental uncertainty. This same study reported that Cu adsorption by composites composed primarily of bacteria adsorbed significantly less than the pure bacterial end-member, which was suggested to arise from interactions between the bacteria and mineral that altered their respective surface charges.

Based on the previous work there is no clear understanding of whether metal(loid) ion adsorption onto bacteria-mineral composites is additive, i.e. whether models developed for the single-sorbent end-member systems are able to predict sorption behavior onto composite mixtures of the two sorbents. This is partially due to the lack of a standard experimental method for conducting these studies, meaning that it is difficult to compare prior studies. The early studies used a single bacteria/mineral ratio^{16–18,22,23,25} and only a handful of studies have used composites with a range of bacteria/mineral ratios.^{19,20,24,26,27} Additionally most studies have used iron oxide which was precipitated abiotically by hydrolysis of Fe(III), rinsed, and only then mixed with bacterial cells to create composites. Prior studies have also used a variety of bacteria which also makes the results difficult to compare. Only Daughney et al. (2011) has investigated the effects of composites formed from Fe(II) in the presence of bacterial cells on ion adsorption.

In this study, the adsorption of Cu(II) cations to *Escherichia coli*-iron oxide composites was investigated during the addition, oxidation, hydrolysis and precipitation of Fe(II)_{aq} to form Fe(III)-oxide. Copper was selected as the sorbate as it has been used in many prior adsorption studies both of single sorbents and mixtures.^{1,14,28–32} Likewise, *E. coli* was selected as the model bacterial species because it has been used in a number of prior adsorption studies.^{1–3,17,33–35} Iron oxides were formed by the introduction, oxidation, hydrolysis, and precipitation of Fe(II)_{aq} and the results can therefore be compared with Fakhri et al. (2008) and Daughney et al. (2011). The behavior of Cu(II) cations was tracked during the formation of the iron oxides, using the same approaches described in Chapter 2 (also similar to the methods used by Daughney et al. 2011). As this thesis has applied the same methods to study Cu(II) and selenate removal, the mechanisms that control non-additive metal(loid) removal could be assessed, principally because selenate adsorbs solely to the mineral phase whereas copper adsorbs mainly to the bacterial cells.

3.2 Methods

3.2.1 Bacterial growth conditions

Escherichia coli AB264 (CGSC) suspensions were pre-cultured in 20-mL of sterilized (121°C, 60 min) trypticase soy broth (TSB) for 24 h in a shaking incubator (27°C, 120 rpm). After 24 h, 20-mL of pre-culture was used to inoculate a 700-mL volume of sterilized TSB and placed in the same incubator for 24 h until late stationary phase was reached. The cultures were rinsed five times with 0.01 M NaNO₃ and recovered via centrifugation (4500 rpm, 10 min) and the supernatant was discarded after each rinse. After rinsing, the bacteria were re-suspended in 0.01M NaNO₃ and the cell density was measured via optical density at 600 nm (OD₆₀₀). The relationship between OD₆₀₀ and bacterial cell dry weight was determined using the same method as in Chapter 2. The cells were diluted with 0.01M NaNO₃ to a final concentration of 0.44 dry g/L. The growth and rinsing procedures employed were similar to previous studies.^{37,38} Cell metabolic state and viability were not evaluated.

3.2.2 Synthesis of abiotic iron oxides

An initial solution of 400 mL 0.01M NaNO₃ in a glass beaker was adjusted to pH 6 with 0.1, 0.01, or 0.001 M HNO₃ or NaOH and then 48.0 ml of FeCl₂ solution ([FeCl₂]=1.25x10⁻²M, [HCl]=2.50x10⁻³M, [NaNO₃]=0.01M) was added at a constant rate of 0.12 ml/min over 6.66 h using a NE-1000 Multi-PhaserTM programmable syringe pump (New Era Pump Systems Inc., Farmingdale, USA). The solution was continuously stirred while in contact with the atmosphere to ensure it was aerated over the experimental period. The initial pH of 6 was maintained by the addition of NaOH solution ([NaOH]=0.03M, [NaNO₃]=0.01M) via a pH stat automatic titrator (Radiometer Analytical model TIM 854, Lyon, France). The iron oxides were aged for up to a total of 24 h (including the period of addition of the FeCl₂ solution). This procedure was similar to previous work by Fakhri et al. (2008), Daughney et al. (2011), and Châtellier et al. (2013). The iron oxides synthesized using this method formed in the absence of bacterial cells and will be referred to as abiotic iron oxides in this paper. As stated in Chapter 2, the surface area of the

abiotic iron oxides, after 24 h aging in suspension, was determined through BET analysis to be 301 m²/g (n=3).

3.2.3 Synthesis of iron oxide-bacteria composites

Suspensions of *E. coli*-iron oxide composites were prepared using the same method as for the abiotic system, except that the initial 400 mL 0.01M NaNO₃ solution contained 0.44 dry g/L bacteria. Similarly to the abiotic iron oxides, these were not collected or rinsed before use and were aged for up to 24 h during the synthesis. The iron oxides formed using this method will be referred to as biotic iron oxides as they were precipitated in the presence of bacterial cells. The surface area of the biotically formed iron oxides could not be determined because the bacterial cells could not be separated from the iron oxide and hence interfered with BET analysis of the mineral component of the composites.

3.2.4 Adsorption to bacteria or iron oxide as a function of pH, Cu(II) to sorbent ratio, and time

Copper adsorption to iron oxide or *E. coli* was monitored over pH 3-8 at fixed ionic strength in triplicate to determine the optimum pH for this study. The optimal pH was selected in order to result in significant adsorption to the bacteria but little or no adsorption onto the iron oxides. These conditions were sought in order to examine the effect of the presence of iron oxides on Cu(II) adsorption to the cells. In Chapter 2 the effect of the presence of bacterial cells on selenate removal was determined. This study therefore complements Chapter 2 and together the two studies can give insight into the causes of any non-additive adsorption behavior that is observed in the presence of bacteria-iron oxide composites.

Bacterial or iron oxide suspensions were prepared as stated above and the iron oxides were aged for 24 h before use. The suspensions were then divided into three 200 mL dilutions in glass beakers for both iron oxide (0.108 g/L, 0.05 g/L, 0.03 g/L) and bacteria (0.44 dry g/L, 0.22 dry g/L, 0.11 dry g/L). 13.18 mL of a solution of copper nitrate (45.52 ppm Cu(NO₃)₂, 0.01 M NaNO₃) was added to each suspension to give a final concentration of 3 ppm Cu in 200 mL total

solution. All suspensions were adjusted to pH 3 or 8 by dropwise addition of 0.1, 0.01, or 0.001 M HNO_3 or NaOH and allowed to equilibrate for 30 min while being stirred continuously in contact with the atmosphere. After the 30 minute equilibration period, a 2-mL sample was collected into a polypropylene microcentrifuge tube, shaken for 1 h, and centrifuged (13200 g, 15 min) to isolate the supernatant. The supernatant was acidified with 1% HNO_3 and analyzed by inductively coupled plasma-optical emission spectroscopy (ICPOES) for $[\text{Cu}_{\text{TOT}}]_{\text{aq}}$ and $[\text{Fe}_{\text{TOT}}]_{\text{aq}}$. There was negligible Fe present in solution for all abiotic iron oxide samples therefore no appreciable dissolution of the mineral occurred. After sampling, the pH was adjusted 0.5 units dropwise with 0.1, 0.01, or 0.001 M HNO_3 or NaOH and allowed to equilibrate for another 30 min whereupon another 2-mL sample was taken. This pattern continued until the final pH of 3 or 8 was reached. Replicates were performed starting from both pH 3 and pH 8 to identify any aging effects of both the bacteria and the iron oxide.

Kinetics experiments were conducted after the optimum pH of 5.2 was selected (see discussion below). Iron oxide and bacterial suspensions were prepared in the same way as for the experiments over a pH range and divided into three separate 200-mL suspensions in glass beakers each with the same iron oxide (0.108 g/L) or bacteria (0.44 dry g/L) concentration, 13.18 mL of the copper nitrate solution was added, and each suspension adjusted to pH 5.2 dropwise with 0.1, 0.01, or 0.001 M HNO_3 or NaOH. The suspensions were stirred continuously while open to the atmosphere and equilibrated for 30 min whereupon a 2-mL sample was taken, centrifuged (13200 g, 15 min), and the supernatant acidified with 1% HNO_3 for ICPOES analysis of $[\text{Cu}_{\text{TOT}}]_{\text{aq}}$ and $[\text{Fe}_{\text{TOT}}]_{\text{aq}}$. Thereafter, samples were taken every 30 min for 7 h. Although the kinetics experiments were only run for 7 h the iron oxide used had already been aged for 24 h so the observed copper adsorption would be most similar to the 24 h samples from the abiotic and composite synthesis experiments described below.

3.2.5 Copper adsorption experiments

The Cu^{2+} adsorption experiments described above were all conducted *after* the sorbent had aged for 24 h. In contrast, the experiments described below were used to track the fate of Cu^{2+} *during* the synthesis and aging of the sorbents. Cu^{2+} adsorption was evaluated in three systems: bacteria only with no added iron; abiotic iron oxide without bacteria; and bacteria-iron oxide composites. All experiments were repeated in triplicate using independently cultured batches of bacteria and independently synthesized iron oxides. All chemical analyses of both the aqueous and solid phases (1,10-phenanthroline, Ferrozine, ICPOES) were performed for all three treatments (bacteria with no added iron, abiotic iron oxide, iron oxide-bacteria composites) and samples were preserved from each replicate for electron microscopy.

All syntheses were initiated with 400 mL of 0.01 M NaNO_3 , continuously stirred in a glass beaker that was left open to the atmosphere. For the experiments that involved the bacteria alone or the bacteria-iron oxide composites, this 400 mL volume contained rinsed *E. coli* cells at a biomass concentration of 0.44 dry g/L; for the experiments conducted with the abiotic iron oxide, this 400 mL solution was free of bacteria. For all experiments this starting solution or suspension was adjusted to pH 6. As per the protocol described above, 48.0 mL of a solution were added to the beaker at a constant rate of 0.12 mL/min while maintaining the suspension at pH 6. For the experiments involving the abiotic iron oxide or the bacteria-iron oxide composites, this solution contained $[\text{FeCl}_2]=1.25 \times 10^{-2}$ M, $[\text{HCl}]=2.50 \times 10^{-3}$ M and $[\text{NaNO}_3]=0.01$ M. For the experiments that involved the bacteria in the absence of iron, this solution contained $[\text{HCl}]=2.50 \times 10^{-3}$ M and $[\text{NaNO}_3]=0.01$ M.

For all experiments, two samples (2 mL and 13.89 mL) of the suspension were collected every 60 min for 10 h and a final sample was collected after 24 h. The first subsample (2-mL) was centrifuged (13200 g, 15 min) and the supernatant was analyzed for $[\text{Fe(II)}]_{\text{aq}}$ using 1,10-phenanthroline, a colorimetric $\text{Fe(II)}_{\text{aq}}$ indicator, to determine the concentration of iron oxide

precipitated prior to copper addition. 0.85-mL $\text{Cu}(\text{NO}_3)_2$ solution was added to the second subsample (13.89-mL) to give a final $\text{Cu}(\text{II})$ concentration of 3 ppm. The sample was then equilibrated for 2 h at $\text{pH } 5.2 \pm 0.03$ by manual dropwise additions of 0.1, 0.01, or 0.001 M HNO_3 or NaOH while being stirred continuously and open to the atmosphere. The 2 h equilibration time was selected on the basis of the kinetics experiments (see below). After the 2 h equilibration period, the 13.89 mL sample (13.89-mL) was divided into three subsamples. One 2-mL subsample was centrifuged (13200 g, 15 min) and the supernatant was analyzed for $[\text{Fe}(\text{II})]_{\text{aq}}$ (1,10-phenanthroline, Ferrozine) using 1,10-phenanthroline. A second 2 mL subsample was centrifuged (13200 g, 2 min), half the supernatant was discarded, then 2.5% glutaraldehyde was added to give a volume ratio of 1:1 for sample relative to glutaraldehyde solution. These samples were stored at 4°C for subsequent analysis by electron microscopy (see below). An ethanol dehydration series was not performed to dry the samples because an environmental scanning electron microscope (ESEM) was used, so drying was unnecessary. The third 2 mL subsample was centrifuged (13200 g, 15 min) and the supernatant was acidified with 1% HNO_3 and analyzed for $[\text{Fe}_{\text{TOT}}]_{\text{aq}}$ and $[\text{Cu}_{\text{TOT}}]_{\text{aq}}$ using ICPOES. The solid (pellet) from the third subsample was digested in 0.5 mL 5 M HCl and the acid digest was analyzed using the ferrozine method and ICPOES for $[\text{Fe}(\text{II})]/[\text{Fe}(\text{III})]$ in the solid phase.

3.2.6 Electron microscopy

Scanning electron microscopy (SEM) samples were preserved as stated previously in Chapter 2 and stored at 4°C until imaging analysis. Back scatter electron (BSE) SEM images were taken under low vacuum (~80 Pa) and at 10.0 kV with a field emission environmental scanning electron microscope (FE-ESEM) (FEI Quanta 200F). Elemental composition was determined using energy dispersive X-ray spectroscopy (EDX) of the solid phase.

Samples for transmission electron microscopy (TEM) analysis were preserved and stored prior to analysis using the same method as for SEM. The samples were shipped to McMaster

University, Hamilton, ON, Canada and microtome sections were prepared on Formvar grids and carbon coated for imaging as stated in Chapter 2. The samples were imaged via field emission transmission electron microscopy (FE-TEM) (FEI Titan 80-300). Bright field (BF) TEM images were collected at 300 kV and energy dispersive X-ray spectra (EDS) were collected in scanning transmission electron microscopy (STEM) mode at a probe size of 1 nm.

3.2.7 Modeling

Surface complexation models (SCM) were developed using FITMOD, a modified version of FITEQL 2.0.^{27,41} All models involved in this study incorporated chemical equilibrium reactions describing the dissociation of water, base, acid, and the electrolyte used in this study (0.01M NaNO₃). The SCMs also included equilibrium reactions for Cu and Fe hydrolysis, reactions with electrolyte ions and reactions with dissolved carbonate. All stability constants were taken from the MINTEQ database (Visual MINTEQ version 3.0).^{42,43} Additionally, the abiotic and composite models used incorporated a triple layer model while the bacteria only and composite systems also used a non-electrostatic model.⁴¹ The stability constants were also adjusted for ionic strength using the Davies equation and all values used were referenced to zero ionic strength, zero surface charge, and 25°C.⁴⁴

Cu(II) adsorption in the presence of *E. coli* was based on the non-electrostatic model used by Borrok et al. (2005) with stability constants from Johnson et al. (2007). This model describes adsorption onto bacterial surfaces with four discrete surface sites denoted here as R₁, R₂, R₃ and R₄, where R represents the cell wall to which the functional group is attached (Table 3.2).

Adsorption onto iron oxide surfaces was based on the triple layer model developed by Peacock and Sherman (2004) using their stability constants and other parameters for Cu adsorption onto lepidocrocite (Table 3.3). Both stability constants and surface site concentrations were optimized because although they have been constrained previously, those prior studies did

not involve the presence of $\text{Fe(II)}_{\text{aq}}$. Although the adsorption model parameters of Peacock and Sherman (2004) were used they did not fully describe the experimental data so an additional input variable to describe the available iron oxide surface sites for co-precipitation was included based on the observations of Karthikeyan et al. (1999). It was assumed that all iron oxides had a surface area of $301 \text{ m}^2/\text{g}$, a formula weight of 88.85 g/mol , and capacitances of 1.0 and 0.2 F/m^2 for the O and B planes respectively from Fukushi et al. (2007). Although the surface area may have varied over time it was assumed to be constant at all times.

The experimental system was described through a series of solution and complexation chemical reactions with different surface sites.^{27,41} The concentrations of iron oxide and bacterial surface sites were optimized to obtain the best fit to the experimental data. The fit of these models was evaluated by the variance of each model, which was denoted by $V(Y)$.⁴¹ In an ideal system $V(Y)$ equals 1, for which the experimental and model errors would be equal. However as no experiment is ideal, $V(Y)$ less than 10 were interpreted as indicating a good fit in this experiment.

3.3 Results and discussion

3.3.1 Copper adsorption to bacterial cells

Bacterial kinetics experiments were performed in triplicate at $\text{pH } 5.2 \pm 0.03$ over a 7 h period with samples taken every 30 min. There was an average of $63.3 \pm 7.4\%$ adsorption over the entire 7 h (Fig. 3.1). After 0.5 h there was $58.2 \pm 2.1\%$ Cu adsorbed which increased to $62.2 \pm 5.0\%$ after 2.0 h. After 2.0 h Cu adsorption was within one standard deviation so an equilibration time of 2.0 h was selected for the biotic copper adsorption experiments for the remainder of the study.

Cu(II) adsorption experiments were conducted over pH 3-8 and with a range of biomass concentrations (Fig. 3.1). As was observed by Borrok et al. (2005), Cu(II) adsorption by the bacteria was at a minimum at pH 3 ($9.4 \pm 7.3\%$) and increased to a maximum at pH 8 ($92.5 \pm 1.4\%$). This is also consistent with prior work by Moon et al. (2011) who observed an adsorption

maximum at pH 6 with approximately 90% Cu adsorbed at that point. However that study was conducted using 0.6 dry g/l bacteria and about 7.0×10^{-5} M (4.4 ppm) Cu(II), as compared to 0.44 dry g/l bacteria and 3 ppm Cu(II) in this study. Also, Moon et al. (2011) used *Bacillus subtilis* which is a Gram positive bacterium and it has been demonstrated that there are approximately 40% more surface sites on Gram positive bacteria than Gram negative bacteria due to the lack of a peptidoglycan outer layer on gram negative cells.⁴⁶

Surface complexation models were created for the experimental data using previously published stability constants for a variety of metals and bacterial surfaces (Table 3.2).^{45,48} This model fit the experimental data from this study well with a variance of 3.7 for the data below pH 7. Data from above pH 7 were excluded from the modeling because under these conditions the solution was supersaturated with respect to CuCO_3 (s) (Fig. 3.1). Although the model underestimated the amount of adsorption that occurred, it was within one standard deviation of the experimental data for all pH values.

As a function of time at pH 5.2 there was an average of $56.5 \pm 8.5\%$ adsorption over the 24 h period which was consistent with the kinetics experiments (Figs. 3.1 and 3.3). The fact that there was little variation over time was likely due to the unchanging concentration of biomass: the cells were in an inert electrolyte (0.01 M NaNO_3) therefore although cell lysis may have occurred the overall concentration of surface sites would have remained approximately constant. The SCM created had a variance of 7.1 and modeled copper adsorption to bacterial cells well over the 24 h period (Fig. 3.3).

3.3.2 Copper adsorption to abiotic iron oxides

Over the 7.0 h period the kinetics experiments showed an average of $2.5 \pm 8.5\%$ Cu adsorbed onto iron oxide (Fig. 3.1). This is similar to the bacterial kinetics as both showed increasing adsorption of Cu until 2 h and then constant adsorption within one standard deviation

from 2 to 7 h. Therefore an equilibration time of 2 h was selected to evaluate Cu(II) adsorption by the abiotic iron oxides and by the bacteria-iron oxide composites.

The experiments conducted over pH 3-8 and a range of mineral concentrations showed similar trends compared to the bacterial experiments. In both cases there was a observed minimum at pH 3 ($0.0 \pm 3.3\%$) and a maximum at pH 8 ($96.9 \pm 4.7\%$) (Fig. 3.1). However there was significantly less adsorption onto the mineral at circumneutral and slightly acidic pH values with only $6.2 \pm 7.4\%$ Cu adsorbed at pH 5. This would indicate that iron oxides have a lower concentration of surface sites than bacterial cells. A model was made using all of the abiotic data over a range of pH below pH 6 as the solution was saturated with respect to CuCO_3 (s) at higher pH and had a variance of 0.9 (Fig. 3.1). The model predicted adsorption within one standard deviation of the experimental data over the pH range included (pH 3-6) and was a good fit.

$[\text{Fe(II)}]_{\text{aq}}$ in samples analyzed before copper addition increased from 0.2 ± 0.7 ppm to a maximum at 2 h of 16.0 ± 8.0 ppm and then decreased to 0.0 ± 0.4 ppm at 24 h (Fig. 3.2). $[\text{Fe(II)}]_{\text{aq}}$ in samples analyzed after a 2 h equilibration with 3 ppm Cu(II) began at 0.0 ± 0.4 ppm at 0 h, increased to 10.4 ± 6.3 ppm and decreased to 0.0 ± 0.5 at 24 h (Fig. 3.2). The samples analyzed before copper addition had higher $[\text{Fe(II)}]_{\text{aq}}$ until 8 h. This is compared to Chapter 2 in which there was no observed difference in $[\text{Fe(II)}]_{\text{aq}}$ between samples with no selenate and those equilibrated for 2 h with 3 ppm selenate so no iron oxide was precipitated during that 2 h. In contrast there was less $\text{Fe(II)}_{\text{aq}}$ in solution in the samples equilibrated with 3 ppm Cu(II) than those with no added Cu(II) so there was iron oxide precipitated during the equilibration time. However, the apparent increased Fe(II) oxidation rate in the presence of copper as opposed to selenate (Figs. 2.2 and 3.2) could simply be due to the higher pH of the copper synthesis experiments (pH 5.2) versus the selenate experiments (pH 4.0). This observed decrease in $[\text{Fe(II)}]_{\text{aq}}$ in the presence of Cu was likely due to the co-precipitation of Cu(II) by iron oxide as was previously observed by Karthikeyan et al. (1999) and was confirmed by the better fit of the

model when co-precipitation reactions from Karthikeyan et al. (1999) were included. There was an average of $18.3 \pm 3.7\%$ Cu adsorbed over the 24 h experimental period in the abiotic samples (Fig. 3.3). There was some slight variation in the extent of Cu sorbed but it was within one standard deviation at all times. This is significantly less than the previously reported Cu(II) adsorption to ferrihydrite by Moon et al. (2012) who found that at pH 5.06 there was 0.27 wt% Cu (12.1 ppm) adsorbed.¹⁹ However the ferrihydrite used by Moon et al. (2012) was synthesized at pH 7.5 and washed prior to their adsorption experiments whereas the iron oxide phase in this study was synthesized at pH 6 and used immediately during and after FeCl_2 addition. Due to these differences it is expected that there are significant differences in the adsorption capacity of the iron oxides used in this study versus those used by Moon et al. (2012).

The model for copper adsorption to iron oxide as a function time was created using stability constants from prior work and had a variance of 5.4 (Table 3.3).^{42,43} This model was run to optimize the concentration of iron oxide surface sites and gave $5.2 \pm 0.2 \times 10^{-4}$ mol sites/g iron oxide as the optimized value with a variance of 0.85. The model included a second type of iron oxide surface site which was used to describe Cu(II) co-precipitation with iron oxide based on an approach used by Karthikeyan et al. (1999) which was adapted for use in this study. The model differs in that in this study the co-precipitation reaction assumes a stoichiometric coefficient of 2 for Cu(II) while Karthikeyan et al. (1999) assumed a coefficient of 1. In this study it was found that a coefficient of 2 gave a better fit. Also the surface area of the iron oxide was determined by BET analysis to be $301 \text{ m}^2/\text{g}$ after 24 h, which was the value used in all models that included iron oxide in this study although there may have been variation in the actual surface area with time. The model provided a good fit although it underpredicted adsorption at the early time points (low iron oxide densities) which was inferred to be due to co-precipitation of copper with iron oxide while the FeCl_2 solution was being added. However the model overestimated removal at the later

time points which was attributed to aggregation of the iron oxide over time leading to a larger surface area and fewer surface sites available per g of iron oxide.

3.3.3 Copper adsorption to bacteria-iron oxide composites

[Fe(II)]_{aq} in samples with no copper at 0 h were 0.0 ± 0.3 ppm which increased to a maximum at 2 h of 24.3 ± 4.0 ppm and decreased at 24 h to 0.0 ± 0.3 ppm (Fig. 3.2). [Fe(II)]_{aq} in samples taken after the 2 h equilibration with copper were 0.0 ± 0.3 ppm at 0 h, increased to 14.0 ± 2.5 ppm at 2 h, and decreased to 0.0 ± 0.03 ppm at 24 h. This is the same overall trend observed in the abiotic treatment but the Fe(II)_{aq} concentrations were greater for the composites with a more significant difference in the samples analyzed before copper was added as compared to those analyzed after the 2 h equilibration. This difference is likely due to the same effect as in the abiotic treatment which was attributed to co-precipitation of Cu with iron oxide. The enhanced Fe(II) oxidation and precipitation rates observed in the abiotic treatment versus the composite were likely due to bacterial inhibition of Fe oxidation and hydrolysis as Fe(II) preferentially adsorbs to bacterial surfaces which prevents Fe(II) hydrolysis and reduces the rate of Fe(II) removal.³⁶

Cu adsorption to composites was $56.6 \pm 2.0\%$ at 0 h and was stable until 8 h when adsorption decreased to a final value of $32.0 \pm 5.2\%$ at 24 h (Fig. 3.3). Most of the adsorption that was observed could be attributed to the bacterial fraction as there was a similar amount of adsorption in the bacterial treatment. This decrease was inferred to be due to masking surface sites in the composite as all Fe was in the solid phase after 8 h (Fig. 3.2). This was observed in both SEM and TEM images collected of the composite material of the 0, 3, 7, 10, and 24 h samples (Figs. 3.4 and 3.5). In a prior study by Daughney et al. (2011) it was been found that the adsorption capacity of composite material is dependent on the ratio of iron oxide/ bacteria present as Fe(II) can compete with metal cations for bacterial surface sites and therefore masks sites from adsorption by other metal cations. Also it was found during modeling that co-precipitation of

Cu(II) with iron oxide occurred prior to 7 h when Fe(II) was still added to solution during modelling which caused there to be more copper removal at early time points than predicted by adsorption alone.²⁹

Composite samples were imaged with both SEM and TEM at the same time points (Figs. 3.4 and 3.5). It was observed using SEM that iron oxide began to appear visibly at 3 h and increased in cell coverage for the course of the experimental period (Fig. 3.4). After 24 h, it was observed through SEM that the iron oxide appeared to be denser and some areas appeared to be partially crystalline with larger nodules formed. The TEM images showed that iron oxide began to form as small nodes at 1 h (Fig. 3.5) which increased in size over time until the cells were completely enclosed at 24 h. Additionally, the iron oxide appeared to be more concentrated at the 10 and 24 h times points with all cells completely surrounded at 24 h (Fig. 3.5). These observations support the hypothesis that the decreased adsorption observed in the composite samples versus the abiotic and biotic samples is likely due to masking of surface sites. Both SEM and TEM images showed increasing coverage of the bacterial cells with more FeCl₂ addition and aggregation over time which corresponds to the observed decrease in Cu adsorption after 8 h. Additionally SEM images were taken of the abiotic iron oxides over time (Fig. 3.6) and showed the progressive aggregation of the iron oxides as a function of time was similar to the composite samples (Fig. 3.4).

The composite SCM was not a good fit to the experimental data with a variance of 20.3 even after the inclusion of the co-precipitation reactions (Fig. 3.3). It overpredicted copper adsorption at early time points (low iron oxide densities) in the experiment and significantly overpredicted Cu removal after 7 h. This was due to the inability of the model to correctly account for decrease in available surface sites due to iron oxide and bacterial site masking as the composites formed. The model used included reactions for Fe(II) adsorption to the bacterial sites which described accurately masking by Fe(II)_{aq} at early time points when FeCl₂ was still added to

the suspension. However there was little $\text{Fe(II)}_{\text{aq}}$ after 7.0 h in the samples equilibrated for 2 h with copper (2.7 ± 1.8 ppm) so these adsorption reactions had a negligible influence on Cu removal after that time. After 7 h surface site masking would have been dominated by iron oxide surface site complexation to bacterial sites however as these reactions were not including in the SCM, it could not account for the experimental decrease in available mineral and bacterial surface sites which led to an overprediction of Cu removal. Models were also run which optimized for the concentration of available iron oxide adsorption surface sites and the percentage of surface sites masked over time which gave variances which were all less than 5 and fit the data perfectly (Fig. 3.3). However the model run over all time points had a variance of 20.3, and could not account for the decrease in both iron oxide and bacterial surface sites due to masking. In this case, it could not fit the data as well as the models that were run separately for each time point.

3.4 Conclusions

Copper removal in the presence of iron oxide-bacteria composites was found to be governed by several processes during the addition and eventual precipitation of $\text{Fe(II)}_{\text{aq}}$ as Fe(III) -oxide including co-precipitation with iron oxide and adsorption by both iron oxide and bacterial cells. At the earlier time points copper was removed mainly through adsorption to the cells and to a lesser extent also through co-precipitation with iron oxide (0-7 h). After 7 h no $\text{Fe(II)}_{\text{aq}}$ was added and most Fe(II) had already been precipitated as iron oxide. Hence after 7 h copper removal was controlled solely adsorption to both bacterial and mineral surface sites however the concentration of available surface sites decreased over time which was inferred to be caused by interactions between the mineral and bacteria (e.g. masking of surface sites). These results imply that in natural systems the interactions between sorbents can significantly decrease sorption capacity leading to decreased metal cation removal. Also co-precipitation of metal cations with iron oxide minerals is a potential removal pathway when $\text{Fe(II)}_{\text{aq}}$ is present. In conclusion this

study demonstrates the significant impact that bacteria-mineral composites can have on metal removal especially during the precipitation of minerals.

Figure 3.1: (A) The percent of copper adsorbed onto iron oxide over pH 3-8 and at mineral concentrations of 0.108 g/l (diamonds), 0.054 g/l (squares), and 0.025 g/l (triangles). Surface complexation models (SCMs) are shown for 0.108 g/l (solid line), 0.054 g/l (dashed line), and 0.025 g/l (dotted line). (B) The percent of copper adsorbed onto *E. coli* cells over pH 3-8 and biomass concentrations of 0.44 dry g/l (diamonds), 0.22 dry g/l (squares), and 0.11 dry g/l (triangles). SCMs are shown for 0.44 dry g/l (solid line), 0.22 dry g/l (dashed line), and 0.11 dry g/l (dotted line). (C) The percent of copper adsorbed over time at pH 5.2±0.03 onto 0.108 g/l iron oxide (closed diamonds) and 0.44 dry g/l bacterial cells (open diamonds). All data are averages with error bars showing one standard deviation (n=3). Models on iron oxide were run over pH 3-6 and onto bacterial cells over pH 3-7 as above those pH values the solutions were saturated with respect to CuCO_3 (s).

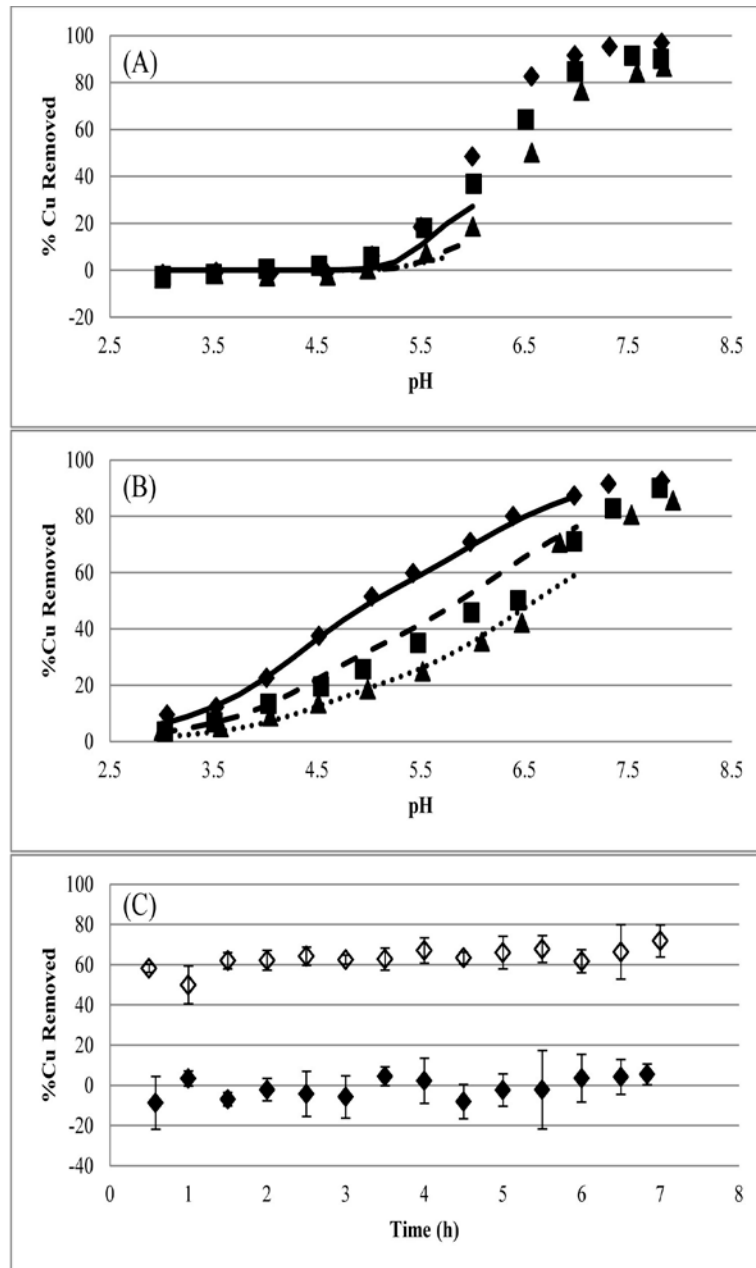


Figure 3.2: $\text{Fe(II)}_{\text{aq}}$ concentrations in ppm obtained using 1,10-phenanthroline are shown for (A) abiotic iron oxide samples and (B) iron oxide-bacteria composite samples over 24 h. $\text{Fe(II)}_{\text{aq}}$ was added for only the first 6.66 h for a total of 48.0-mL FeCl_2 added. In both graphs the samples analyzed before Cu(II) addition (solid diamonds) and samples analyzed after a 2 h equilibration with Cu(II) (open diamonds) are shown with errors bars of one standard deviation ($n=3$). There was variation between replicates (e.g. temperature, humidity) which slightly affected the rate of Fe(II) oxidation and led to larger standard deviations. However, this was accounted for in the surface complexation models by modelling all data for all replicates simultaneously.

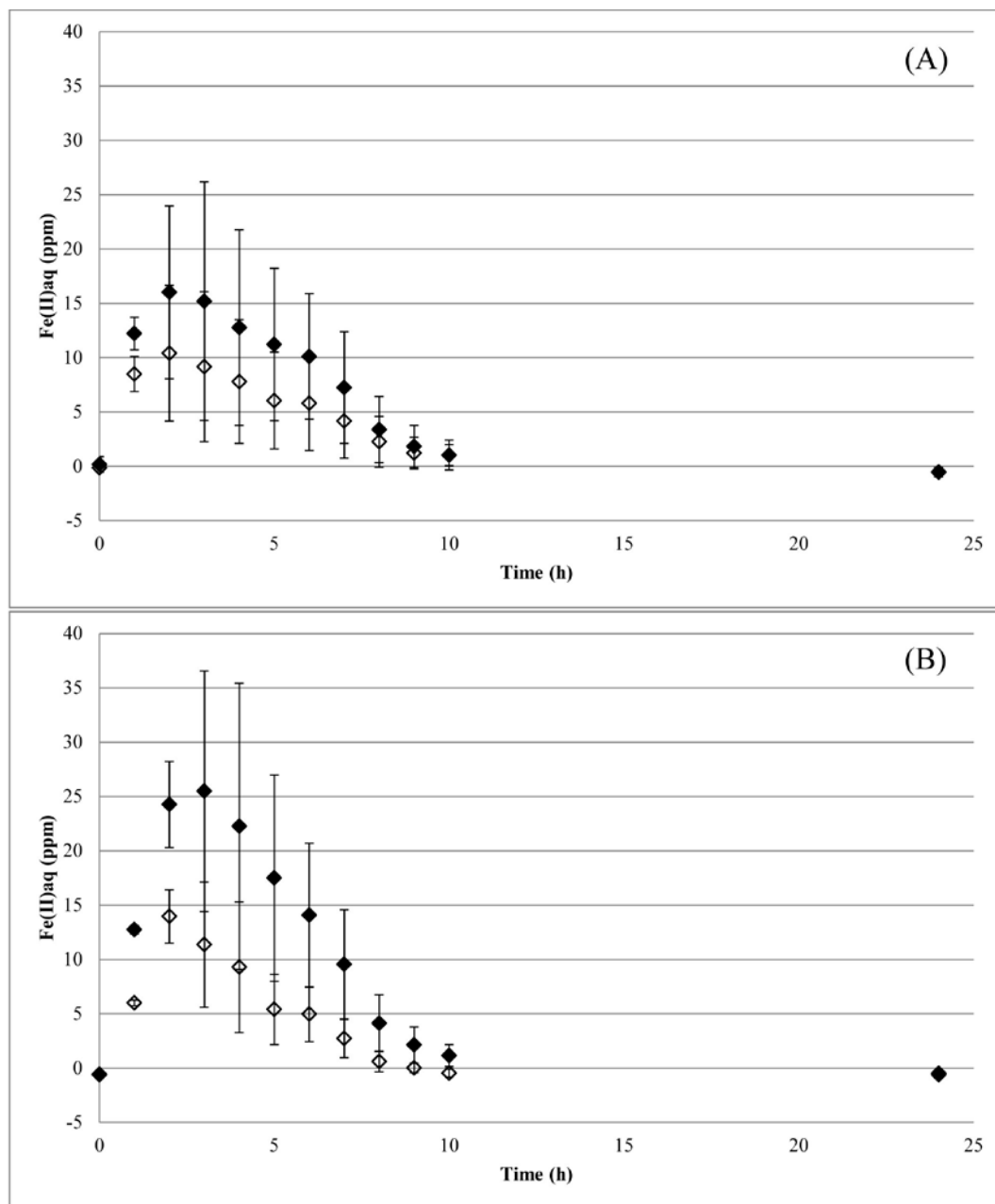


Figure 3.3: The percentage of copper removed of the 3 ppm Cu(II) initially added to each sample is shown over 24 h with the abiotic (closed diamonds), biotic (open diamonds), and composite (shaded diamonds) results shown with error bars of one standard deviation (n=3). Surface complexation modeling results over all time points are shown for the abiotic (solid line), biotic (dashed line), and composite (dotted line) samples. The composite model run separately for each time point to optimize for the concentration of iron oxide surface sites with a different percentage of iron oxide and bacterial surface sites masked is also shown (dash-dot line).

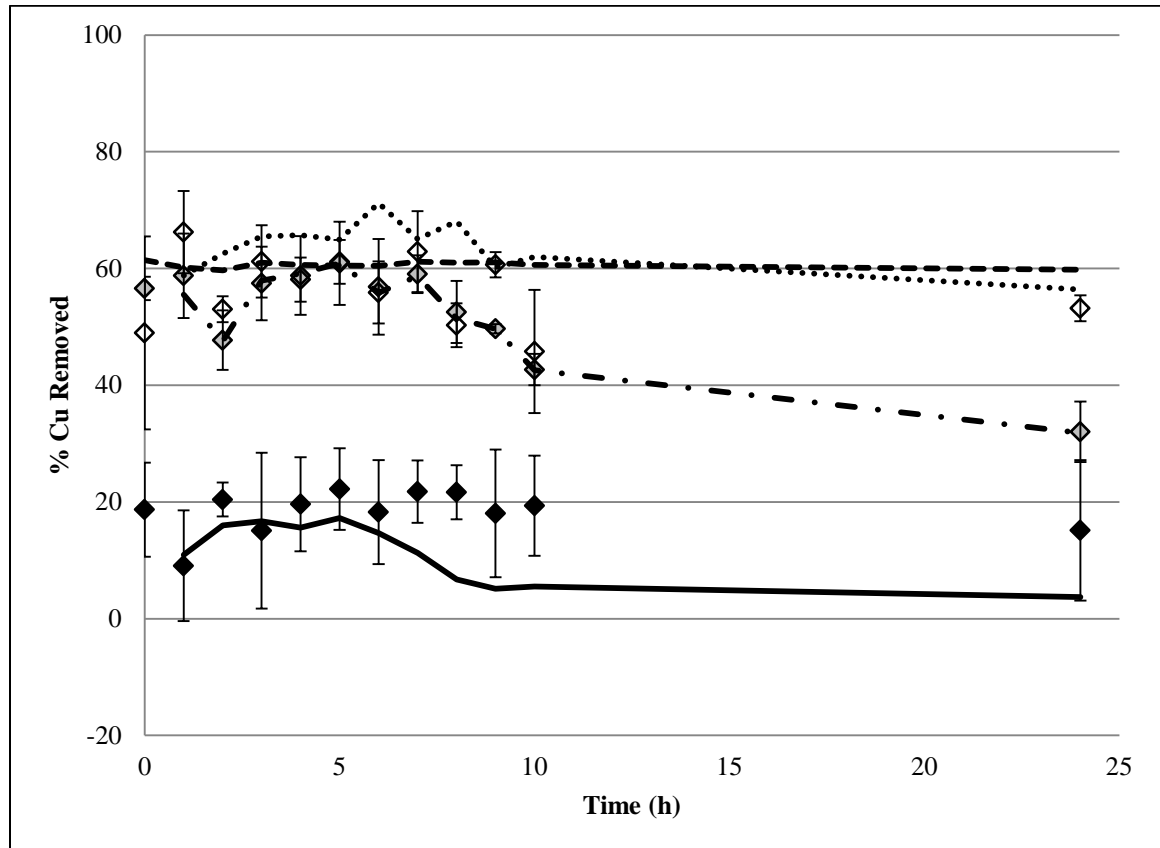


Figure 3.4: Backscatter electron-scanning electron microscopy (BSE-SEM) images of composite samples after a 2 h equilibration with 3 ppm Cu showing (A) 1 h, (B) 3 h, (C) 7 h, (D) 10 h, and (E) 24 h at 2000x magnification and white scale bars denoting 20 μm . (F) 1 h, (G) 3 h, (H) 7 h, (I) 10 h, (J) 24 h at 4000x magnification with white scale bars denoting 10 μm . All images were taken at 10.0 kV and ~ 80 Pa.

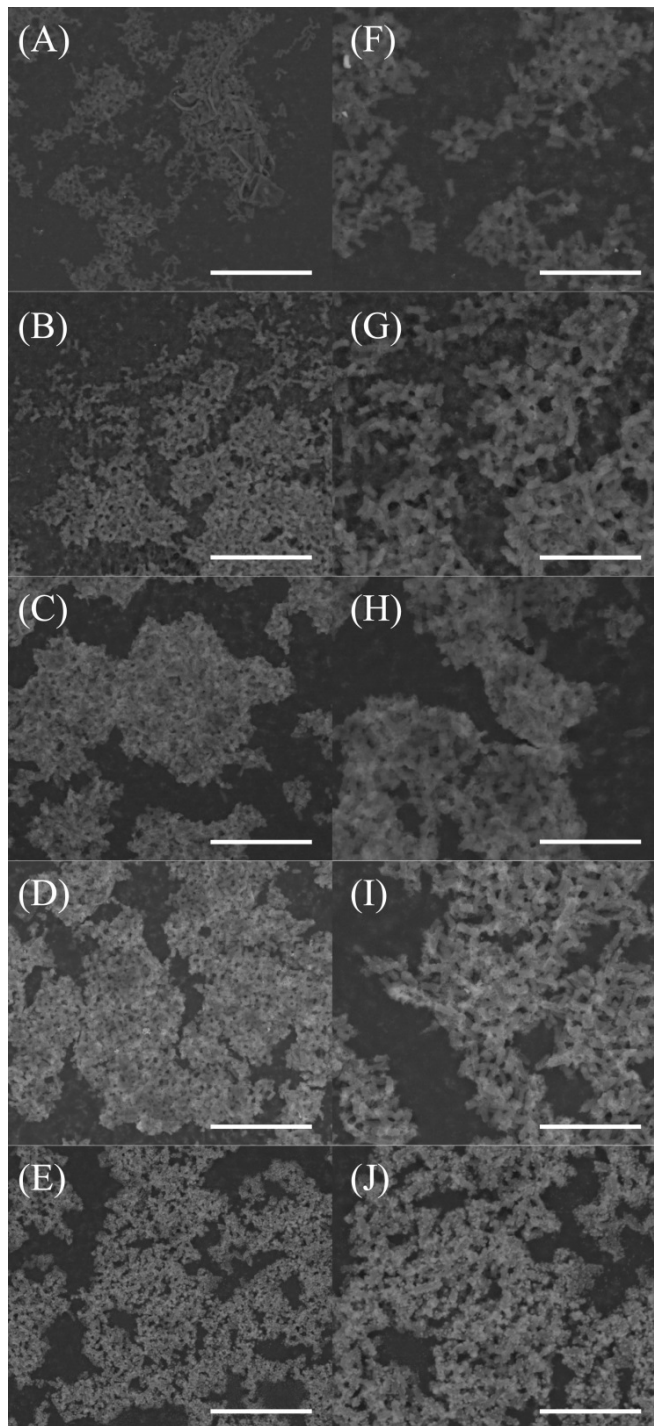


Figure 3.5: Transmission electron microscopy (TEM) micrographs of (A) 1 h, (B) 3 h, (C) 7 h, (D) 10 h, and (E) 24 h composite samples with 3 ppm added copper and white scale bars denoting 0.2 μm . (F) 1 h, (G) 3 h, (H) 7 h, (I) 10 h, and (J) 24 h composite samples with 3 ppm added copper and white scale bars showing 0.1 μm .

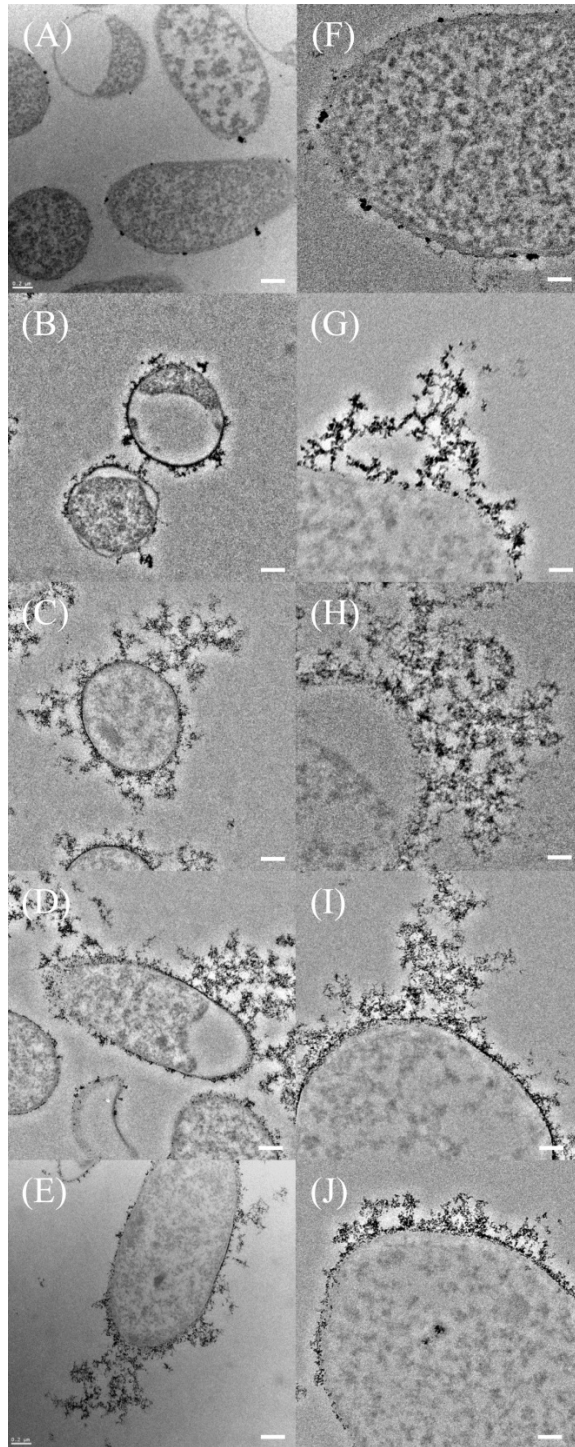


Figure 3.6: Backscatter electron-scanning electron microscopy (BSE-SEM) images of abiotic iron oxides equilibrated with 3 ppm copper for 2 h at (A) 3h, (B) 10 h, and (C) 24 h. All white scale bars denote 10 μm . The cubic objects in (C) were identified as salt (NaCl) crystals by scanning electron microscopy-energy dispersive x-ray spectroscopy (SEM-EDS).

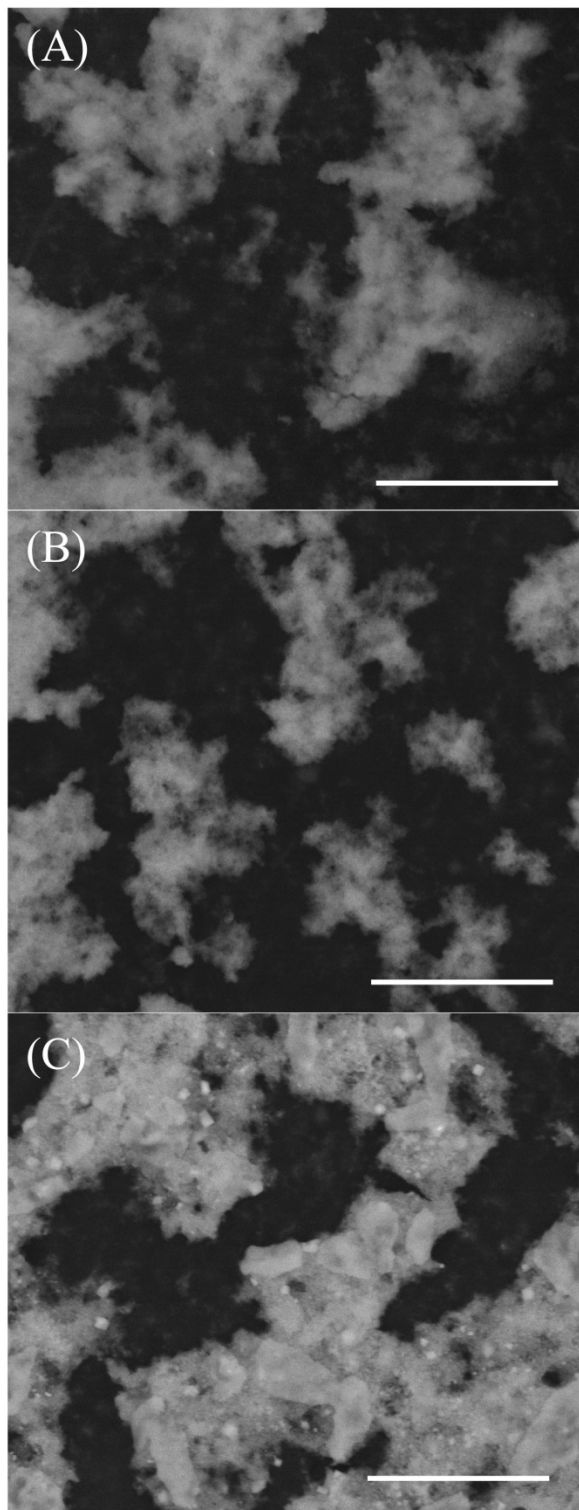


Table 3.2: Overview of prior studies examining metal(loid) cation and oxyanion adsorption onto composite mixtures of bacteria and iron oxide minerals with the sorbate, the observed dominant sorbent, and the observed additive or non-additive behavior of the system shown.

Study	Sorbate	Dominant Sorbent	Additive?
Small et al. (1999)	Sr^{2+}	Bacteria	No
Templeton (2003a,b)	Pb^{2+}	Mineral	Yes
Martinez et al. (2004)	Cd^{2+}	Bacteria	No
Kulczycki et al. (2005)	Cd^{2+} , Pb^{2+}	Bacteria	No
Chen et al. (2008)	Cu^{2+} , Zn^{2+}	Bacteria	Yes
Langley et al. (2009)	Sr^{2+}	Not determined	Not determined
Song et al. (2009)	Cd^{2+}	Both	No
Daughney et al. (2011)	Cd^{2+}	Bacteria	No
Moon et al. (2012, 2013)	Cu^{2+}	Both	Both

Table 3.2: Characteristics of the *E. coli* cells used in surface complexation modeling of the biotic system after Borrok et al. (2005) and Johnson et al. (2007).

Characteristic	Mean \pm σ	Source
Dry biomass concentration (g/l)/optical density (600 nm)	0.6528	This study
Site 1 concentration (10^{-4} mol/l)	2.86 ± 0.76	Borrok et al. (2005)
Site 2 concentration (10^{-4} mol/l)	3.23 ± 0.23	Borrok et al. (2005)
Site 3 concentration (10^{-4} mol/l)	2.21 ± 0.23	Borrok et al. (2005)
Site 4 concentration (10^{-4} mol/l)	1.68 ± 0.17	Borrok et al. (2005)
$\text{Log } K, R_1\text{-H} + \text{Cu}^{2+} \rightleftharpoons R_1\text{-Cu} + \text{H}^+$	-0.34	Johnson et al. (2007)
$\text{Log } K, R_2\text{-H} + \text{Cu}^{2+} \rightleftharpoons R_2\text{-Cu} + \text{H}^+$	-0.97	Johnson et al. (2007)
$\text{Log } K, R_3\text{-H} + \text{Cu}^{2+} \rightleftharpoons R_3\text{-Cu} + \text{H}^+$	-2.29	Johnson et al. (2007)
$\text{Log } K, R_4\text{-H} + \text{Cu}^{2+} \rightleftharpoons R_4\text{-Cu} + \text{H}^+$	-2.60	Johnson et al. (2007)
$\text{Log } K, R_1\text{-H} \rightleftharpoons R_1^- + \text{H}^+$	-3.1	Johnson et al. (2007)
$\text{Log } K, R_2\text{-H} \rightleftharpoons R_2^- + \text{H}^+$	-4.7	Johnson et al. (2007)
$\text{Log } K, R_3\text{-H} \rightleftharpoons R_3^- + \text{H}^+$	-6.6	Johnson et al. (2007)
$\text{Log } K, R_4\text{-H} \rightleftharpoons R_4^- + \text{H}^+$	-9.0	Johnson et al. (2007)
$\text{Log } K, R_1\text{-H} + \text{Fe}^{2+} \rightleftharpoons R_1\text{-Fe} + \text{H}^+$	-0.32	This study
$\text{Log } K, R_2\text{-H} + \text{Fe}^{2+} \rightleftharpoons R_2\text{-Fe} + \text{H}^+$	-0.25	This study
$\text{Log } K, R_3\text{-H} + \text{Fe}^{2+} \rightleftharpoons R_3\text{-Fe} + \text{H}^+$	-1.59	This study
$\text{Log } K, R_4\text{-H} + \text{Fe}^{2+} \rightleftharpoons R_4\text{-Fe} + \text{H}^+$	-1.46	This study

Table 3.3: Characteristics of the iron oxide minerals used in surface complexation modeling of the abiotic system after the triple layer models of Peacock and Sherman (2004) for lepidocrocite and co-precipitation stability constant from Karthikeyan et al. (1999).

Characteristic	Mean \pm σ	Source ^b
Iron oxide surface area (m ² /g)	301 ^a	This study
Iron oxide concentration (g/l)	0.109 \pm 0.001	This study
Iron oxide site concentration (10 ⁻⁵ mol/l)	5.23 \pm 0.21	This study
Iron oxide molar mass (g/mol)	88.85	1
Capacitance 0 (F/m ²)	1.0	2
Capacitance B (F/m ²)	0.2	2
Log K, 2 \equiv FeOH + Cu ²⁺ + 2H ₂ O \rightleftharpoons (FeO) ₂ Cu(OH) ₂ ²⁻ + 2H ⁺	-2.45	3
Log K, 3 \equiv FeOH + 2Cu ²⁺ + 3H ₂ O \rightleftharpoons (Fe ₃ O(OH) ₂)Cu ₂ (OH) ₃ + 4H ⁺	-4.28	3
Log K(co-precipitation), \equiv FeOH + 2Cu ²⁺ \rightleftharpoons FeOCu ₂ ³⁺ + H ⁺	4.61	4 ^c
Log K, \equiv FeOH + H ⁺ \rightleftharpoons FeOH ₂ ⁺	6.9	5
Log K, \equiv FeOH \rightleftharpoons \equiv FeO ⁻ + H ⁺	-10.9	5
Log K, \equiv FeOH + Na ⁺ \rightleftharpoons \equiv FeO ⁻ Na ⁺ + H ⁺	-9.6	5
Log K, \equiv FeOH + NO ₃ ⁻ \rightleftharpoons \equiv FeOH ₂ ⁺ NO ₃ ⁻	8.4	5
Log K, \equiv FeOH + H ₂ CO ₃ \rightleftharpoons \equiv FeOCOO ⁻ + H ⁺ + H ₂ O	-2.68	5
Log K, \equiv FeOH + H ₂ CO ₃ \rightleftharpoons \equiv FeOCOOH + H ₂ O	2.15	5
Log K, \equiv FeOH + H ₂ CO ₃ + Na ⁺ \rightleftharpoons \equiv FeOCOONa + H ⁺	-3.23	5

^aThe surface area was assumed to be 301 m²/g at all times.

^b Sources: 1) Langmuir (1997), 2) Fukushima and Sverjenski (2007); 3) Peacock and Sherman (2004), 4) Karthikeyan et al. (1999), and 5) Villalobos and Leckie (2001).

^c The stability constant (log K) for co-precipitation was optimized during this study but the co-precipitation reaction was similar that used by Karthikeyan et al. (1999).

3.5 References

- (1) Mullen, M. D.; Wolf, D. C.; Ferris, F. G.; Beveridge, T. J.; Flemming, C. A.; Bailey, G. W. Bacterial sorption of heavy metals. *Appl. Environ. Microbiol.* **1989**, *55*, 3143–9.
- (2) Ferris, F. G.; Beveridge, T. J. Site specificity of metallic ion binding in *Escherichia coli* K-12 lipopolysaccharide. *Can. J. Microbiol.* **1986**, *32*, 52–55.
- (3) Ferris, F. G.; Beveridge, T. J. Binding of a paramagnetic metal cation to *Escherichia coli* K-12 outer-membrane vesicles. *FEMS Microbiol. Lett.* **1984**, *24*, 43–46.
- (4) Kulczycki, E.; Ferris, F. G. Impact of cell wall structure on the behavior of bacterial cells as sorbents of cadmium and lead. *Geomicrobiol. J.* **2002**, *19*, 553–565.
- (5) Boyanov, M. I.; Kelly, S. D.; Kemner, K. M.; Bunker, B. A.; Fein, J. B.; Fowle, D. A. Adsorption of cadmium to *Bacillus subtilis* bacterial cell walls: A pH-dependent X-ray absorption fine structure spectroscopy study. *Geochim. Cosmochim. Acta* **2003**, *67*, 3299–3311.
- (6) Wightman, P.; Fein, J. Iron adsorption by *Bacillus subtilis* bacterial cell walls. *Chem. Geol.* **2005**, *216*, 177–189.
- (7) Yee, N.; Fein, J. Cd adsorption onto bacterial surfaces: A universal adsorption edge? *Geochim. Cosmochim. Acta* **2001**, *65*, 2037–2042.
- (8) Burnett, P. G. G.; Daughney, C. J.; Peak, D. Cd adsorption onto *Anoxybacillus flavithermus*: Surface complexation modeling and spectroscopic investigations. *Geochim. Cosmochim. Acta* **2006**, *70*, 5253–5269.
- (9) Daughney, C. J.; Fowle, D. a; Fortin, D. E. The effect of growth phase on proton and metal adsorption by *Bacillus subtilis*. *Geochim. Cosmochim. Acta* **2001**, *65*, 1025–1035.
- (10) Dzombak, D. A.; Morel, F. M. M. *Surface Complexation Modeling, Hydrous Ferric Oxide*; Wiley Interscience: New York, 1990.
- (11) Cox, J. S.; Smith, D. S.; Warren, L. a; Ferris, F. G. Characterizing heterogeneous bacterial surface functional groups using discrete affinity spectra for proton binding. *Environ. Sci. Technol.* **1999**, *33*, 4514–4521.
- (12) Daughney, C. J.; Hetzer, A.; Heinrich, H. T. M.; Burnett, P. G. G.; Weerts, M.; Morgan, H.; Bremer, P. J.; McQuillan, a J. Proton and cadmium adsorption by the

archaeon *Thermococcuse zilligii*: Generalising the contrast between thermophiles and mesophiles as sorbents. *Archaea* **2010**, 273, 1–42.

- (13) Spadini, L.; Schindler, P. W.; Charlet, L.; Manceau, A.; Vala Ragnarsdottir, K. Hydrous ferric oxide: evaluation of Cd-HFO surface complexation models combining Cd(K) EXAFS data, potentiometric titration results, and surface site structures identified from mineralogical knowledge. *J. Colloid Interface Sci.* **2003**, 266, 1–18.
- (14) Karthikeyan, K.; Elliott, H. Surface complexation modeling of copper sorption by hydrous oxides of iron and aluminum. *J. Colloid Interface Sci.* **1999**, 220, 88–95.
- (15) Small, T. D.; Warren, L. A.; Ferris, F. G. Influence of ionic strength on strontium sorption to bacteria, Fe(III) oxide, and composite bacteria-Fe(III) oxide surfaces. *Appl. Geochemistry* **2001**, 16, 939 – 946.
- (16) Small, T. D.; Warren, L. A.; Roden, E. E. Sorption of strontium by bacteria, Fe(III) oxide, and bacteria-Fe(III) oxide composites. *Environ. Sci. Technol.* **1999**, 33, 4465–4470.
- (17) Kulczycki, E.; Fowle, D.; Fortin, D.; Ferris, F. G. Sorption of cadmium and lead by bacteria–ferrihydrite composites. *Geomicrobiol. J.* **2005**, 22, 299–310.
- (18) Templeton, A. S.; Spormann, A. M.; Brown Jr., G. E. Speciation of Pb(II) sorbed by *Burkholderia cepacia*/goethite composites. *Environ. Sci. Technol.* **2003**, 37, 2166–2172.
- (19) Moon, E. M.; Peacock, C. L. Adsorption of Cu(II) to ferrihydrite and ferrihydrite–bacteria composites: Importance of the carboxyl group for Cu mobility in natural environments. *Geochim. Cosmochim. Acta* **2012**, 92, 203–219.
- (20) Moon, E. M.; Peacock, C. L. Modelling Cu(II) adsorption to ferrihydrite and ferrihydrite–bacteria composites: Deviation from additive adsorption in the composite sorption system. *Geochim. Cosmochim. Acta* **2013**, 104, 148–164.
- (21) Daughney, C. J.; Fakihi, M.; Châtellier, X. Progressive sorption and oxidation/hydrolysis of Fe(II) affects cadmium immobilization by bacteria-iron oxide composites. *Geomicrobiol. J.* **2011**, 28, 11–22.
- (22) Templeton, A. S.; Trainor, T. P.; Spormann, A. M.; Newville, M.; Sutton, S. R.; Dohnalkova, A.; Gorby, Y.; Brown, G. E. Sorption versus biomineralization of Pb(II) within *Burkholderia cepacia* biofilms. *Environ. Sci. Technol.* **2003**, 37, 300–307.

- (23) Martinez, R. E.; Pedersen, K.; Ferris, F. G. Cadmium complexation by bacteriogenic iron oxides from a subterranean environment. *J. Colloid Interface Sci.* **2004**, *275*, 82–9.
- (24) Chen, X.; Chen, L.; Shi, J.; Wu, W.; Chen, Y. Immobilization of heavy metals by *Pseudomonas putida* CZ1/goethite composites from solution. *Colloids Surf. B. Biointerfaces* **2008**, *61*, 170–5.
- (25) Langley, S.; Gault, A. G.; Ibrahim, A.; Takahashi, Y.; Renaud, R. O. B. Sorption of strontium onto bacteriogenic iron oxides. *Environ. Sci. Technol.* **2009**, *43*, 1008–1014.
- (26) Song, Y.; Swedlund, P. J.; Singhal, N.; Swift, S. Cadmium(II) speciation in complex aquatic systems: A study with ferrihydrite, bacteria, and an organic ligand. *Environ. Sci. Technol.* **2009**, *43*, 7430–7436.
- (27) Daughney, C. J.; Châtellier, X.; Chan, A.; Kenward, P.; Fortin, D.; Suttle, C. A.; Fowle, D. A. Adsorption and precipitation of iron from seawater on a marine bacteriophage (PWH3A-P1). *Mar. Chem.* **2004**, *91*, 101–115.
- (28) Craven, A. M.; Aiken, G. R.; Ryan, J. N. Copper(II) binding by dissolved organic matter: Importance of the copper-to-dissolved organic matter ratio and implications for the biotic ligand model. *Environ. Sci. Technol.* **2012**, *46*, 9948–9955.
- (29) Karthikeyan, K.; Elliott, H.; Chorover, J. Role of surface precipitation in copper sorption by the hydrous oxides of iron and aluminum. *J. Colloid Interface Sci.* **1999**, *209*, 72–78.
- (30) Fang, L.; Huang, Q.; Wei, X.; Liang, W.; Rong, X.; Chen, W.; Cai, P. Microcalorimetric and potentiometric titration studies on the adsorption of copper by extracellular polymeric substances (EPS), minerals and their composites. *Bioresour. Technol.* **2010**, *101*, 5774–5779.
- (31) Button, K. S.; Hostetter, H. P. Copper sorption and release by *Cyclotella meneghiniana* and *Chlamydomonas reinhardtii*. *J. Phycol.* **1977**, *13*, 198–202.
- (32) Gibert, O.; de Pablo, J.; Cortina, J. L.; Ayora, C. Sorption studies of Zn(II) and Cu(II) onto vegetal compost used on reactive mixtures for in situ treatment of acid mine drainage. *Water Res.* **2005**, *39*, 2827–38.
- (33) Beveridge, T. J.; Koval, S. F. Binding of metals to cell envelopes of *Escherichia coli* K-12. *Appl. Environ. Microbiol.* **1981**, *42*, 325–335.

- (34) Fang, L.; Cai, P.; Chen, W.; Liang, W.; Hong, Z.; Huang, Q. Impact of cell wall structure on the behavior of bacterial cells in the binding of copper and cadmium. *Colloids Surfaces A Physicochem. Eng. Asp.* **2009**, *19*, 553–565.
- (35) Châtellier, X.; West, M. M.; Rose, J.; Fortin, D.; Leppard, G.; Ferris, F. G. Characterization of iron-oxides formed by oxidation of ferrous ions in the presence of various bacterial species and inorganic ligands. *Geomicrobiol. J.* **2004**, *21*, 99–112.
- (36) Fakih, M.; Châtellier, X.; Davranche, M.; Dia, A. *Bacillus subtilis* bacteria hinder the oxidation and hydrolysis of Fe^{2+} ions. *Environ. Sci. Technol.* **2008**, *42*, 3194–3200.
- (37) Burnett, P.-G.; Heinrich, H.; Peak, D.; Bremer, P. J.; McQuillan, a. J.; Daughney, C. J. The effect of pH and ionic strength on proton adsorption by the thermophilic bacterium *Anoxybacillus flavithermus*. *Geochim. Cosmochim. Acta* **2006**, *70*, 1914–1927.
- (38) Burnett, P.-G. G.; Handley, K.; Peak, D.; Daughney, C. J. Divalent metal adsorption by the thermophile *Anoxybacillus flavithermus* in single and multi-metal systems. *Chem. Geol.* **2007**, *244*, 493–506.
- (39) Châtellier, X.; Grybos, M.; Abdelmoula, M.; Kemner, K. M.; Leppard, G. G.; Mustin, C.; West, M. M.; Paktunc, D. Immobilization of P by oxidation of Fe(II) ions leading to nanoparticle formation and aggregation. *Appl. Geochemistry* **2013**, *35*, 325–339.
- (40) Smeaton, C. M.; Fryer, B. J.; Weisener, C. G. Intracellular precipitation of Pb by *Shewanella putrefaciens* CN32 during the reductive dissolution of Pb-jarosite. *Environ. Sci. Technol.* **2009**, *43*, 8086–91.
- (41) Westall, J. C. FITEQL: A computer program for the determination of chemical equilibrium constants from experimental data **1982**, Report 82–01.
- (42) Peacock, C. L.; Sherman, D. M. Copper(II) sorption onto goethite, hematite and lepidocrocite: A surface complexation model based on ab initio molecular geometries and EXAFS spectroscopy. *Geochim. Cosmochim. Acta* **2004**, *68*, 2623–2637.
- (43) Villalobos, M.; Leckie, J. O. Surface complexation modeling and FTIR Study of carbonate adsorption to goethite. *J. Colloid Interface Sci.* **2001**, *235*, 15–32.
- (44) Langmuir, D. *Aqueous Environmental Geochemistry*; Prentice Hall: Upper Saddle River, 1997.

- (45) Johnson, K.; Szymanowski, J.; Borrok, D.; Huynh, T.; Fein, J. Proton and metal adsorption onto bacterial consortia: Stability constants for metal–bacterial surface complexes. *Chem. Geol.* **2007**, *239*, 13–26.
- (46) Borrok, D. A universal surface complexation framework for modeling proton binding onto bacterial surfaces in geologic settings. *Am. J. Sci.* **2005**, *305*, 826–853.
- (47) Moon, E. M.; Peacock, C. L. Adsorption of Cu(II) to *Bacillus subtilis*: A pH-dependent EXAFS and thermodynamic modelling study. *Geochim. Cosmochim. Acta* **2011**, *75*, 6705–6719.
- (48) Borrok, D.; Aumend, K.; Fein, J. Significance of ternary bacteria–metal–natural organic matter complexes determined through experimentation and chemical equilibrium modeling. *Chem. Geol.* **2007**, *238*, 44–62.
- (49) Cornell, R. M.; Schwertmann, U. *The Iron Oxides: Structure, Properties, Reactions, Occurrences and Uses*; 2nd ed.; Wiley & Sons, 2003.
- (50) Appelo, C. A. J.; Van Der Weiden, M. J. J.; Tournassat, C.; Charlet, L. Surface complexation of ferrous iron and carbonate on ferrihydrite and the mobilization of arsenic. *Environ. Sci. Technol.* **2002**, *36*, 3096–3103.
- (51) Hiemstra, T.; van Riemsdijk, W. H. Adsorption and surface oxidation of Fe(II) on metal (hydr)oxides. *Geochim. Cosmochim. Acta* **2007**, *71*, 5913–5933.
- (52) Liger, E.; Charlet, L.; Van Cappellen, P. Surface catalysis of uranium(VI) reduction by iron(II). *Geochim. Cosmochim. Acta* **1999**, *63*, 2939–2955.
- (53) Maithreepala, R. A.; Doong, R.-A. Synergistic effect of copper ion on the reductive dechlorination of carbon tetrachloride by surface-bound Fe(II) associated with goethite. *Environ. Sci. Technol.* **2004**, *38*, 260–8.

CHAPTER 4

CONCLUSIONS

4.1 Summary

The main goal of this thesis was to investigate the effect of the presence of bacteria-mineral composites on metal(loid) ion adsorption during the addition, oxidation, hydrolysis, and precipitation of Fe(II) to form Fe(III)-oxide under controlled laboratory conditions. A secondary goal was to assess the ability of surface complexation models to fit the experimental data. This was accomplished by conducting experiments in triplicate for selenate or copper adsorption onto iron oxide, bacteria, or bacteria-iron oxide composites. The selenate and copper experiments were conducted at pH 4.0 and pH 5.2 respectively, based on observed adsorption in the end-member single-sorbent systems (iron oxide or bacteria) over the range pH 3-8. All adsorption experiments involved a 2.0 h equilibration time, based on preliminary kinetics experiments. Aqueous phase Fe(II), selenate, and copper concentrations were monitored via 1,10-phenanthroline and ICPOES and solid phase Fe(II) and Fe(III) concentrations were determined by acid digestion followed by Ferrozine analysis.^{1,2} SEM and TEM images were taken to characterize the progressive formation of iron oxide. The BET approach was used to measure the surface area of the abiotic iron oxides after aging for 24 h; this method was found to be unsuitable for measuring the surface area of the bacteria or the bacteria-iron oxide composites.

Chapter 2 describes the adsorption of selenate onto abiotic iron oxide (no bacteria present), bacteria (no iron oxide present) and bacteria-iron oxide composites. Selenate did not adsorb to *E. coli* under any of the experimental conditions used in this study. This result is consistent with the only previous study that has investigated selenate adsorption onto bacterial cells, given the difference in experimental conditions employed.³ Selenate adsorption onto abiotic iron oxide decreased with increasing pH and increasing selenate-to-mineral concentration ratio.⁴ Experiments that tracked the adsorption of selenate during the oxidation of Fe(II) and

progressive precipitation of abiotic iron oxide revealed that 1) the presence of selenate did not affect Fe(II) oxidation rates; 2) selenate removal was due only to adsorption and not co-precipitation within the iron oxide; and 3) the density of adsorption sites on the iron oxide (mol/g) decreased with time, inferred to be the result of progressive aggregation of initially small particles. Parallel experiments were conducted to track the adsorption of selenate in the presence of *E. coli* cells during the oxidation of Fe(II) and resulting formation of bacteria-iron oxide composites. These experiments showed that 1) the presence of the bacteria decreased the rate of iron oxide precipitation, inferred to be due to Fe(II) adsorption onto the cells and resulting stabilization against ambient oxidation^{3,5}; and 2) selenate adsorption onto the bacteria-iron oxide composites was significantly reduced compared to the bacteria-free system, particularly for the longest reaction times. Surface complexation models (SCMs) developed to fit the experimental data suggested that the iron oxide particles formed in the presence of the bacteria initially had significantly higher adsorption site densities (mol/g) than the abiotic iron oxides formed in the absence of the cells but under otherwise identical conditions. The SCMs also indicated that the observed decrease selenate adsorption by the bacteria-iron oxide composites over time was due to masking of iron oxide adsorption sites by the bacteria, in addition to the aggregation of the mineral over time as observed in the abiotic system.

Chapter 3 evaluated copper adsorption onto abiotic iron oxide, bacteria, and bacteria-iron oxide composites. Copper adsorption onto the bacteria (in the absence of iron oxides) increased with increasing pH and increasing bacteria-to-copper concentration ratio, in agreement with previous studies.^{6,7} Similarly, in agreement with previous studies,^{6,8,9} copper adsorption onto the abiotic iron oxide (in the absence of bacteria) increased with increasing pH and increasing mineral-to-copper concentration ratio. Previously developed SCMs provided a good fit to the observed adsorption in the copper-bacteria and copper-iron oxide systems evaluated in this study.⁸⁻¹² As for the case with selenate, experiments were undertaken to track the adsorption of

copper during the oxidation of Fe(II) and progressive precipitation of abiotic iron oxide. The experiments with copper were conducted at pH 5.2, and hence the rate of Fe(II) oxidation was enhanced relative to the experiments with selenate, which were conducted at pH 4.0. As a result, some iron oxide precipitation occurred while copper was present in the system, meaning that copper was removed from solution by co-precipitation as well as adsorption, the latter being the dominant mechanism, whereas the selenate removal was entirely due to adsorption. Experiments were also conducted to track the adsorption of copper in the presence of *E. coli* cells during the oxidation of Fe(II) and resulting formation of bacteria-iron oxide composites. As observed in the selenate experiments, these experiments with copper showed that 1) the presence of the bacteria decreased the rate of iron oxide precipitation, inferred to be due to Fe(II) adsorption onto the cells and resulting stabilization against ambient oxidation^{3,5}; and 2) copper adsorption onto the bacteria-iron oxide composites was significantly reduced compared to the bacteria-free system, particularly for the longest reaction times. SCMs developed to fit the experimental data suggested that the copper adsorbed primarily to the bacterial fraction of the composites, with adsorption to or co-precipitation within the iron oxide being relatively minor. The SCMs indicated that the observed decrease copper adsorption by the bacteria-iron oxide composites over time was due to masking of bacterial adsorption sites by the iron oxide, in addition to the aggregation of the mineral over time as observed in the abiotic system.

4.2 Discussion

It would be easiest to directly compare the results from Chapters 2 and 3, however several variables should first be considered. First, the inherent differences between cations and anions cause copper and selenate to behave fundamentally differently. This was demonstrated by the fact that selenate does not adsorb to *E. coli* whereas copper adsorbs to both the bacterial cells and iron oxide (with the former sorbent being dominant for copper removal under the experimental conditions used in this study). The experiments that were performed to track the adsorption of selenate during the oxidation of Fe(II) were conducted at pH 4.0, whereas the

comparable experiments to track the fate of copper were conducted at pH 5.2. As a result, the rate of iron oxide precipitation was enhanced in the experiments performed with copper. The rate of iron oxide precipitation appeared to affect the size of the particles: it was observed by TEM imaging that the mineral phase produced at pH 5.2 had relatively larger particles than produced at pH 4.0 (Figs. 2.5 and 3.8). Moreover, the enhanced rate of oxidation in the copper experiments meant that some copper removal occurred via co-precipitation as well as via adsorption, whereas the selenate removal was only via adsorption. The co-precipitation of copper within the iron oxide may have also affected the crystallinity, morphology or surface area of the particles, which in turn may have affected their reactivity as a sorbent.

Despite differences in the conditions employed in the selenate and copper experiments, the approach of studying cationic and anionic sorbates provided greater insight into the system than could have been obtained by investigating only one sorbate. Under the conditions of each experiment, a significant fraction of either selenate or copper was removed from solution. The bacteria-free systems revealed that aggregation of the abiotic iron oxide over time led to reduced removal of both selenate and copper. The similarity of behavior of selenate and copper in the abiotic systems supports the conclusion that a common mechanism is responsible for the reduced adsorption over time, namely the progressive aggregation of initially small particles. The experiments performed with the bacteria-iron oxide composites showed that the adsorption of both selenate and copper was significantly reduced compared to the bacteria-free system, particularly for the longest reaction times. Note however that the selenate removal from solution was primarily due to adsorption onto the mineral component of the composites, whereas the copper removal was primarily due to adsorption by the bacterial component. Again, the similarity of behavior of selenate and copper points to a common mechanism, inferred to be caused by the masking of adsorption sites. For the selenate experiments the iron oxide adsorption sites were masked by the bacteria, and for the copper experiments the bacterial adsorption sites

were masked by the iron oxide. To the knowledge of the author, this is the first study that has identified the mutual masking effect caused by interactions between the two sorbents.

Based on the numbers, similar amounts of selenate and copper were removed from solution by the composites after 24 h (Figs. 2.3 and 3.3). This was expected to occur as the experimental conditions (e.g. pH, sorbate concentration) were selected on the basis of selenate or copper removed in the end-member systems such that any effects of the composites would be noticeable experimentally. However it would be difficult to find such simple systems with the right environmental conditions (e.g. pH, ionic strength) in nature. Therefore in the future more complex experiments should be performed to account for the effects of varied pH and ionic strength, temperature, diverse bacterial communities, the presence/absence of $\text{Fe(II)}_{\text{aq}}$, and varied sorbate/sorbent ratios. Although this thesis did not consider the mentioned variables it is the basis for future laboratory and field work and offers the first look at the adsorption of metal oxyanions onto bacteria-mineral composites. Additionally the effect of the presence of bacterial cells on selenate removal and the presence of iron oxide on copper removal allowed for the elucidation of the effects that bacteria-iron oxide composites may have on the removal of metal(loid)s and the mechanisms of those effects.

4.3 Conclusions

The initial hypothesis was “that a decrease in adsorption (e.g. non-additive behavior) will be observed in the presence of bacteria-iron oxide composites as compared to adsorption in the end-member systems (e.g. bacteria or iron oxide).” This was observed in both the selenate and copper adsorption experiments after 24 h. However the extent of adsorption in the selenate composite experiments was consistently intermediate to the abiotic and biotic systems while in the copper composite experiments there was an equivalent amount of adsorption to the biotic system until 7 h after which there was less adsorption in the composite. Overall similar amounts of adsorption were observed in the selenate and copper experiments, however they were

conducted under different pH conditions. A comparison of these two studies highlights the need for more adsorption experiments that compare the sorption of different metal(loid)s using the same experimental protocols. Additionally, as there have been no prior studies on metal oxyanion adsorption in the presence of composites, more work should be undertaken with a variety of metal oxyanions both with and without $\text{Fe(II)}_{\text{aq}}$ present to better understand metal oxyanion adsorption behavior. The two studies conducted as part of this thesis help us to better understand the differences between metal(loid) adsorption with both bacteria and minerals present versus only a single sorbent. This helps us to better understand selenate and copper cycling in contaminated systems and to potentially predict their remediation via adsorption.

4.4 Future work

The major gap in knowledge in this field currently is the lack of complexity of the studies being performed. Few dual sorbent adsorption experiments have been undertaken (Tables 2.1 and 3.1), and more should be conducted with a variety of bacterial species and metal(loid) sorbates. Additionally as Chapter 2 is the first study to examine metal(loid) oxyanion adsorption onto bacteria-iron oxide composites more studies that incorporate metal(loid) oxyanions should be performed as well. Studies that examine different types of complexity including multiple sorbates or multiple bacterial species would be a start. Also, Chapters 2 and 3 are the second and third studies to observe the effect of $\text{Fe(II)}_{\text{aq}}$ addition, oxidation, hydrolysis, and precipitation on metal(loid) adsorption.⁶ As significant effects have been observed, this is another avenue for further study. The overarching objective of these future studies should be the eventual understanding of adsorption behavior and metal(loid) removal in natural systems.

4.5 References

- (1) Viollier, E.; Inglett, P. W.; Hunter, K.; Roychoudhury, A. N.; Van Cappellen, P. The ferrozine method revisited: Fe(II)/Fe(III) determination in natural waters. *Appl. Geochemistry* **2000**, *15*, 785–790.
- (2) Stookey, L. L. Ferrozine---a new spectrophotometric reagent for iron. *Anal. Chem.* **1970**, *42*, 779–781.
- (3) Daughney, C. J.; Fakhri, M.; Châtellier, X. Progressive sorption and oxidation/hydrolysis of Fe(II) affects cadmium immobilization by bacteria-iron oxide composites. *Geomicrobiol. J.* **2011**, *28*, 11–22.
- (4) Kenward, P.; Fowle, D.; Yee, N. Microbial selenate sorption and reduction in nutrient limited systems. *Environ. Sci. Technol.* **2006**, *40*, 3782–6.
- (5) Fakhri, M.; Châtellier, X.; Davranche, M.; Dia, A. *Bacillus subtilis* bacteria hinder the oxidation and hydrolysis of Fe²⁺ ions. *Environ. Sci. Technol.* **2008**, *42*, 3194–3200.
- (6) Moon, E. M.; Peacock, C. L. Adsorption of Cu(II) to ferrihydrite and ferrihydrite–bacteria composites: Importance of the carboxyl group for Cu mobility in natural environments. *Geochim. Cosmochim. Acta* **2012**, *92*, 203–219.
- (7) Borrok, D.; Borrok, M. J.; Fein, J. B.; Kiessling, L. L. Link between chemotactic response to Ni²⁺ and its adsorption onto the *Escherichia coli* cell surface. *Environ. Sci. Technol.* **2005**, *39*, 5227–5233.
- (8) Karthikeyan, K.; Elliott, H.; Chorover, J. Role of surface precipitation in copper sorption by the hydrous oxides of iron and aluminum. *J. Colloid Interface Sci.* **1999**, *209*, 72–78.
- (9) Peacock, C. L.; Sherman, D. M. Copper(II) sorption onto goethite, hematite and lepidocrocite: A surface complexation model based on ab initio molecular geometries and EXAFS spectroscopy. *Geochim. Cosmochim. Acta* **2004**, *68*, 2623–2637.
- (10) Borrok, D. A universal surface complexation framework for modeling proton binding onto bacterial surfaces in geologic settings. *Am. J. Sci.* **2005**, *305*, 826–853.
- (11) Johnson, K.; Szymanowski, J.; Borrok, D.; Huynh, T.; Fein, J. Proton and metal adsorption onto bacterial consortia: Stability constants for metal–bacterial surface complexes. *Chem. Geol.* **2007**, *239*, 13–26.

- (12) Karthikeyan, K.; Elliott, H. Surface complexation modeling of copper sorption by hydrous oxides of iron and aluminum. *J. Colloid Interface Sci.* **1999**, 220, 88–95.

VITA AUCTORIS

NAME:	Rachel E. Franzblau
PLACE OF BIRTH:	New York City, NY, USA
YEAR OF BIRTH:	1989
EDUCATION:	Ann Arbor Pioneer High School, Ann Arbor, MI, USA 2007 University of Michigan, BSc Chemistry, Ann Arbor, MI, USA 2011